Hexa-X-II | WP4 | D4.3

Early results of 6G Radio Key Enablers

Hexa-X-II

hexa-x-ii.eu

30/04/2024

Outline

- Objectives
- Overview of value-based holistic radio design
  - Representative use cases and radio scenarios, radio design framework, transceiver architecture
- Channel modelling
  - sub-THz channel models, JCAS channel modeling
- MIMO transmission
  - D-MIMO schemes and architectures, massive MIMO schemes and architectures, RIS-aided transmissions
- Waveforms and modulations
  - Sub-THz waveforms and constellations, waveforms enhancements
- Intelligent radio air interface design
  - Waveform learning, AI- based CSI acquisition, AI-based MIMO transmissions, AI for HW impairments
- Joint communications and sensing
  - Deployment, resource optimization
- Flexible spectrum access solutions
  - Spectrum sharing and coexistence, low-latency access, NT/NTN integration, proactive resource management
- Trustworthiness
  - Secret key generation, jamming classification, jammer localization, JCAS security and privacy
- Proof of concepts and simulators
  - AI-native air interface, bistatic JCAS, power consumption for JCAS, EMF assessment

Objectives

Analyse of 6G radio design and spectrum access requirement and identify key 6G radio enablers

Towards THz communications

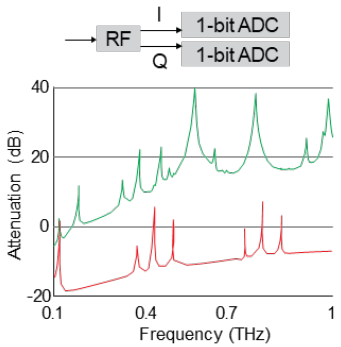

WPO 4.2: Provide a suitable channel model and develop novel broadband air-interface techniques to enable energy-efficient operations in the (sub-)THz bands, including new energy-efficient waveforms and modulations, and advanced massive MIMO techniques.

Joint communications and sensing

WPO 4.3: Provide solutions that enable flexible, cross-functional joint communication and sensing over a unified radio infrastructure, including new architectures, signals, methods, and protocols.

Intelligent radio air-interface design (FR1, FR2)

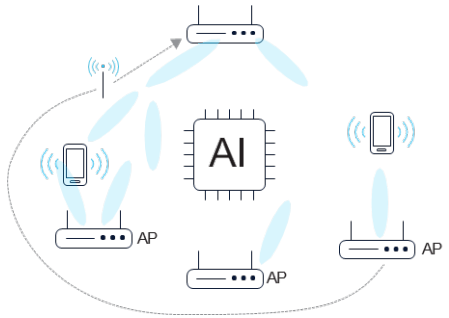

WPO 4.4: Design intelligent radio air interface to improve one or a combination of KPIs including spectral efficiency, energy efficiency, coverage, or lower cost at FR1 and FR2 spectrum.

Flexible spectrum access solutions

WPO 4.5: Develop spectrum sharing and medium access mechanisms for enabling an efficient transition to 6G (coexistence) and low-latency service access.

WPO 4.1: Develop an inclusive, trustworthy, and flexible radio design tailored to meet given 6G KPIs and KVI requirements through analysis and integration of HW architectures, transmission schemes and security solutions.

KVI: key value indicator
KPI: key performance indicator

Sustainable, trustworthy and inclusive holistic radio design

Overview of value-based holistic radio design

Radio design process

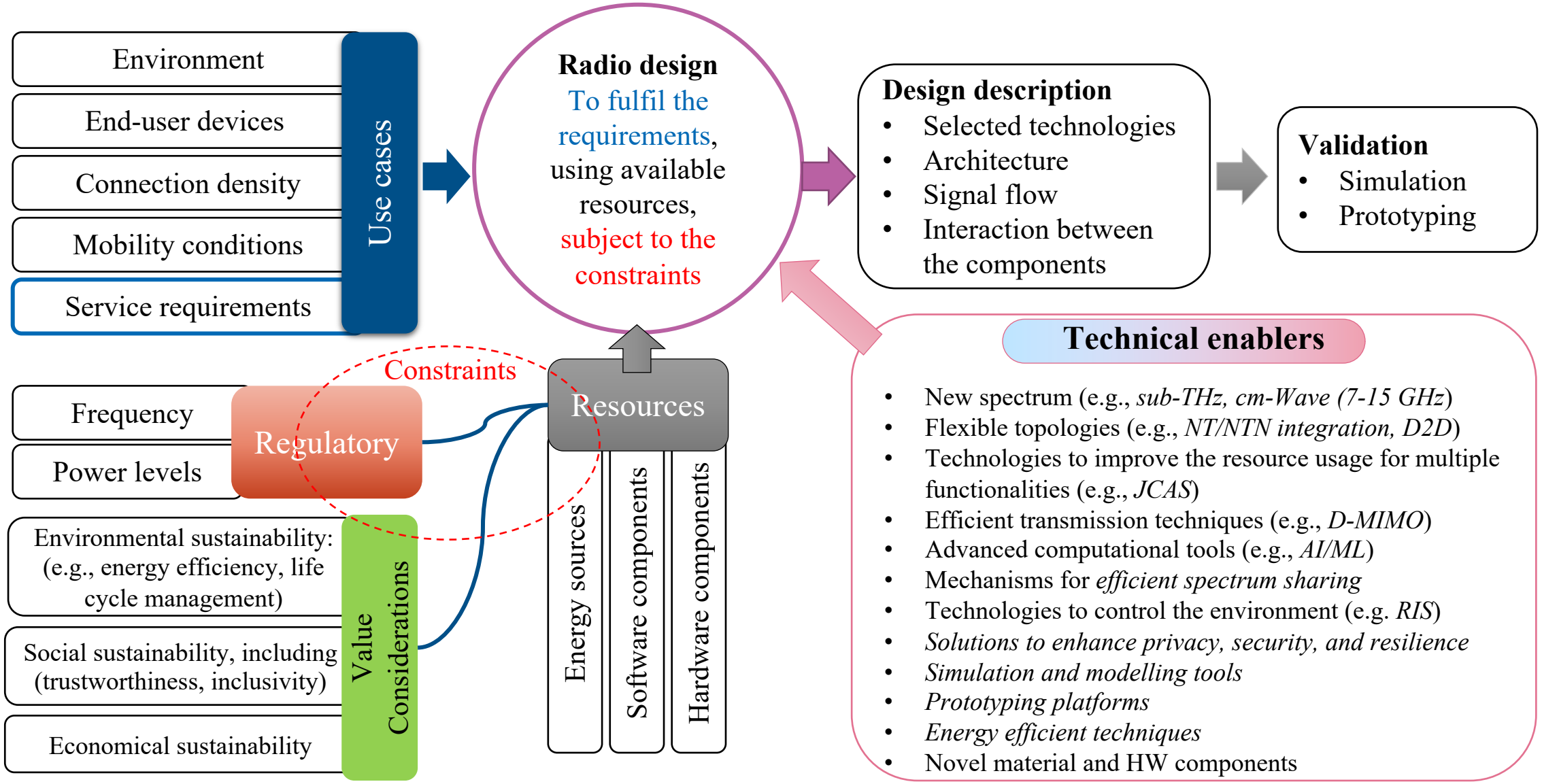

Use cases analysis and scenarios

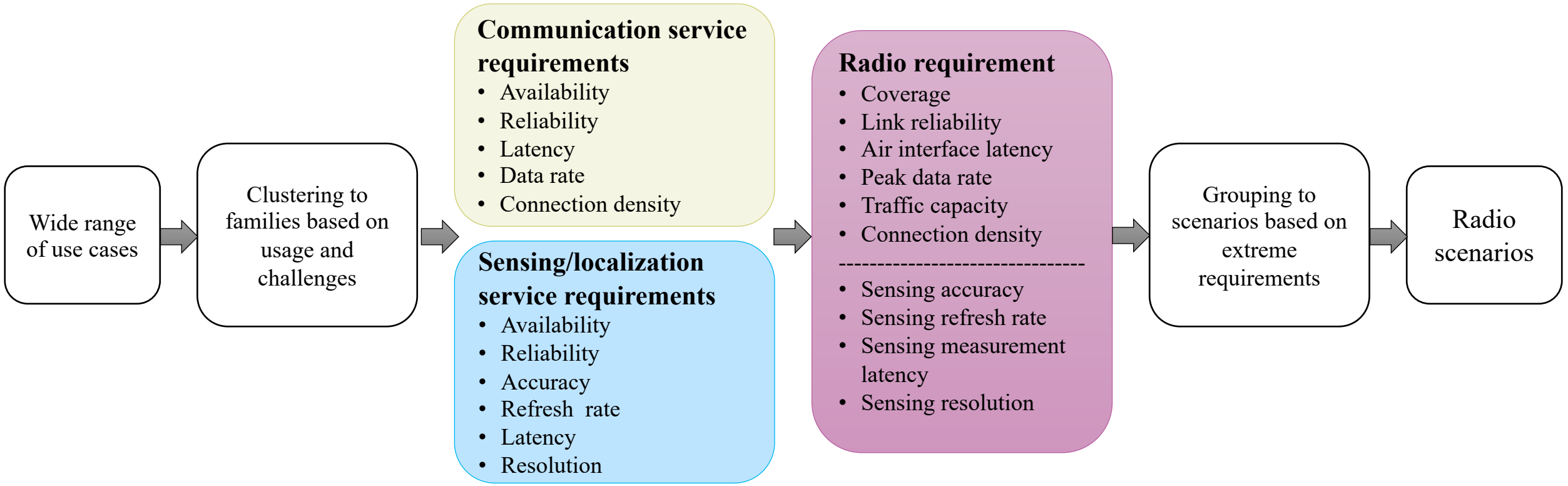

5G scenarios (IMT-2020)

- eMBB
- URLLC
- mMTC

6G scenarios (IMT-2030)

- Immersive communication
- Hyper RLLC
- Massive communication
- Ubiquitous connectivity
- AI and communication
- Integrated sensing and communication

Hexa-X-II radio scenarios

- Extreme data rate
- Extreme RLLC
- Extreme connection density
- Extreme coverage

AI and sensing are included in each scenario

RLLC: reliable an low-latency communication

Radio scenarios KPIs

- Derived by analysing the service requirements of representative use cases and mapping to radio requirements

Radio scenario	ITU usage scenarios	HEXA-X-II use case family (representative)	Peak data rate	Link reliability	Air interface latency	Connection density	Coverage	Sensing capabilities
Extreme coverage	Ubiquitous connectivity	Fully connected world (Ubiquitous network) Physical awareness (Network-assisted mobility)	Low Medium < 1 Gbit/s	Variable	Variable	Variable	Ultra-wide Extreme-wide Availability (99.99%-99.999999%)	Variable
Extreme data rate	Artificial intelligence and communication Immersive communication	Immersive experience (Seamless immersive reality)	Ultra-high Extreme-high (10-100 Gbit/s)	Variable	Variable	Low Medium <10^4 device/km^2	Local	Variable
Extreme connection density	Immersive communication Massive communication	Digital twins (Realtime digital twins) Trusted environment (Human-Centric Services)	Medium High < 10 Gbit/s	Variable	Variable	Ultra-high Extreme-high (10^6-10^8) device/km^2	Variable	Variable
Extreme low latency and high reliability	Hyper reliable and low-latency communication Integrated sensing and communication	Collaborative robots (Cooperative mobile robots)	Low < 10 Mbit/s	Ultra-high Extreme-high (99.999%-99.99999%)	Ultra-low Extreme-low (0.1-10) ms	Variable	Local	Ultra-high Positioning accuracy (0.1-1) cm

Radio scenarios parameters

- Sub-scenarios can be defined by different combinations of scenario parameters

Radio scenario	Environment	Deployment option	Radio devices	Mobility	Frequency	Example
Extreme coverage	Mobile indoor Public indoor Outdoor (urban, suburban, rural)	Long range Short range Fixed/temporary Mobile infrastructure TN/NTN integration	Enhanced 5G (mMTC, eMBB) devices Energy neutral devices	Static, up to 300 km/h	Sub-GHz Sub-6 GHz 7-15 GHz Satellite frequency ranges	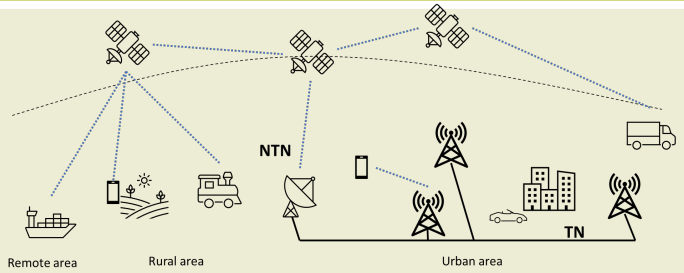
Extreme data rate	Controlled and semi-controlled indoor and outdoor	Small cell D2D Fixed access Sensor network with a gateway	Access points for backhaul Gateway for sensors Local devices (sensors, actuators)	Static, up to 10 km/h, controlled mobility (velocity information available)	mmWave or sub-THz Mixed and unlicensed for local connections	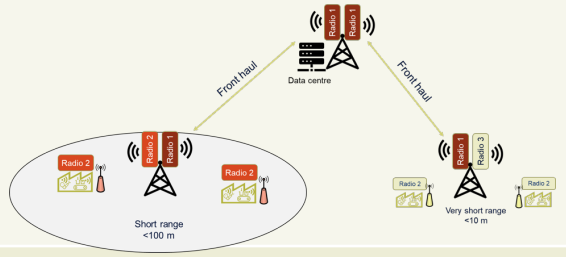
Extreme connection density	Urban indoor/outdoor with high density of users High-rise	High density of cells Macro cell Micro cell Cell-free	Reliable high data rate with bounded latency devices	Static, up to 100 km/h	Sub-6 GHz 7-15 GHz mmWave	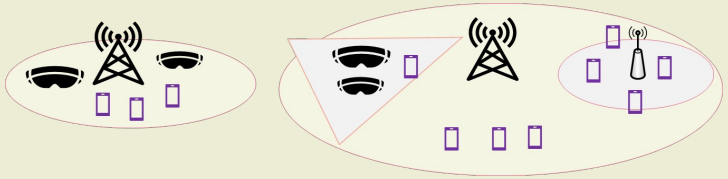
Extreme low latency and high reliability	Indoor Embedded network	Small cell On premises infrastructure Sensor network	High reliability & low latency devices	Static, up to 20 km/h, controlled mobility (velocity information available)	Private frequency Sub-GHz Sub-6 GHz 7-15 GHz mmWave, sub-THz for sensing	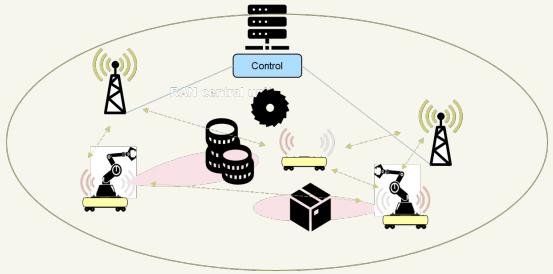

6G Radio design requirements

- Performance requirements related to services

Air interface communication requirements	Performance metrics
Data rate	Peak data rate, throughout, capacity, spectral efficacy, sum rate, average rate, packet rate.
Coverage	Range (spatial separation distance), beamwidth, signal-to-noise ratio (SNR), coverage probability, outage probability.
Air interface latency	The time needed to transmit and receive L2 packet successfully.
Air interface reliability	Bit error rate (BER), frame error rate (FER), block error rate (BLER), symbol error rate (SER), normalized mean square error (NMSE).
Radio sensing requirements	**Performance metrics**
Location/sensing accuracy	Error norm value (distance between true and estimated value) corresponding to a certain percentile of the location error norm.
Sensing latency	The time between initialization of sensing/localisation procedure and acquiring localisation/sensing estimate.
Orientation accuracy	The orientation error norm value corresponding to a certain percentile (e.g., 90%, 99%) of the orientation error norm.
Location coverage	The area or volume or fraction of a space in which the localization error is below a certain limit.
Sensing resolution	The smallest difference in a dimension (e.g., range, angle, Doppler) between objects to have measurably different values.
Sensing detection probability	The probability that a target is detected given that it is present .

- General performance requirements

Implementation and operation	Performance metrics
Energy efficiency	Ratio of output power to the total consumed power, energy consumption to achieve certain performance goal (such as energy required to transfer a bit).
Complexity	Amount of hardware resources, computational complexity of algorithms.
Cost	Cost of design, implementation, deployment, and operation.

- Design value requirements

Value requirements	Performance metrics
Inclusiveness	Coverage, global standard, proper number of manageable interfaces, affordable devices.
Trustworthiness	Reliability, security, resilience, integrity.
Sustainability	Values and needs of the end-users, energy consumption, life cycle assessment (LCA) of material, electromagnetic field (EMF) exposure.

Holistic radio design framework and enablers

Holistic radio design considers the entire radio system as a whole, and the interdependencies between different elements.

Value focused radio solutions: for trustworthiness, inclusiveness, etc.

Upper-layers: radio functions and protocols

AI/ML models

Logical channels

MAC

Access and resource allocation functions

Transport channels

PHY

TX-DSP (Transmitter functions)

RX-DSP (Receiver functions)

HW and channel abstraction

RU

TX DSP-frontend, (DAC), Bandwidth

RF-TX (LP, Conversion), Frequency band

TX RF-frontend (beamforming, PA, antennas), Frequency band

RX DSP-frontend, (ADC), Bandwidth

RF-RX (Conversion, LP), Frequency band

RX RF-frontend (beamforming, LNA, antennas), Frequency band

Propagation

Type of environment

Mobility

Type of deployment

Flexible spectrum access solutions: Sharing, coexistence, low-latency access

Signal processing and algorithms

Waveform, modulation, coding, radio resource allocation, AI/ML schemes

Radio link modelling

Channel modelling, HW modelling, link-level signal modelling

Architecture and deployment

Radio HW architecture, RIS, D-MIMO, JCAS deployment

End-to-end radio optimization

RF transceiver architectures

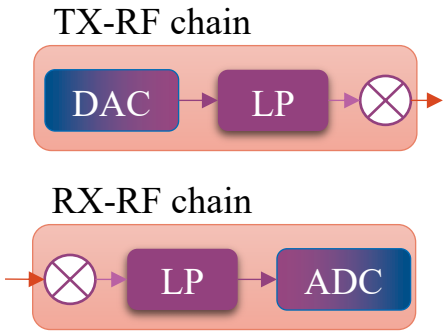

- MIMO with analogue beamforming
  - Antenna arrays/lenses
  - Fully analogue beamforming
  - Hybrid digital and analogue
  - Subarray based
- MIMO
  - Point-to-point MIMO
  - Multiuser MIMO
  - Massive MIMO/digital beamforming
- Architectures with various combination of ADC/DAC resolution
  - 1-bit DAC and 1-bit ADC
  - High resolution DAC, 1-bit ADC

MIMO with analogue beamforming

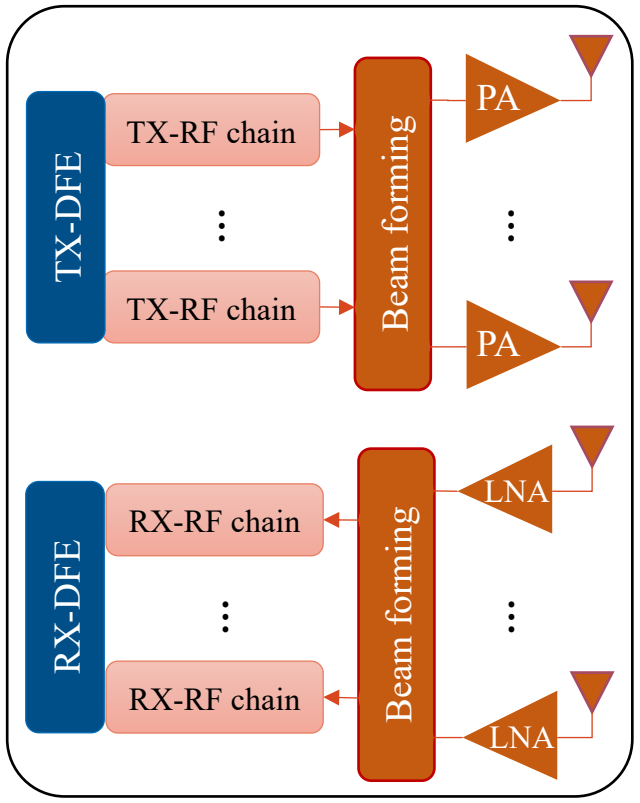

Architecture for mmWave, sub-THz

MIMO

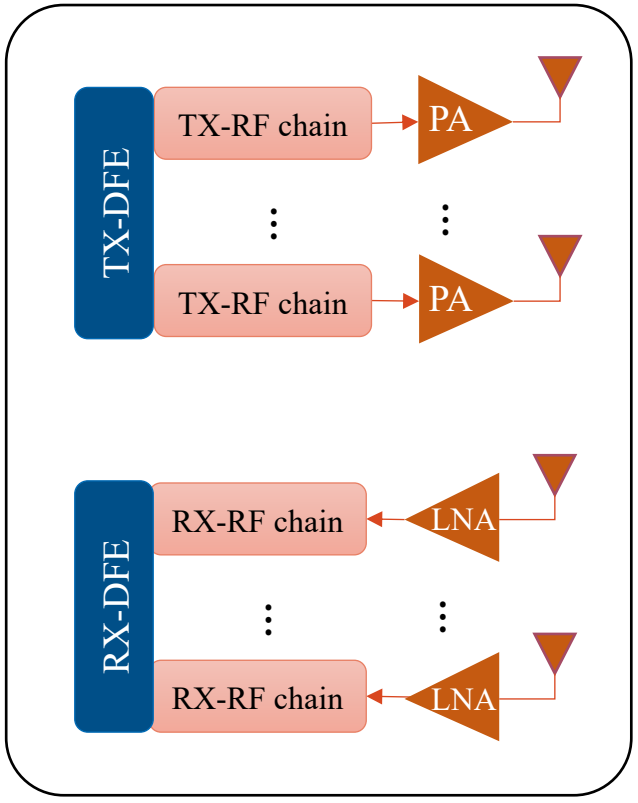

Architecture for mMIMO with digital beamforming, MU-MIMO

Radio architecture and deployment options

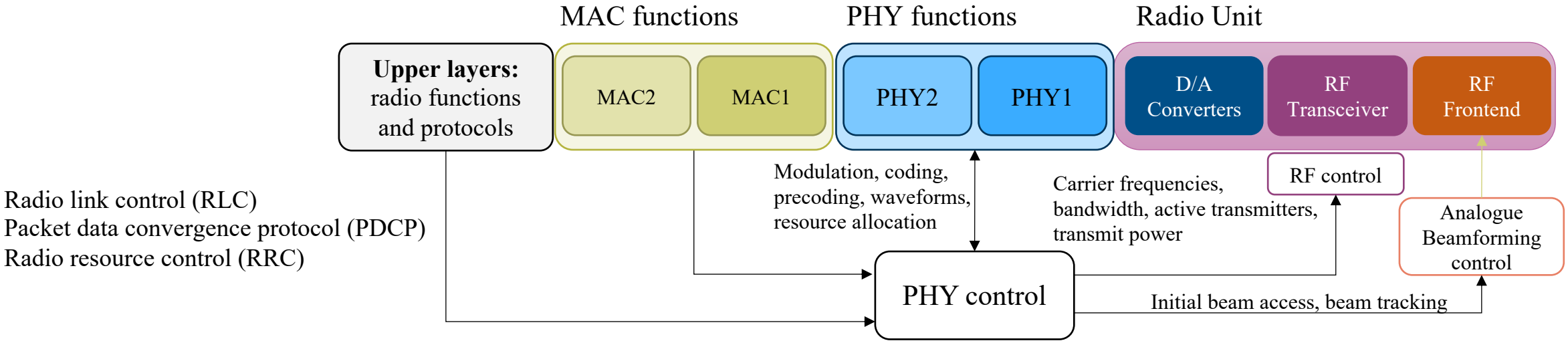

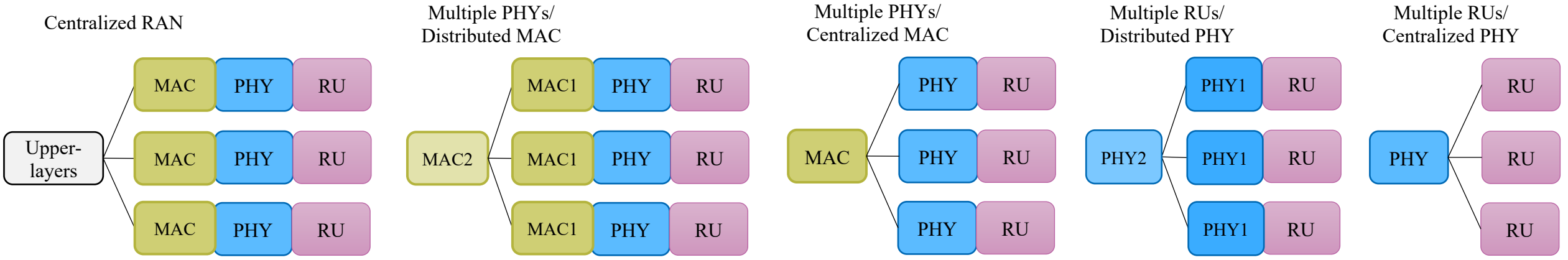

Link modelling

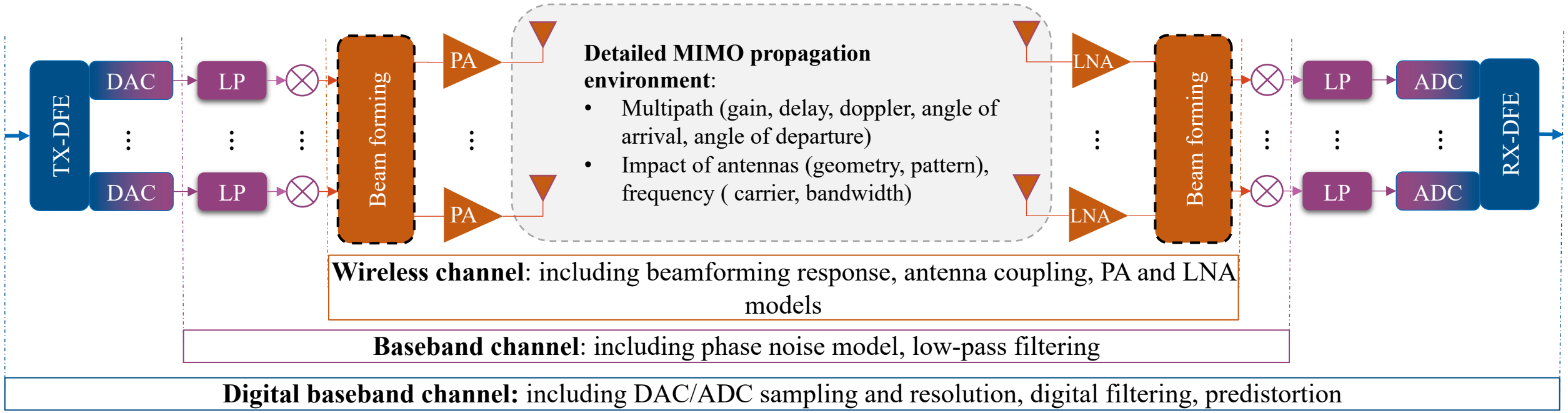

Signal processing and algorithms

- Abstracted processing model
  - Need to be adapted to the scenario, such as multiuser uplink, multiuser downlink, considering the radio architecture and deployment
  - Processing should consider the architecture, such as centralized/distributed processing, per user / joint processing

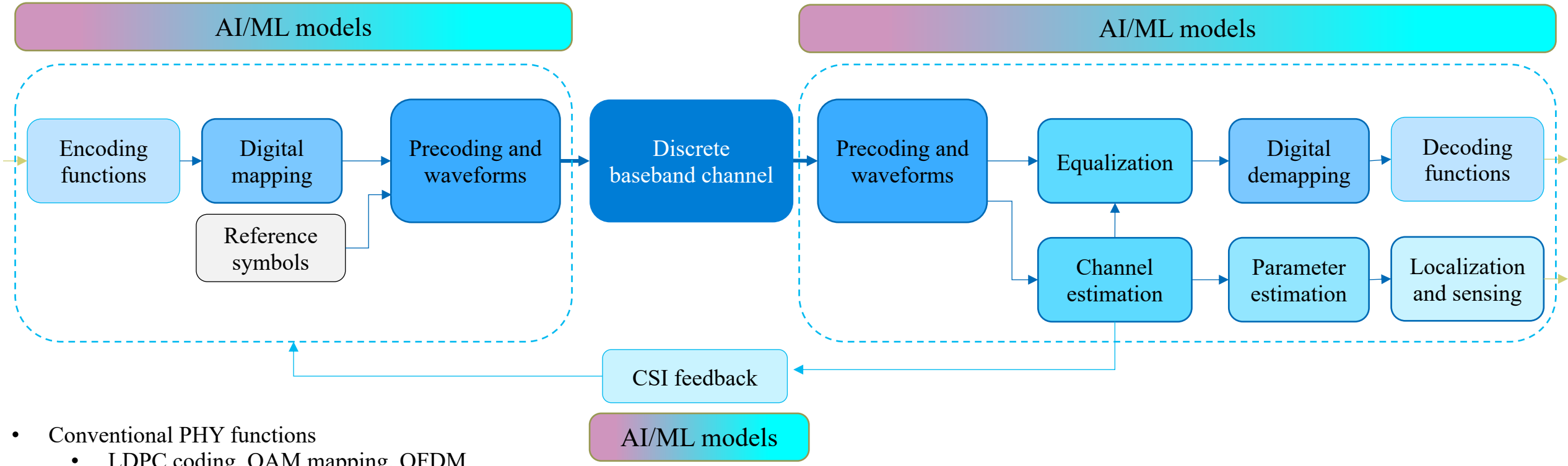

- Conventional PHY functions
  - LDPC coding, QAM mapping, OFDM
- AI/ML based functions
  - Learned constellation
  - Learned waveform/precoding
  - Learned multiple functions

Channel modelling

Summary

- In Chapter 3, the channel models related to the use of the sub-THz and THz bands, and new technologies like reconfigurable intelligent surfaces (RIS) and joint communication and sensing (JCAS) are covered. It presents extensions of existing standard channel models such as the channel parameter values at the sub-THz band; a modification to account for near-field effects; the reflection coefficient of various materials at the sub-THz band; and coverage reduction due to the increased path loss at THz frequencies. In addition, the signal model in an environment with RIS; and JCAS use cases, channel model features relevant to sensing, and their relation to existing channel models are discussed in Chapter 3.

3GPP-like channel model (T4.2, AAU)

Problem Statement	The standardized stochastic channel model 3GPP TR 38.901 is a commonly used model for generating wideband propagation channels with statistically consistent results. However, it currently only supports frequencies up to 100 GHz. The input channel parameter values needed to generate channels using 3GPP TR 38.901 for the 140 GHz band are provided here.
Methodology	Double-directional multipath data from channel measurement campaigns in the indoor entrance hall and outdoor residential environments from 140 – 144 GHz. Derive channel model parameters such as large-scale, small-scale, and cross-correlation parameters.

Results

Channel model parameter values listed in Tables A.1-1, A.1-2, A.1-3 in Appendix section of D4.3.

Large-scale Parameters (LSP)			LoS						NLoS				
			Delay Spread (ns)	Angular Spread (°)	Shadow Fading (dB)	K - factor (dB)	Distance-dependent coefficient (dB)	Path loss Offset	Delay Spread (ns)	Angular Spread (°)	Shadow Fading (dB)	Distance-dependent coefficient (dB)	Path loss Offset
Indoor	PE (%)	Office [38.901]	37	43	71	8	2	21	45	9	9	5	26
		Entrance Hall	9	12	0	5	0	0	12	8	0	0	1
Outdoor	PE (%)	Urban-Micro [38.901]	28	55	73	10	3	15	57	51	5	27	19
		Residential	32	54	0	8	0	1	82	75	0	7	6

PE: Percent error of μ_{LSP} between measured and generated channels.

These parameter values can be utilized to create realistic channels, which are helpful for evaluating links and systems in the sub-THz band.

Channel model component for near-field condition (T4.2, OUL)

Problem Statement	Provide a simple modification to the legacy channel modelling 3GPP TR 38.901. In physical reality, antenna elements of Tx and Rx arrays have slightly different propagation lengths on LoS and NLoS paths. These slightly different path lengths cause frequency-dependent phase offsets between signals on antenna elements.

Methodology

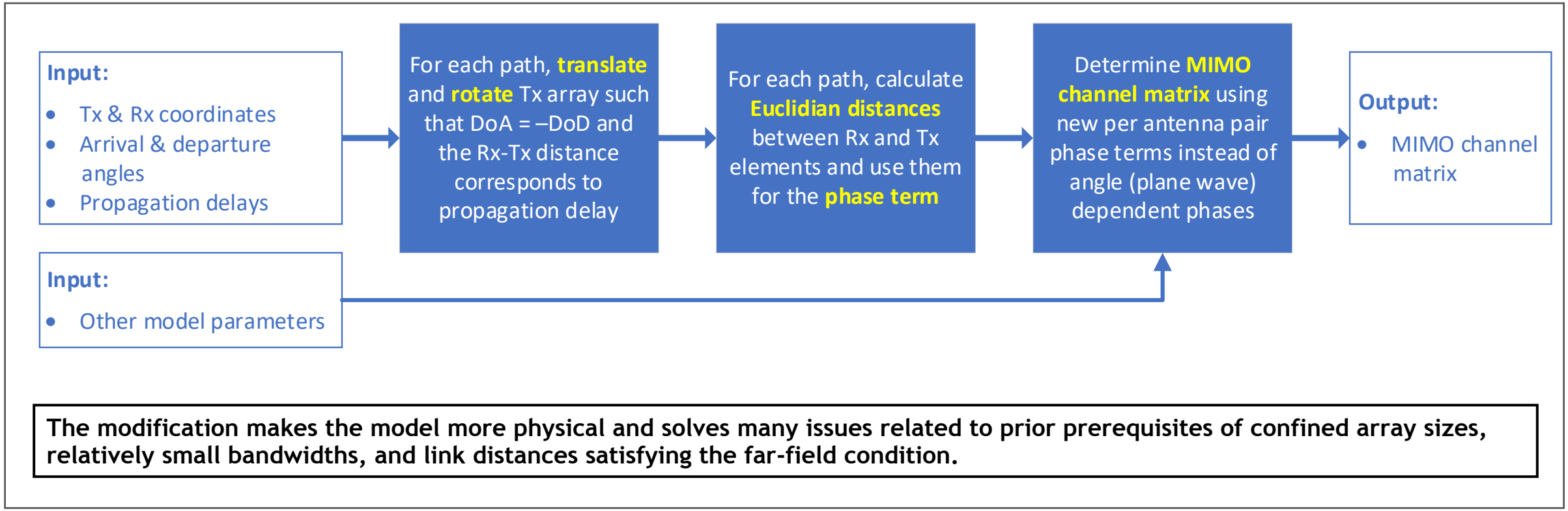

The modification makes the model more physical and solves many issues related to prior prerequisites of confined array sizes, relatively small bandwidths, and link distances satisfying the far-field condition.

Coverage analysis at THz frequencies (T4.2, TIM)

Problem Statement	THz frequencies provide increased bandwidths compared to the ones achievable with mmWave, leading to meet the demands for increased data rates up to Tbps. The countereffect is a significant reduction of radio coverage compared to the one achievable with mmWave, due to high propagation loss.
Methodology	Theoretical analysis of path loss and coverage reduction at 100 GHz and 600 GHz.

Results

Path loss [dB]	Benchmark	Achievement	Impact on the system
	mmWave @ 100 GHz	THz @ 600 GHz	THz @ 600 GHz vs mmWave @ 100 GHz
	d_{3D} mmWave [m]	d_{3D} THz [m]	Coverage reduction [%]
110	150	10	99.57%
130	600	45	99.44%
147.6	N/A	100	N/A

THz frequencies are therefore suitable for providing focused coverage spots, in a range up to roughly 100 m, depending on the acceptable path loss requirements of the overall system.

Impact of rough and coated surfaces on reflection coefficients (T4.2, ORA)

Problem Statement	The goal is to address the reflection coefficient deviation of rough surface materials compared to material with smooth surface as assumed by the ITU-R P2040 model. Deterministic simulations useful for evaluation of wireless radio interfaces and coverage prediction rely on the use of these reflection coefficients.
Methodology	Measurement using vector network analyzer and frequency extenders covering the frequency bands 5-40 GHz, 110-170 GHz, 170-260 GHz. Materials measured: mortar, patterned glass, and carpet tile.

Results

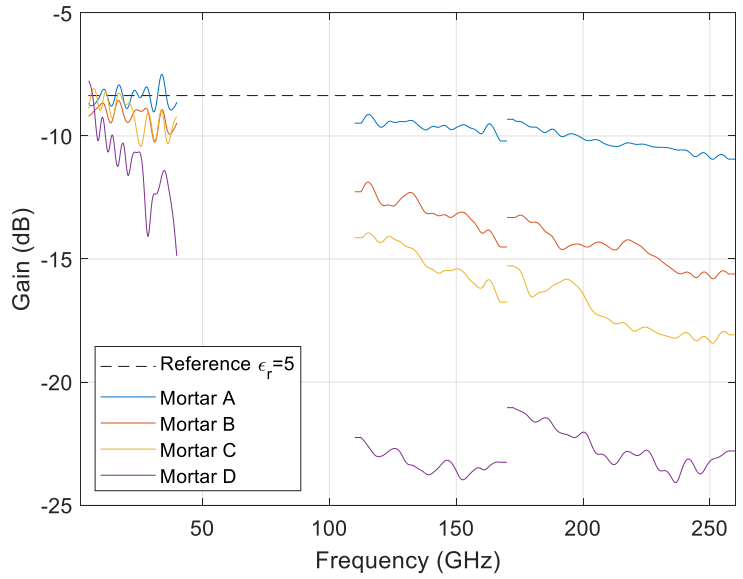

Averaged reflection gain measured at a normal incidence from different rough surfaces and comparison with a flat surface reference material

The averaged reflection gain off a rough surface compared to a smooth surface may be reduced from a few dB to 15 dB depending on the surface roughness at frequency above 100 GHz.

Conclusions on rough mortars can be extended to non-flat indoor material such as carpet or patterned glass.

Signal level analysis for RIS in a simplified scenario (T4.4, TIM)

Problem Statement	A signal model for calculation of the signal-to-noise ratio (SNR) at the user receiver is derived, considering both passive and active RIS. The effect of RIS on the signal received by the user is then determined in a simplified propagation scenario.
Methodology	SISO with RIS and RX in the far-field region of Tx and RIS. Assumed frequency is 26 GHz and number of RIS elements is 256. Geometry shown below. RIS moved horizontally with a 10 meter step.

Results

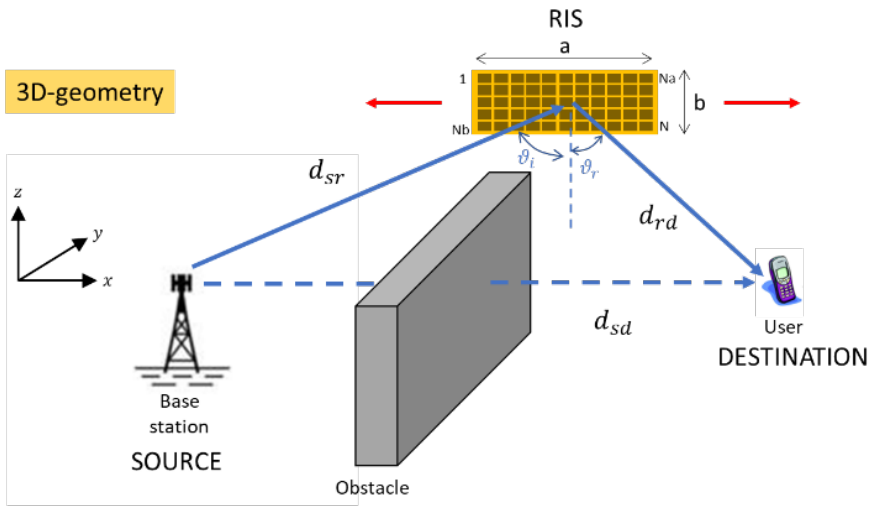

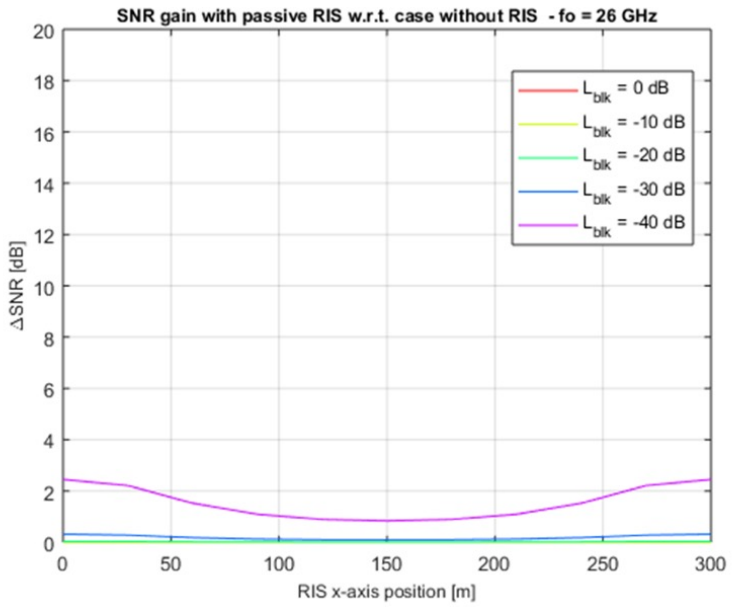

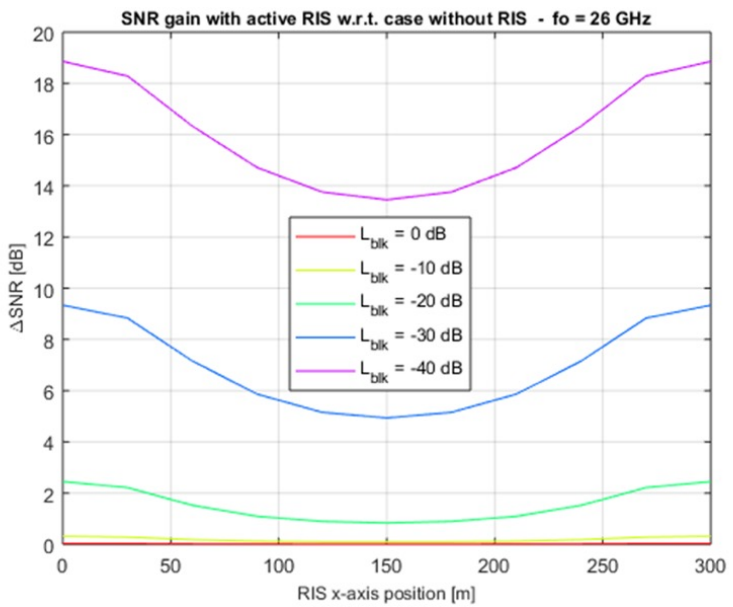

A simple model of a communication link with RIS was derived, revealing the negligible and significant SNR gains of the passive RIS and active RIS.

JCAS channel models (WP4)

Problem Statement	Delve deeper in the models needed to support sensing and JCAS use cases.
Methodology	Sensing use cases are first reviewed, based on which a set of relevant sensing aspects or features are determined that the JCAS channel models should support. A selection of currently available models is then provided and related to these features.

Results

Supported | Partially or conditionally supported | Not supported

JCAS feature	Objects in a coordinate system	Different object types	Radar cross section	Extended objects	Doppler due to the mobility of communicating devices	Doppler and Micro-Doppler due to motions of wave scattering objects	Space/time consistency	Near-field	Data sets for classification use cases	Communication and sensing channel compatibility, and reciprocity
Statistical geometric models										
Site-specific models (Deterministic)										
Hybrid models (Deterministic + Statistical)										
Stored channel model										

Stored channel models can support all features, provided the corresponding data is present. This analysis indicates that for performance evaluation purposes, hybrid models or site-specific models may be preferred over the classical statistical geometric models.

MIMO Transmission

Summary

- Within the framework of 6G, MIMO is expected to have a significant role, offering the potential to enhance the capacity and efficiency of wireless communication systems even further to satisfy future communication demands. Chapter 5 focuses on exploring three techniques of MIMO within the context of 6G: **D-MIMO, massive MIMO, and RIS**.
- **D-MIMO:** It focuses on both coherent and non-coherent transmission, and explores decentralized transmission and analogue fronthaul, as well as investigates the rotary antenna and one-bit ADC system. Additionally, it discusses the sub-THz D-MIMO assisted by a sub-6GHz macro network.
- **Massive MIMO:** It includes the analysis of enhanced data detection using a 1-bit ADC, and explores the design of a beamformer for sub-THz frequencies, as well as the investigation of hybrid analogue-digital architectures for MIMO. Additionally, it discusses the multi-user MIMO and location-dependent coded caching.
- **RIS-assisted transmission:** It focuses on the discussion of D-MIMO-assisted with RIS and RIS-assisted IAB. In addition, this section investigates the channel estimation of RIS, RIS reflecting modulation (RIS-RM), and non-radiative RIS transmission.

MIMO Transmission

D-MIMO schemes and architectures

Non-coherent Space-time Coded Transmission

Problem Statement	The mmWave frequency band faces challenges in reliable communication due to high path loss and shadowing. Besides, channel estimation can be tricky in several scenarios, e.g., high mobility, lack of uplink/downlink reciprocity, hardware calibration conditions and pilot contamination. NC-JT schemes defined in 3GPP can be used to address these issues, however, it is not clear how to use them with distributed and massive number of antennas. The aim is to explore robust transmission modes in challenging conditions by using orthogonal space time frequency block codes (STFBC) in D-MIMO precoding to enhance diversity at the UE side and maintain certain data rates even without precise CSI.
Methodology	Proposed solutions: • An RU-UE clustering is carried out to establish disjoint clusters of RUs jointly serving UEs, within each of which a suitable STFBC is going to be applied. • Alamouti-like orthogonal codes are used to realize the robust transmission mode, which use time, frequency and space diversity at the UE side.

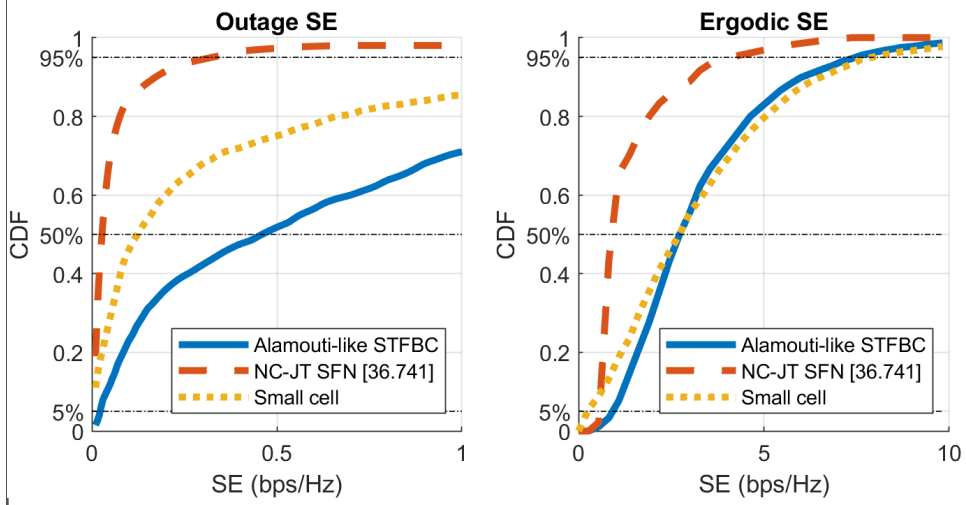

- **Simulation settings:** Numerical simulations are performed in an indoor factory of area 120×60 meters, where operating frequency is 28 GHz with 200 MHz bandwidth.
- Path loss and shadowing is set as in 3GPP 38.901, and small-scale channel model is Rayleigh distributed. Maximum transmission power is 0.2W and UE noise figure is 9 dB.
- **Results:** the per-UE cumulative distribution functions (CDFs) for outage and ergodic SEs.
- STFBC together with optimized clustering outperforms baseline methods.
- A significant enhancement on 5th percentile user ergodic SEs can be achieved with STFBCs, while the mean values are similar both for STFBC and small-cell
- The clustering can optimize the worst-case SEs by maintaining a similar performance for all users on average.

Distributed OTA cooperative beamforming design

Problem Statement	The DMIMO configuration diminishes intercell interference, making it especially well-suited for small-cell applications. In the literature on non-cooperative beamforming strategies, where each AP locally designs its beamformer without exchanging CSI through backhaul fronthaul links, recent studies highlight the potential for cooperative beamforming strategies to yield even greater performance gains. However, the cooperative beamforming design requires the CSI exchange via fronthaul links, which may not be feasible due to the fronthaul bandwidth limitations and not scalable. This work provides a cooperative beamforming design without exchanging the CSI via fronthaul links, using the bi-directional training.
Methodology	Proposed solutions: • Considering the downlink communication, the cooperative beamformers is designed using bi-directional training, where the UEs update their combiners using downlink pilots (DL), and APs update their precoders using uplink pilots (UL-1 and UL-2) using iterative bi-directional training. • The complexity of the proposed method is much less than the CPU based design.

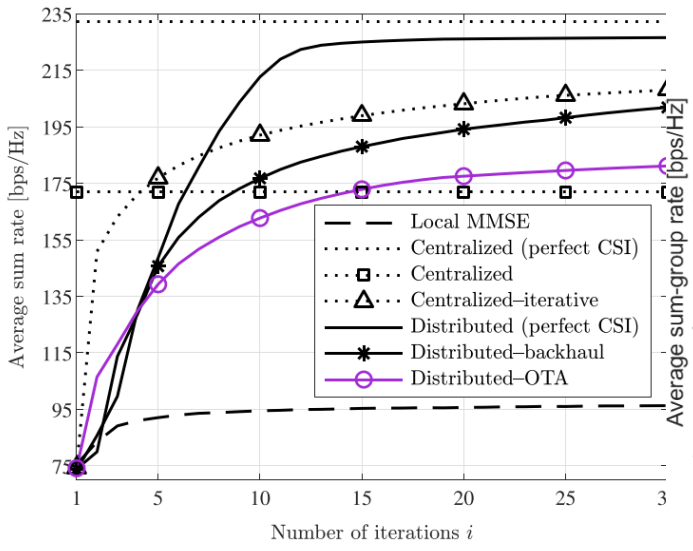

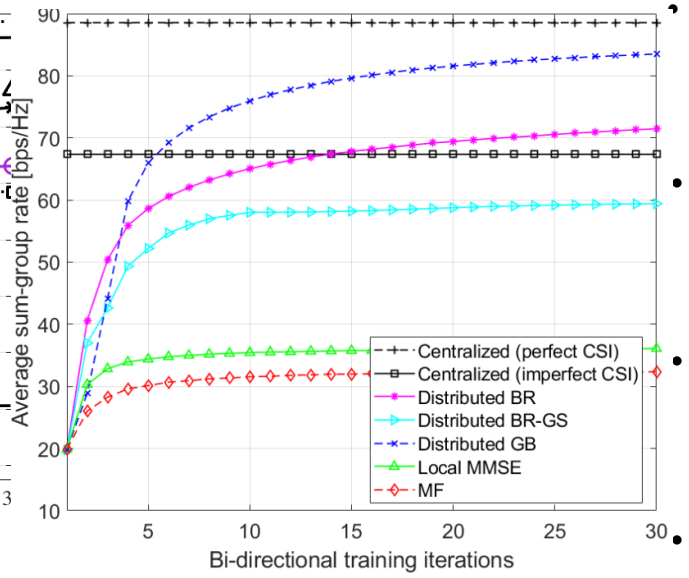

- **Simulation settings:** Consider 25 BS placed on square grid of 500m×500m area. 16 multiantenna UEs are randomly placed. The channel between UEs and APs follows Rayleigh fading, and the carrier frequency is 2.5 GHz.
- **Results:** The proposed method with OTA signalling, i.e., distributed-OTA, distributed GB, BR, BR-GS outperform the local MMSE, MF and centralized methods in both unicasting and multicasting.
- The number of OTA resources required for unicasting depends on the number of UEs, while the number of OTA resources required for multicasting depends on the number of multicasting groups.
- Note that the imperfect channel includes AWGN at APs and UEs.

D-MIMO with rotary ULAs

Problem Statement	Traditional wireless communication systems adopt static antennas, that is, antennas or antenna arrays without any movement capabilities. Movable antennas can exploit wireless channel variation in the continuous spatial domain. This additional degree of freedom can enhance the quality of wireless links, and consequently the communication performance. In this contribution, the performance of MU-MIMO systems where the APs are equipped with rotary ULA is studied. Considering an indoor industrial scenario, the numerical results show that the adoption of APs equipped with rotary ULAs can significantly enhance the mean per-user achievable SE when compared to deployments with static APs.
Methodology	• Single antenna devices are randomly and uniformly distributed on the coverage area. A random subset of K devices is active and seeks to transmit data in the uplink in each time slot. All devices are positioned at the same height. • Fully centralized processing is considered, where all the APs simultaneously serve all the devices, and they are connected to a common CPU through fronthaul connections. The CPU is responsible for performing all the signal processing tasks of the system. • Assume that there are no hardware impairments, and there is perfect synchronization among the APs. Moreover, CSI is available at the APs. CPU has estimated of the positions of all the devices subscribed to the network. The optimal position of the Q APs is jointly computed by the CPU.

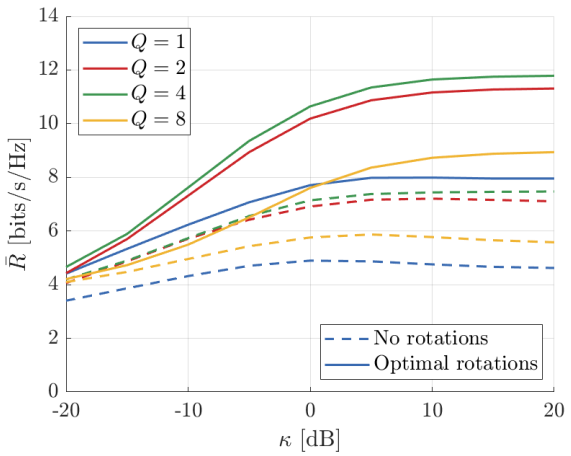

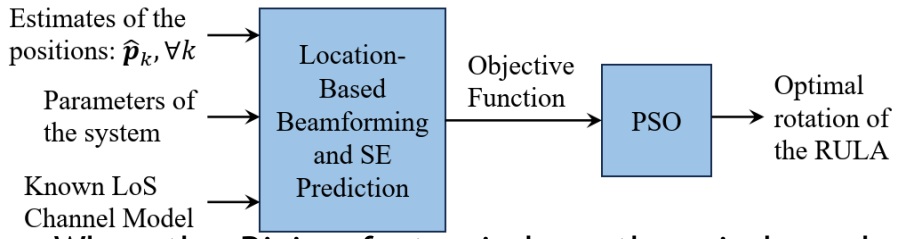

- **Results:** The results for the APs equipped with static ULAs are compared to the results for the case of APs with the rotary ULAs. The curves the performance improvement of the rotary ULAs grows with the Rician factor.
- When the Rician factor is low, the wireless channels are dominated by NLoS components, andthe rotation of the ULAs does not bring performance gains.
- When the Rician factor grows, the power of the LoS components increases. The rotation of the ULAs brings significant enhancement to the spectral efficiency.
- Q=2 and Q=4 achieve the best performance, which shows that there is a “sweet spot” between the number of APs and number of antenna elements per AP that yields the best performance.

Distributed-MIMO with analogue fronthaul

Problem Statement	D-MIMO introduces new challenges related to higher demands on bandwidth, synchronization, and power consumption. Therefore, innovative solutions are essential to harness the potential of D-MIMO in a cost-effective manner. Coherent joint transmission (CJT) involving two or more transmit/receive points (TRxPs) must be supported. However, meeting the stringent synchronization requirements with sub-nanosecond precision becomes crucial for CJT. One practical approach to achieving CJT is by employing analogue fronthaul (FH) links in combination with centralized processing since channel estimation includes the phase and amplitude change of both the wired path (i.e., FH) and wireless path of each transmitter, providing all the necessary information for CJT precoding.
Methodology	• A simple multiple-input single-output (MISO) setup is assumed involving an N-TRxP D-MIMO network and a single user equipment (UE). Both the UE and all TRxPs within the network are assumed to have a single antenna.

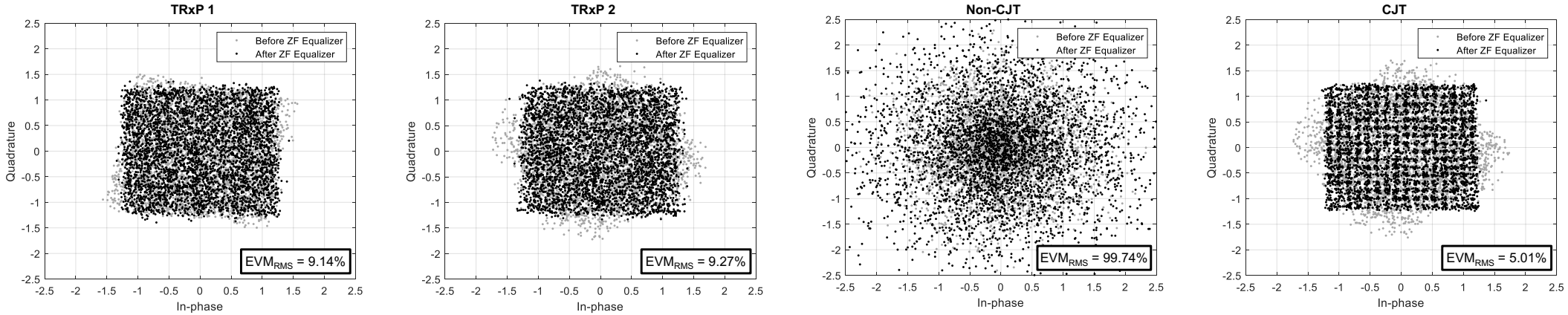

Results: 10 MHz OFDM signal carrying high-order 256-QAM symbols across all subcarriers. To assess D-MIMO flexibility with analogue FH links, TRxP 1 has an 800m fibre FH link, while TRxP 2 uses a 1.2m coaxial cable, resulting in a ~3.897 µs delay difference.

- For fair CJT evaluation, the EVM performance for both TRxPs is nearly identical during separate transmissions. The measured delay difference of 3.906 µs closely aligns with the theoretical 3.897 µs.
- For CJT, separate channel estimation is performed for TRxP 1 and TRxP 2. These estimates are used to compute the precoder for the TRxP 2 signal. The precoded signal is aligned in time in accordance with the measured delay difference between FH links.
- The CJT gain approximates ~5.35 dB when compared to TRxP 2 alone and approximately ~5.22 dB in comparison to TRxP 1.

One-bit ADC for multi-cell setup

Problem Statement	The next generation of wireless systems, beyond 5G, may operate at extremely high frequencies up to 1 THz with large bandwidths, which requires larger antenna arrays and increasingly sharp beamforming to maintain a consistent signal-to-noise ratio. However, the ADCs /DACs used in current systems consume a lot of power. One solution is to use low-resolution ADCs / DACs with 1 to 4 quantization bits to enable the use of massive MIMO arrays, which require hundreds or thousands of antennas.
Methodology	• The distributed massive MIMO system consists of B RRHs and K single antenna UEs. The RRHs are separated by 100 m and UEs are clustered and move in-between the RRHs. The RRHs are connected to a CPU via fronthaul connections. This study focuses on the uplink scenario. • The min-power and max-min SINDR designs are considered to optimize the UE power levels and the BS noise levels. The following equation represents the max-min-SINDR problem used for optimization. For a fixed noise level at the RRHs, the power of UEs can be optimized using a gradient, fixed-point iteration, or BCD methods. For the noise level optimization (which is more than the thermal noise), linear search is applied over the possible noise values.

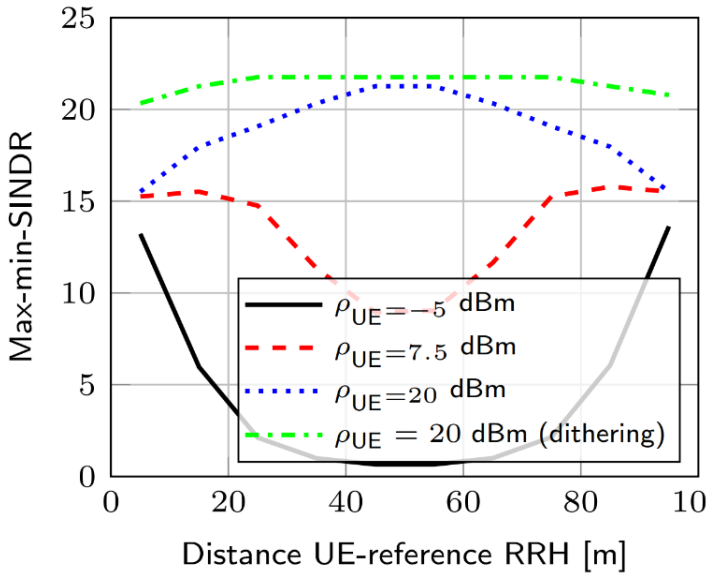

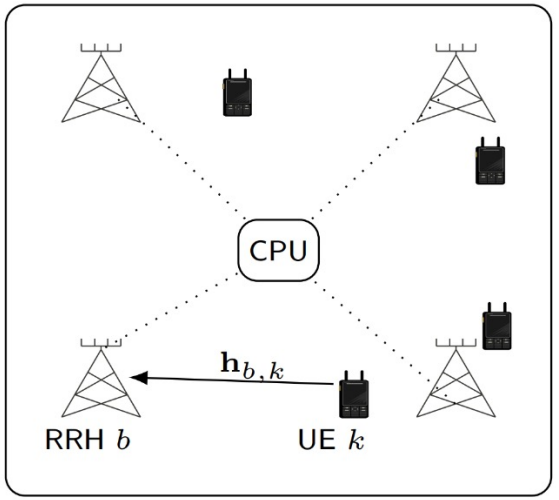

Results: The evaluation considers 2 RRH placed with 100 m distance between them. The carrier frequency is 28 GHz, Rayleigh fading channel is used. the UEs are moved from one RRH to other RRH, and UEs transmit powers and RRH noise levels are optimized for each distance from the reference RRH. The power control with dithering tuning improved the SINDR of the UEs. The impact of dithering (i.e., RRH artificial noise level) is more pronounced when the UEs are closer to an RRH.

sub-THz D-MIMO assisted by a sub-6 GHz macro network

Problem Statement	Link quality at sub-THz frequencies is sensitive to blockage. A D-MIMO network in form of sub-THz radio access nodes connected to a CPU ensures high probability of LoS at sub-THz frequencies. When a device moves or rotates, the serving beam needs to be updated. This entails a beam search procedure where the network sends reference signals in candidate beams and the device measures and reports the best beams. In a system with many APs and many beams per AP (can be on the order of 1000 or 10000 beams in the entire D-MIMO system), the beam search procedure over all the beams in the system will take a prohibitively long time, incurring latency and/or system capacity reduction.
Methodology	• Using the uplink channel characteristics at a frequency substantially lower than sub-THz (concretely, below 6 GHz) to infer the candidate list for a beam search in the downlink of the sub-THz D-MIMO network towards the target UE. • Beam candidate list can be obtained by NN classifier. One such classifier architecture is a feedforward NN with cross-entropy loss function and softmax output activation function. • Two strategies: Sort p_k in descending order, pick K beams with highest p_k . • Sort p_k in descending order, sum sorted p_k until the cumulative sum > threshold.

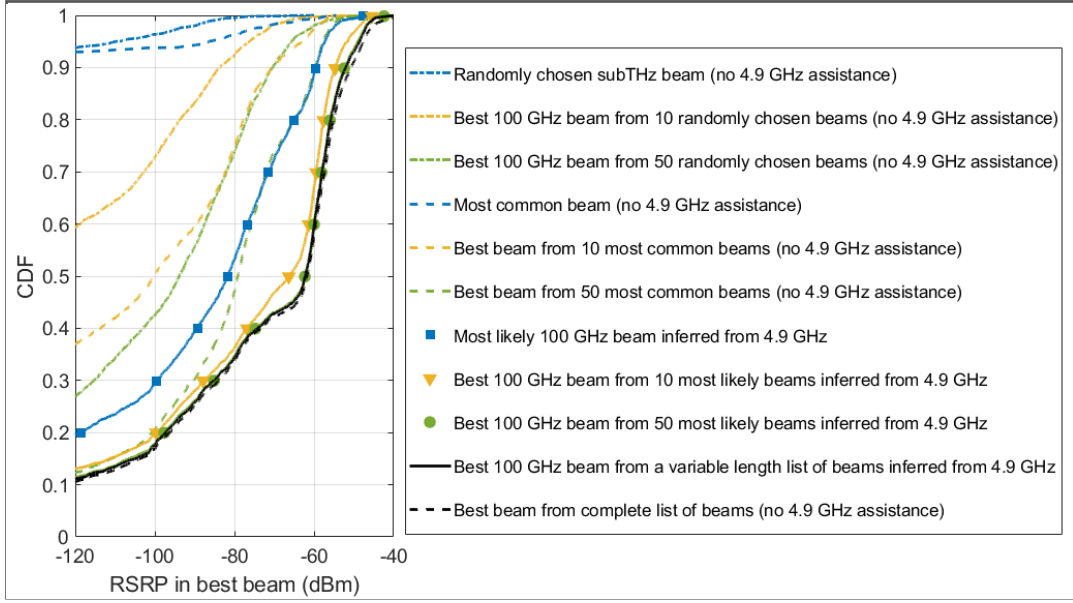

- **Results:** Data is collected from an emulated 3D deployment, where a ray-tracing, spatially consistent channel model is used to generate channels. User positions are distributed over a 4×4 meter grid, for a total of 8504 positions over the shown coverage area. Data from 5000 positions, sampled uniformly over the coverage area, are used for training, 1000 for model validation and 2504 for testing. There is a total of 128*20 = 2560 beams in the system.
- When a list of 50 beams is compiled based on the suggestion by ML based on sub-6 GHz data, the performance comes a few fractions of dB within the exhaustive search (black dashed line). The number of scanned beams in the 50 beam list example is only 50/(128*20) = 1.9% of the total number of beams in the system, indicating an enormous resource overhead reduction when applying the proposed scheme.

MIMO Transmission

Massive MIMO schemes and architectures

Enhanced data detection for massive MIMO with 1-bit ADCs

Problem Statement	New insightful results are presented on the uplink multi-user data detection for massive MIMO systems with 1-bit ADCs. On one hand, the former works perform an exhaustive search over the set of expected values of the soft-estimated symbols corresponding to the target UE resulting from all the possible data symbol vectors, whose size grows exponentially with the number of UEs; on the other hand, it does not take advantage of the interdependence among the soft-estimated symbols of the interfering UEs as it treats each UE individually.
Methodology	• A new data detection strategies are proposed based on the minimum distance criterion with respect to the expected values of the soft-estimated symbols. • A joint data detection strategy is proposed, which considers parallel data detection over all the UEs and exploits the interdependence among their soft-estimated symbols. • Furthermore, a low-complexity variant of the joint detection is presented, which is obtained by reducing the size of the search space.

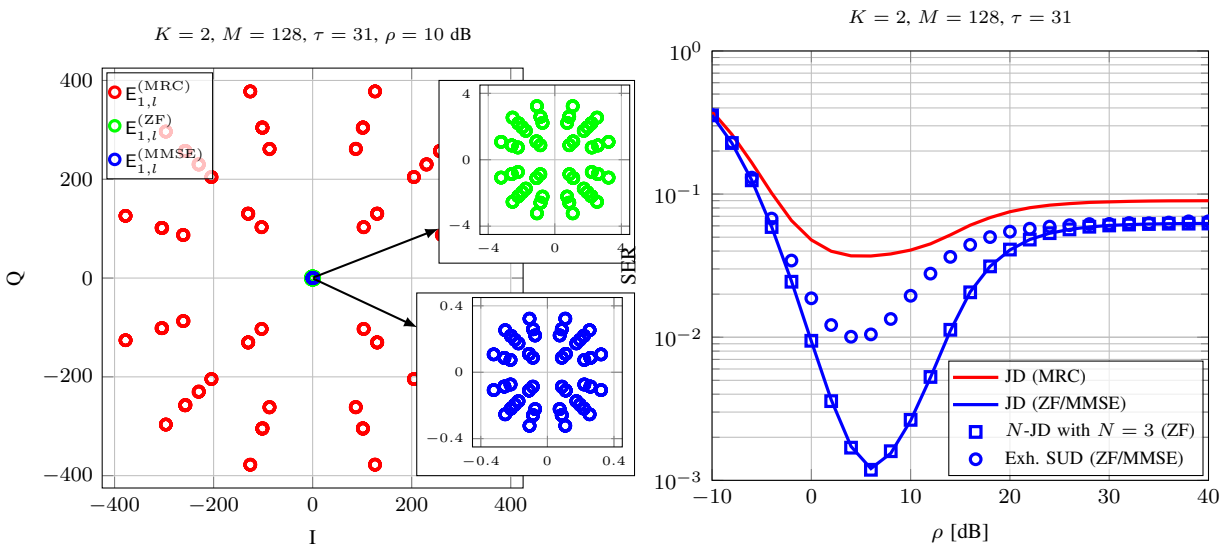

- **Results:** 16-QAM data symbols are considered. The channel covariance matrices are generated based on the one-ring channel model with no pathloss. The expected values with ZF/MMSE can be obtained by simple scaling of their MRC counterparts.
- Numerical results show that ZF and MMSE provide substantial gains in terms of SER compared with MRC.
- The proposed joint detection and its low-complexity variant greatly outperform the exhaustive single-UE data detection method described in since the latter does not account for the interdependence among the soft-estimated symbols of the interfering UEs.

Massive MIMO with 1-bit DACs and ADCs

Problem Statement	Enabling communications in the (sub-)THz band will call for massive MIMO arrays at either the transmit- or receive-side, or at both. To scale down the complexity and power consumption when operating across massive frequency and antenna dimensions, a sacrifice in the resolution of the DACs/ADCs will be inevitable. Simple 1-bit DACs/ADCs can also alleviate the overall complexity and power consumption of the RF chains.
Methodology	• Considering a point-to-point system, the Bussgang decomposition is utilised to unfold the relation between the transmitted data symbols (at the input of the transmitter's 1-bit DACs) and the soft-estimated symbols acquired via linear combining of the quantized received signal (at the output of the receiver's 1-bit ADCs). • Assuming perfect CSI, a tractable approximation of MSE between the transmitted data symbols and their soft estimates is derived along with the combining strategy that minimizes it.

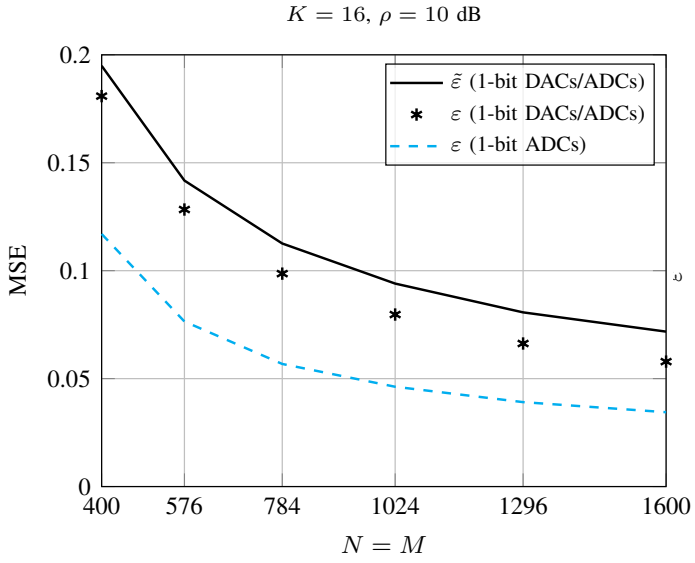

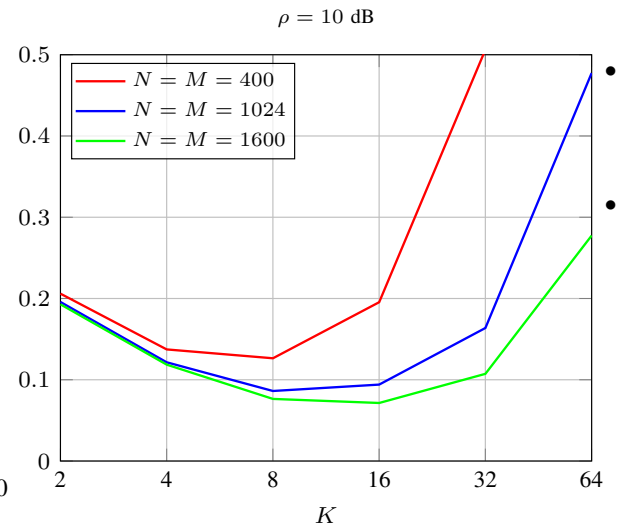

- **Results:** Assuming 16-PSK data symbols, remarkably small SER values can be obtained with truly massive antenna arrays at both the transmitter and receiver.
- A doubly 1-bit quantized massive MIMO system with very large antenna arrays can deliver an impressive performance in terms of MSE and SER, which is not far from that of a massive MIMO system with full-resolution DACs and 1-bit ADCs. In particular, replacing the 1-bit DACs with full-resolution ones provides a modest MSE or SER gain at the cost of much higher RF complexity and power consumption at the transmitter.

Energy efficient beamforming architecture and deployment for sub-THz

Problem Statement	Scope of this study is the spectral and energy efficiency trade-off of different beamforming architectures and BS placements, with focus on indoor scenarios and hybrid beamforming at the BS. With system level simulations the coverage and throughput of different deployment arrangements with different numbers of BS and randomly distributed UEs is evaluated. To assess the related energy efficiency, the power consumption is derived with a refined power consumption model based on that introduced in.
Methodology	An indoor scenario with a size of 30m × 60m is considered. Base stations are located equally spaced at the walls of the longer side at a height of 4 meters and transmitting towards the room. In the initial scenario 8 BS are applied which transmit with a grid of beams (GoB) of 4 × 4 beams. For a fixed number of randomly distributed UEs (4, 8 and 16) the average UE throughput for different transmit power of the BS, the number of BS and the number of UEs is analysed. A first coarse power consumption assessment is given.

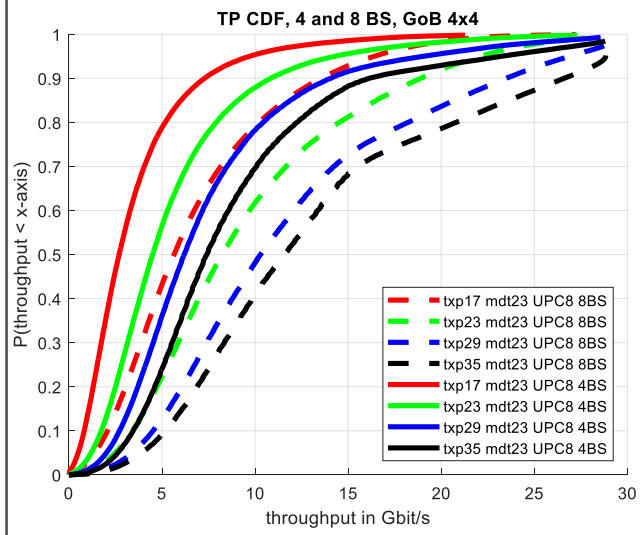

8 simultaneous UEs

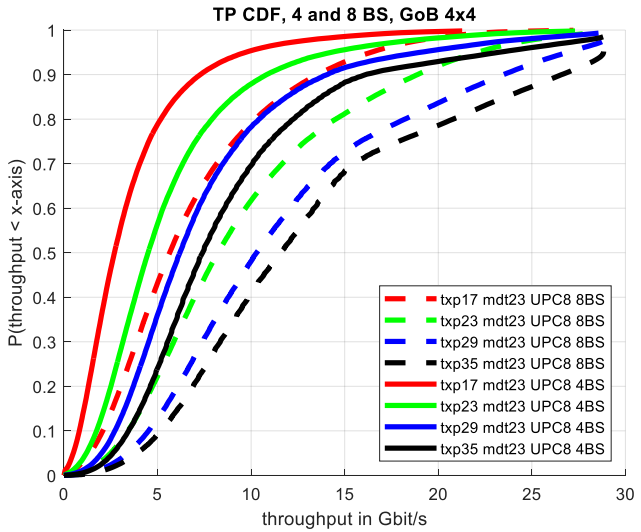

16 simultaneous UEs

Simulation Assumptions: Transmit power of the BS, antenna characteristics (Uniform rectangular array, with selection of ideal beam from a GoB) and a 3GPP channel model adapted to 140 GHz based on Hexa-X measurements. The assumed carrier frequency is 144 GHz, the signal bandwidth is approximately 4 GHz.

Results: The expected outcome is to be in the position to derive most efficient deployment in terms of meeting coverage/throughput requirements with best energy efficiency.

MU-MIMO optimization in diverse device scenarios

Problem Statement	MU-MIMO is a key tool for increasing the capacity of cell or user groups, using multiple antennas at both the transmitter and receiver, and allowing multiple users to access simultaneously the same channel. This work focuses on DL MU-MIMO for TDD scenario, where challenges include the accurate channel knowledge at BS due to weak UE transmit power and impracticality of frequent updates, the communication with different users in a way that reduces or eliminates interference among them, as well as the complexity (both hardware and computational) originating from multiple antennas and implementation of MU-MIMO schemes.
Methodology	The approach of dimensionality reduction via “effective antennas” (EAs). The term EA, for receiver (RX) or transmitter (TX) antenna array, is defined as a set of linear combinations over RX or TX array with the purpose of transforming the actual channel into more tangible effective channel related to virtual EAs (instead of physical antennas). These “clean” from interference channels can be then the aim for the MU-MIMO DL precoder. AI/ML tools can be used together with the flexible EA approach to address computationally intensive steps within the communication procedure and optimise trade-offs between system performance and complexity/energy cost on the BS and UE sides.

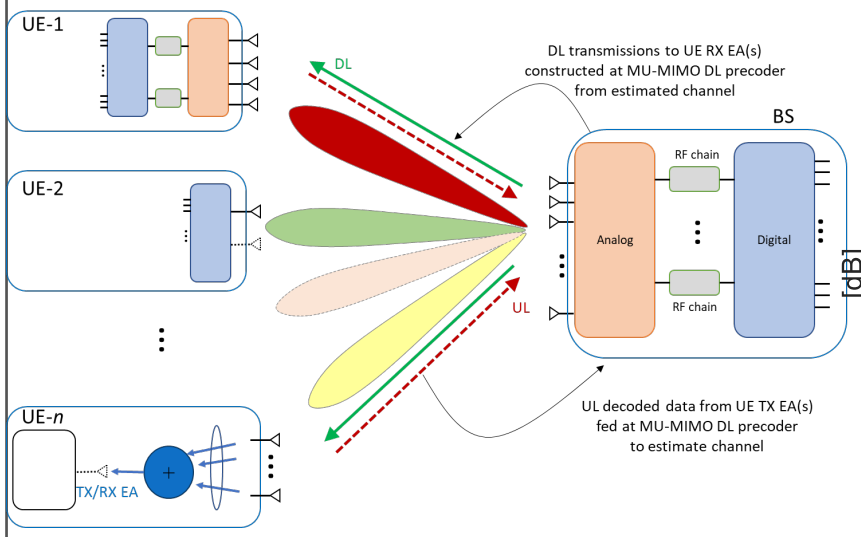

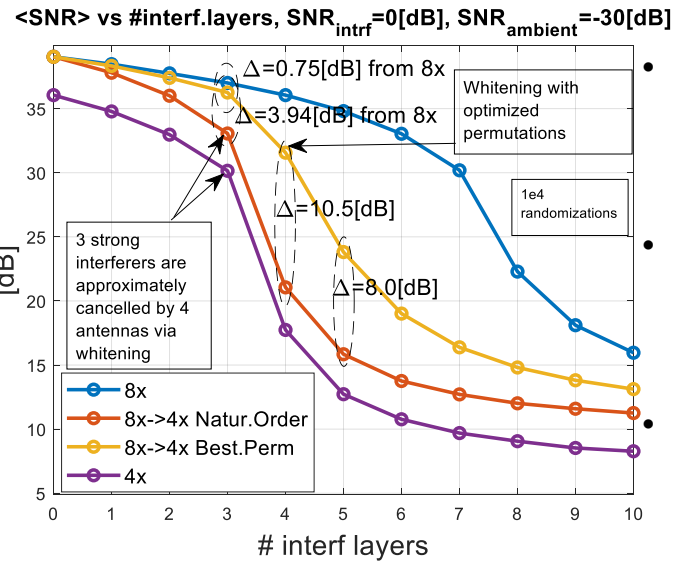

- **Results:** Preliminary numerical simulations of the interference rejection scenario have been also run to confirm the importance and potential of optimizations using the proposed approach.
- The performance comparison among different single-user MIMO (systems, with and without dimensionality reduction, shows significant gain potential from an optimized EA approach.
- AI/ML tools can help to harness fully this potential when system dimensions and computational complexity increase.

Multi-antenna location-dependent coded caching

Problem Statement	New data-intensive services like wireless extended reality (XR) applications driven by 5G and beyond demand stringent quality of service (QoS), requiring both low latency and high throughput. Coded caching (CC) has garnered attention for its superior global caching gain compared to traditional schemes, achieved through intelligent utilization of aggregate cache memory across the network. This scalability appeals particularly to multi-user collaborative scenarios like XR applications, with CC also leveraging spatial multiplexing gains from multi-antenna transmissions. However, there is a research gap in applying multi-antenna CC techniques to XR setups, especially in exploiting their location-dependent content access characteristics.
Methodology	• A location-dependent memory allocation strategy is implemented based on predicted data rates to reduce the delivery time at each location, reflecting wireless connectivity quality. • Equal memory portions are assigned to all files, necessitating a new packet generation approach to accommodate varying cache ratios. • A multicast beamforming scheme with multi-rate modulation is proposed to simultaneously leverage global caching and multiplexing gains, thereby enhancing QoS compared to existing methods.

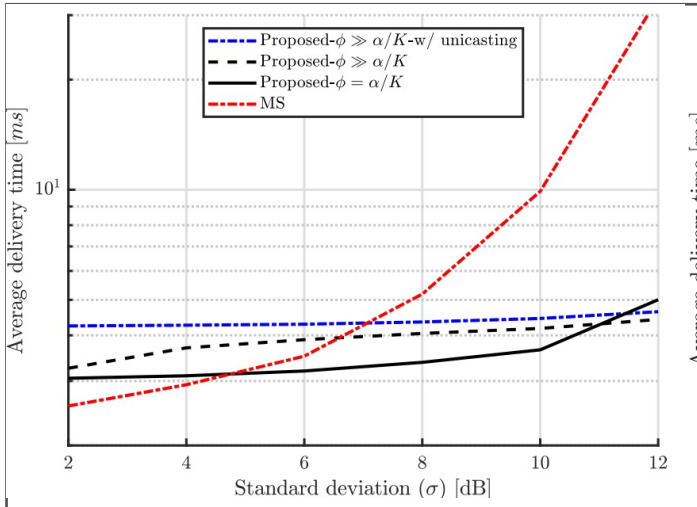

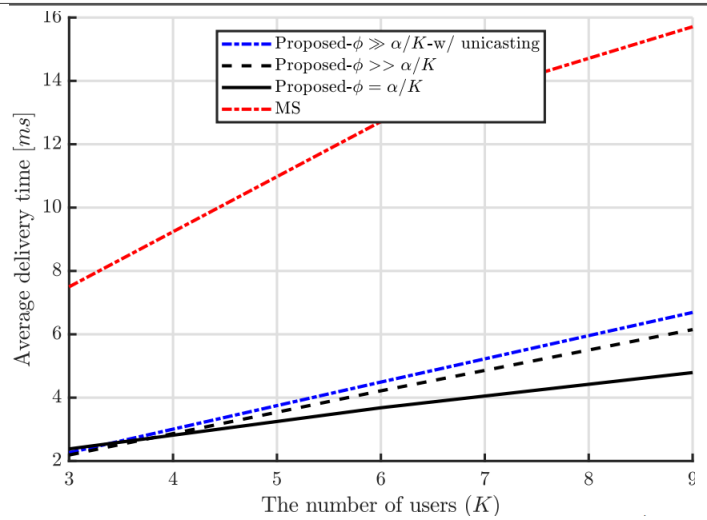

- **Results:** Considering the Rayleigh fading channel with pathloss.
- For less variation in large-scale fading among states, the traditional MS scheme outperforms other methods.
- For more attenuated states, the MS scheme performs worse than the proposed schemes.
- Considering the effect of the network size K, the delivery time generally grows with the number of users.
- The number of users served in parallel (i.e., the DoF) also increases for larger K, resulting in an overall performance improvement for all the CC-based schemes.

MIMO Transmission

RIS-assisted transmission

D-MIMO assisted with RIS

Problem Statement	In evolving 5G and future 6G networks, scalability of D-MIMO systems to large networks in a practically feasible way is challenging. Exploitation of cost-effective and energy-efficient dynamic clustering techniques, and densification enablers is crucial for such systems to sustain. RIS is well regarded as a low cost, rapidly deployable, energy-efficient candidate offering extra diversity in the spatial domain. This work explores RIS-aided multi-AP systems attaining certain prescribed KPIs, while considering the energy consumption in the system.
Methodology	• To understand how RISs can help improve current communications systems, this study compares the performance of • A system consisting of 18 APs, each equipped with 16 antennas, communicating with 18 single-antenna UEs • The same system assisted by 18 RISs, each comprising 64 reflective elements • The system with RISs but with single-antenna APs • With M_RIS=256. • For easy of simulation, it is assumed assume that the RISs are always located with LoS to both the AP and the UE they assist.

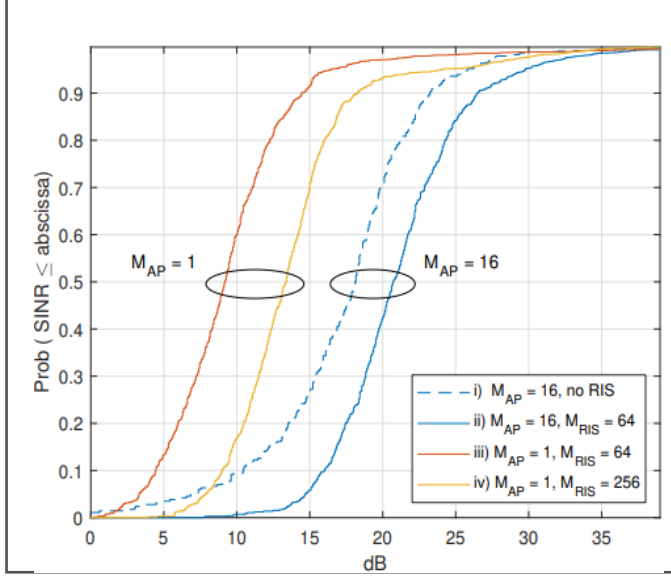

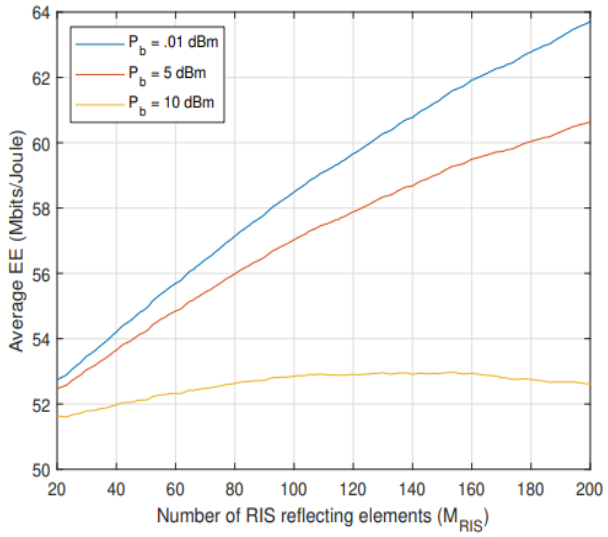

- **Results:** The CDFs of the SINR experienced by the Ues and the feasible energy efficiency (EE) gains provided by RISs.
- For the case of 16-antenna APs: RISs can improve the median SINR from 18 dB to 21 dB. More importantly, the 10-percentile SINR is improved by about 6 dB.
- The right figure shows that even with P_b power dissipation values as high as 10 dBm per reflecting element, deploying RISs holds the potential for improving the system's energy efficiency.

RIS assisted integrated access and backhaul

Problem Statement	The sub-urban IAB networks have been impacted by the tree foliage on signal propagation. The attenuation and scattering of wireless signals caused by leaves and branches can lead to a considerable performance degradation in these networks. Consequently, it is of utmost importance for network designers and operators to adopt innovative strategies, cope with such issues, especially in maintaining reliable and sufficient data rates in the backhaul links. RISs due to their unique capabilities, can be helpful in bypassing the tree foliage affected direct backhaul links. This work explores RIS-aided IAB system attaining certain prescribed KPIs, including service coverage probability.
Methodology	• The work is to optimize the network and address the tree foliage issue in IAB networks, for the sub-urban areas, focusing on the backhaul links. • A mmWave channel model is adapted, with 5G channel model (5GCM) urban macro (Uma) close in model for pathloss modelling. • Codebook-based beamforming is used due to its less complexity and better efficiency as it replaces the normal beamforming strategy with a comparatively simpler amplitude and phase-changing method.

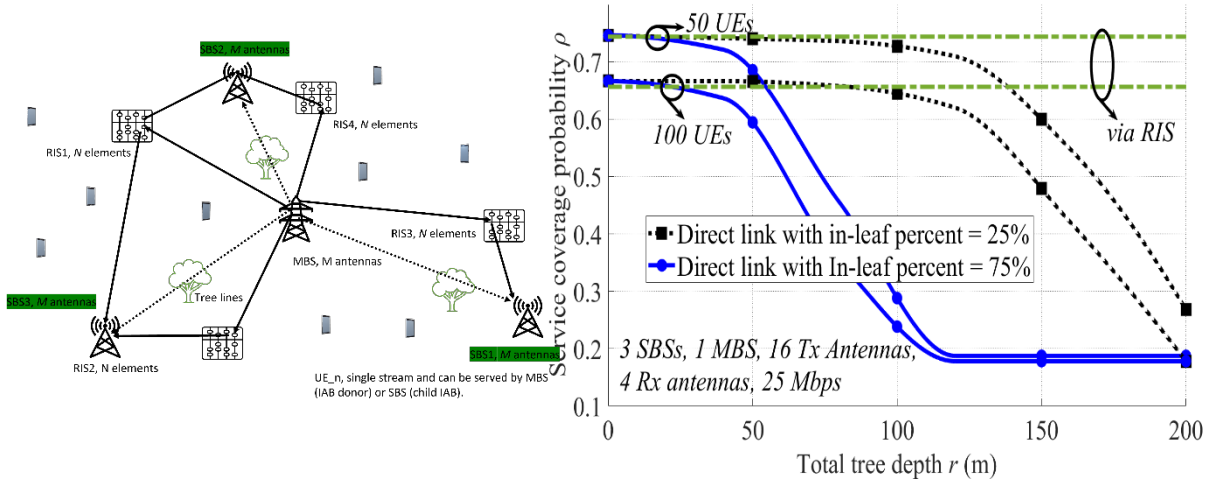

- **Results:** The figure depicts the service coverage probability as a function of tree depth r for sub-urban use case considering in-leaf percentages, i.e., the percentages of leaf cover in the trees of 25% and 75% resembling the seasonal variations.
- For small r values, the traditional IAB network is depicting similar performance to a RIS-aided network.
- As the r becomes larger, the RIS-aided network outperforms the IAB only backhauled network.

Channel estimation for RIS

Problem Statement	Considering a passive RIS, the uplink channel estimation schemes rely on the feedback received at the base station by transmitting a pilot sequence to estimate the channel. Further, a large number of reflecting elements are required at RIS to facilitate a satisfactory performance, which requires a large pilot overhead. Furthermore, the mobility of vehicles demands frequent channel estimation, thus creating an intolerable pilot overhead. This work focusses on uplink channel estimation under mobility in an RIS aided mm wave communication system. The objective of the study is to improve channel estimation accuracy while utilizing fewer pilot resources.
Methodology	• The study considers a pilot sequence corresponding to phase shifts at RIS obtained from a codebook. The received pilot symbols are used to estimate the channel parameters. • The resulting optimization problem is non-convex due to the coupling of optimization variables. Still, an approximate solution can be found using alternative optimization. • The accuracy of the solution is compromised due to power leakage caused by non-ideal angular grid. Therefore, a machine learning based approach is proposed to predict the AoAs.

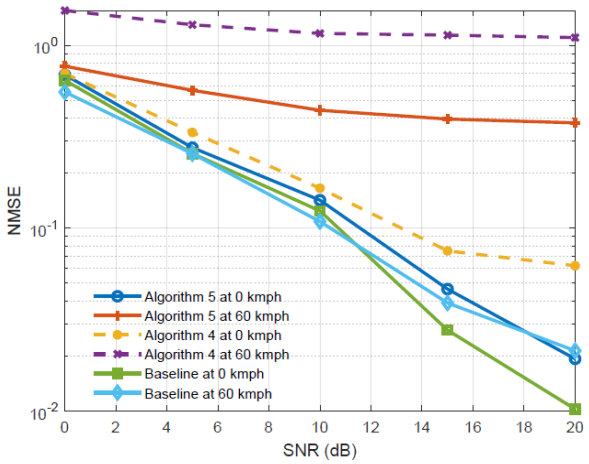

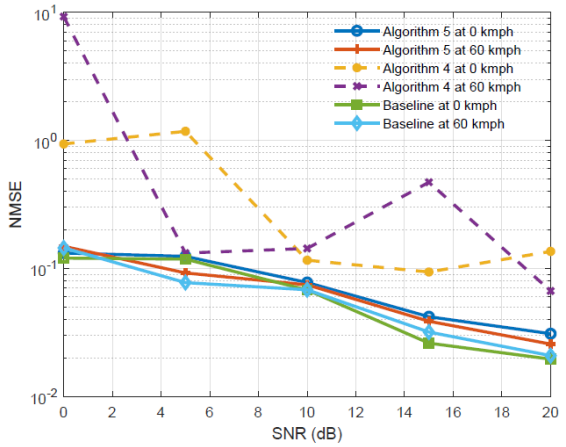

- **Results:** The results compare the NMSE of the direct and RIS channels when using different channel estimation algorithms.
- The DeepMIMO dataset is used to generate channel parameters (i.e., AoAs, AoDs and complex path gains) for a system with career frequency 28 GHz.
- The figures show the NMSE performance of the proposed machine learning-based channel estimation algorithm (denoted as Algorithm 5 in the figure) in comparison to optimisation-based algorithm (denoted as Algorithm 4 in the figure) and the baseline with known AoAs, for stationary and mobile user scenarios.
- It can be observed that the machine learning solution outperform optimisation -based algorithm in both stationary and mobile user cases.

Control procedures for non-radiative RIS

Problem Statement	There is a distinction between infrastructure RIS and personal RIS, where the latter is assumed to be located close to UEs, operate in mmWave or sub-THz spectrum and be transparent or non-transparent to the network. Given the considered target use cases of personal RIS and high frequency indoor propagation, the wireless control of RIS can be split between the UE, a local RIS controller and a remote controller of RIS whose placement is flexible. An investigation is carried out for the options of functionality split to identify the best one from the perspective of signalling overhead, latency and implementation complexity.
Methodology	• The first option is based on the exchange of control model. In this case, remote controller periodically computes a control model and provides it to the local controller. • The second option is based on the exchange of a pair of a codebook and a control model for UE. By codebook an enumerated set of RIS configurations is considered, where each configuration corresponds to a set of reflecting coefficients.

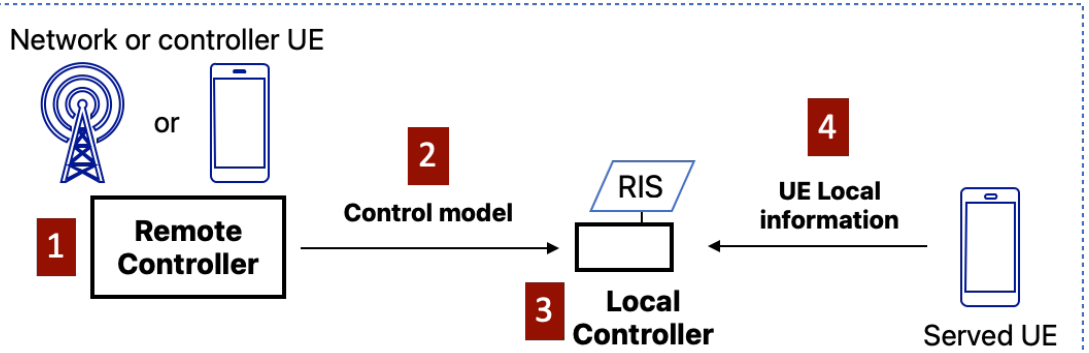

First option

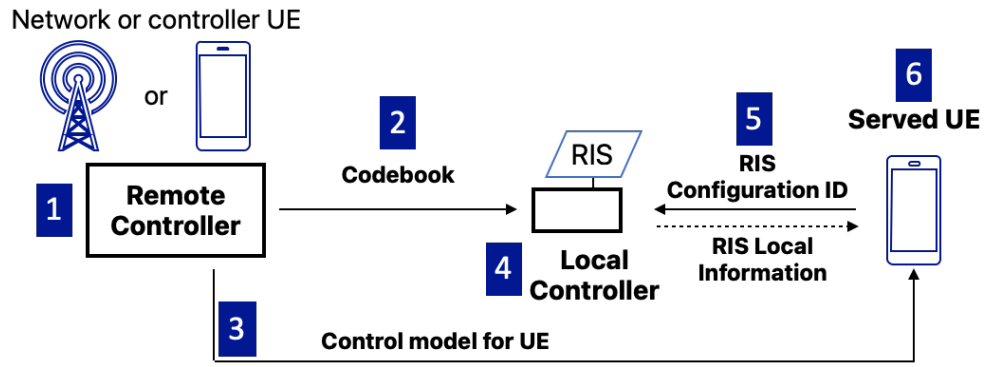

Second option

- **Results:** The following advantages compared with baseline option without control split:
- Reduced communication overhead.
- Assistance for coverage extension.
- Privacy preserving.

Learn RIS reflecting modulation

Problem Statement	RIS-based communications with reflection modulation (RM) have garnered attention in literature as the RIS does not require additional RF chains to modulate information. The aim of this work is to provide a more scalable, less restricted solution that reduces BER for the more general application Jointly mapped RM, such that the RIS reflection patterns and transmit signals are jointly incorporated for the constellation design. In cases where the AP and user equipment (UE) direct link is NLoS, JRM can effectively deliver information to the user with the aid of the RIS and the joint constellation design.
Methodology	• A single-user downlink system is studied under the full CSI assumption. The joint constellation is designed such that each constellation point comprises of a tuple of a transmit signal and a RIS reflection pattern. • The neighbouring RIS elements are grouped to have the same reflection coefficient to improve scalability and lower complexity in the design of the constellation and beamforming. • The RIS phase shifts are designed to align the phase of the effective channel, thus in jointly mapped quadrature RM, for a given reflection pattern, a group of elements are tuned to be orthogonal to the effective channel. In jointly mapped reflection pattern modulation (JRPM), a group of elements are turned off. An alternating optimization algorithm is used for the jointly active and passive beamforming design.

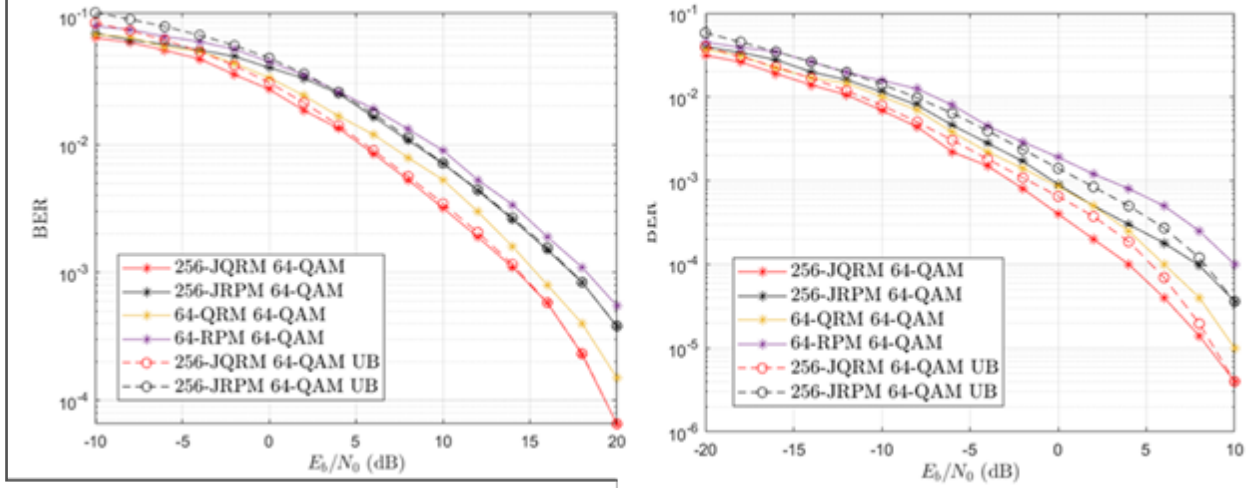

- **Results:** the BER performance of the proposed JQRM and JRPM schemes are compared with their respective theoretical upper bounds and equivalent SRM schemes, i.e., QRM and RPM, for SISO and MISO systems respectively.
- Both JQRM and JRPM shows superior BER performance compared to their separately mapped counterparts due to higher energy per bit achieved by the joint constellation design. The simulated BER of both JRPM and JQRM performs below their respective theoretical upper bounds. Overall, the QRM-based methods outperform the RPM-based methods due to the full aperture gain achieved by having all the RIS elements turned on.

Waveforms and Modulations

Summary

Waveforms and modulation schemes are important assets to meet 6G's requirements on spectral and energy efficiency. With (sub)-THz communications, the system's bandwidth will increase, affecting its power consumption and other performance metrics. Chapter 6 introduces extended and novel waveform and modulation schemes envisioning (sub-)THz communications. These include the analysis of standardized waveforms and their numerology, the design of 1-bit quantized zero crossing modulation (ZXM) and polar hardware-friendly constellations, and the proposal of an adaptive multicarrier modulation scheme resistant to Doppler shifts and out-of-ban emissions, a new matrix design for low-density parity check (LDPC) codes, and an optimized delayed bit interleaved coded modulation (DBICM).

Evolution of New Radio numerology and waveforms towards sub-THz frequencies

Problem Statement	Current 5G New Radio (5G NR) specifications do not cover operations in the sub-THz frequencies. Hence, this contribution explores 5G NR numerology, i.e., subcarrier spacing (SCS) and cyclic prefix (CP) length, and standardized waveforms, i.e., CP-OFDM and DFT-s-OFDM, to support sub-THz communications in the face of known hardware limitations.
Methodology	The adopted SCSs for sub-THz communications are 120, 240, 480, 960, 1920, and 3840 kHz, and the waveforms employed are CP-OFDM and DFT-s-OFDM. The analysis is focused on enabling Tbps rates, increasing robustness to PN, and reducing the PAPR of the waveform.

Results

- SCSs from 960 kHz to 1920 kHz can provide a good baseline for sub-THz communications supporting Tbps rates and large bandwidths and allowing the necessary enhancement to mitigate PN for both CP-OFDM and DFT-s-OFDM.
- 3840 kHz SCS provides widest contiguous bandwidth, but short CP can be a problem and, thus, a more conservative value of 1920 kHz should be first explored.
- DFT-s-OFDM can provide better coverage due to larger power amplifier output power when compared to CP-OFDM.

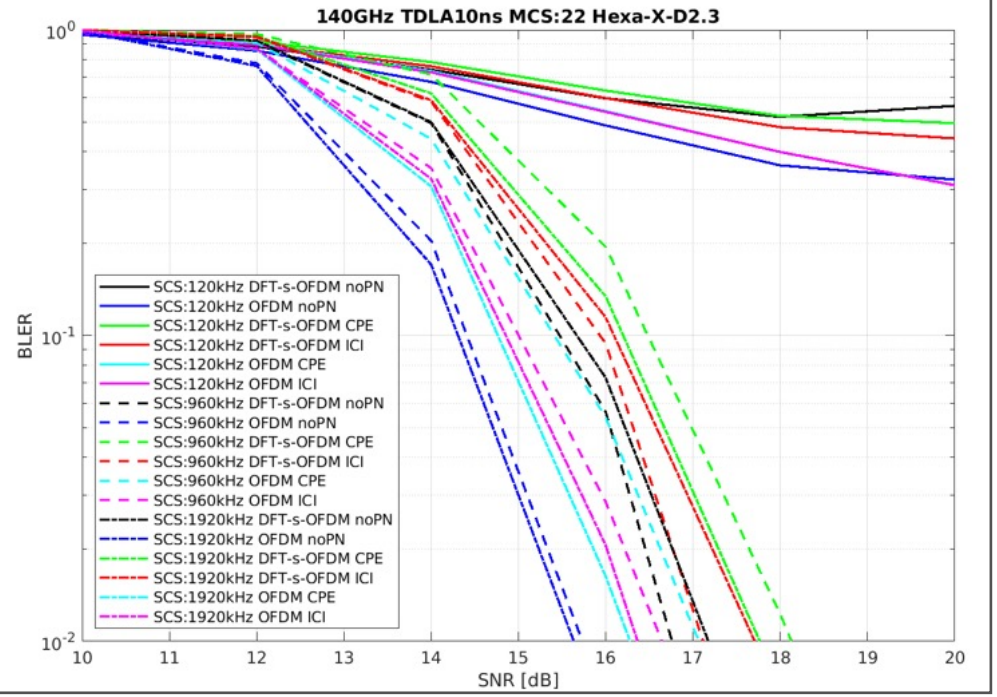

Energy-efficiency of 1-bit quantized zero crossing modulation

Problem Statement	The usage of high bandwidths at sub-THz carriers necessitates high sampling frequencies since the power consumption of ADCs increases quadratically with the signal bandwidth. Hence, by employing 1-bit ADCs will shift the information-carrying signal domain from the amplitude to the time domain. The scope is to estimate the energy efficiency of the ZXM approach in comparison to conventional M-QAM with high ADC amplitude resolution for sub-THz frequencies.
Methodology	The energy consumption of the frontend components are estimated by employing a power consumption model wherein the ADC samples at the same rate as the DAC and the ADC power consumption scales linearly with the FTN factor used in ZXM. With these models, the energy per bit is minimized over the transmit power and the bandwidth given a required data rate. The achievable spectral were evaluated analytically and through Monte-Carlo simulations for hard demapping QAM and ZMX, respectively.

Results

- The minimum energy per bit was obtained for ZXM and 64 and 256 QAM modulations with $f_c = 120\ \mathrm{GHz}$, $\mathrm{B_{max}} = 12\ \mathrm{GHz}$, $P_{\max} = 10\ \mathrm{W}$ at the transmitter antenna, distance of $d = 20\ \mathrm{m}$, antenna gain of receive and transmit antenna of $6\ dB$ and path loss exponent of $\beta = 2$.
- ZXM is significantly more energy efficient up to a rate of about 30 Gbps. Interestingly, a FTN signalling factor of $M_{\mathrm{tx}} = 2$ seems to be most efficient in the considered setting for most rates.

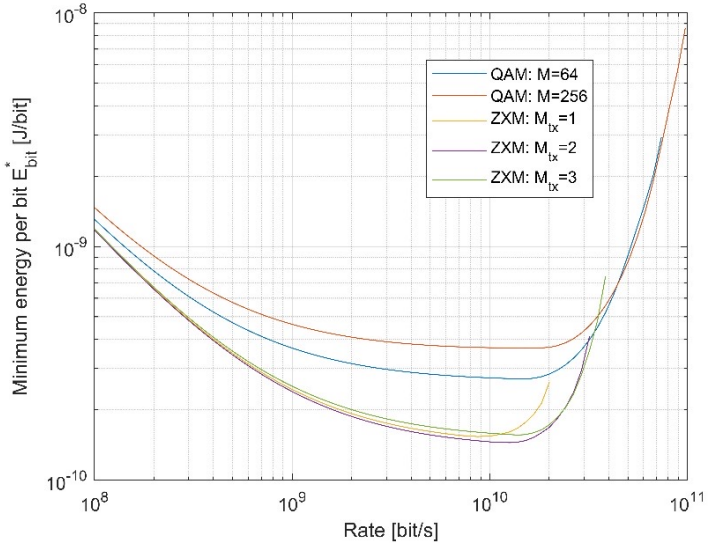

Polar constellations

Problem Statement	The polar constellations are an alternative to the classical QAM Mapping. It is especially well-adapted for FR2 bands and THz bands where the oscillators integrated on the devices are not very accurate leading consequently to a greater lack of synchronization and phase noise. The goal is to create new types of constellations robust to phase noise and Doppler shift.
Methodology	At the transmission, the polar constellations are combined to CP-OFDM, and, at the receiver side, the new demodulator will correct CPE of the polar symbols. The system's performance (BER or BLER) were evaluated in two scenarios: for AWGN channels with Doppler shift effect and 3GPP channels with Doppler shift model.

Results

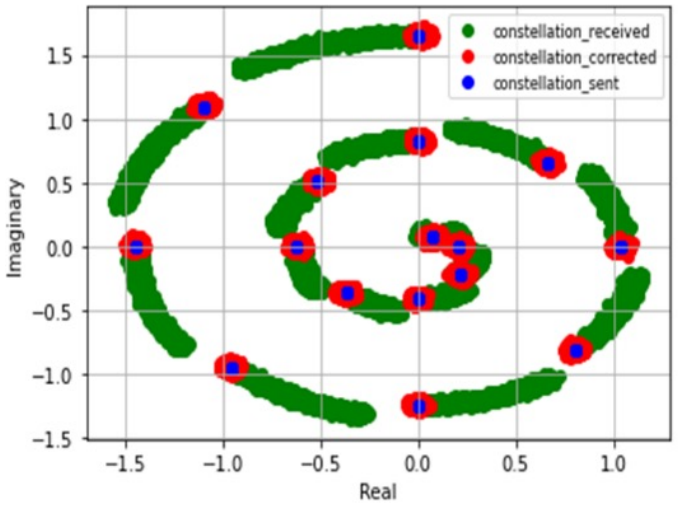

Spiral constellation at the transmitter/receiver.

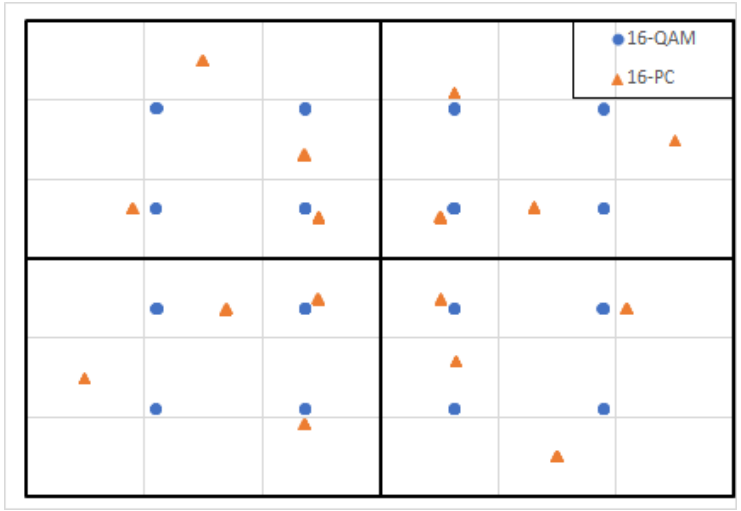

16-Polar Constellation and 16QAM at the transmitter.

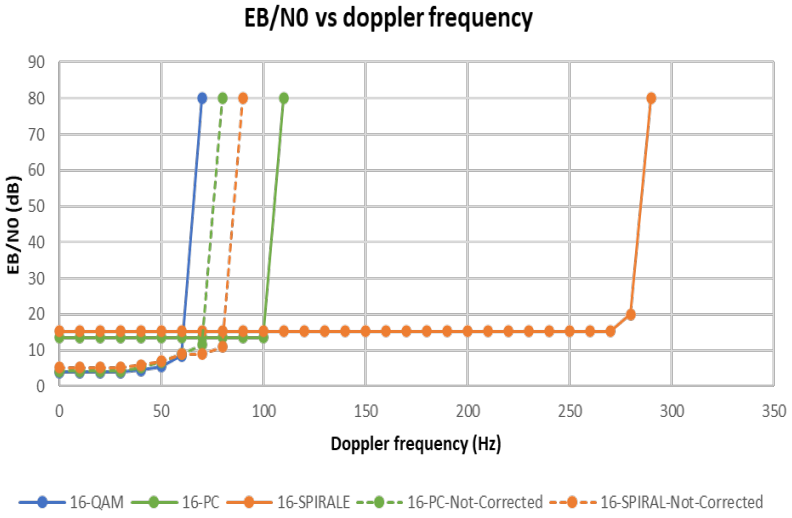

$EB/N0$ performance of 16-QAM, 16-PC, 16 spiral as function of Doppler shift at BER = 10^{-3}.

Hardware-friendly waveforms

Problem Statement	Systems employing single carrier frequency domain equalization (SC-FDE) can reduce PAPR level by selecting suitable constellation patterns and pulse shaping filter. The feasibility of these hardware-friendly waveforms needs validation through a real-world sub-THz hardware setup.
Methodology	SC-FDE waveform with standardized square constellations will be evaluated through over-the-air transmissions using an in-house demonstrator operating at 144 GHz. First results will focus on EVM analysis for different QPSK, 16 to 256 QAM modulations.

Results

- The obtained EVMs are well below the 3GPP recommend values for all modulation orders.
- The coded BER performance over a transmission of 260 symbols is as follows: 0 for QPSK, 0 for 16QAM, 3.2×10^{-7} for 64QAM and 3.5×10^{-7} for 256QAM.

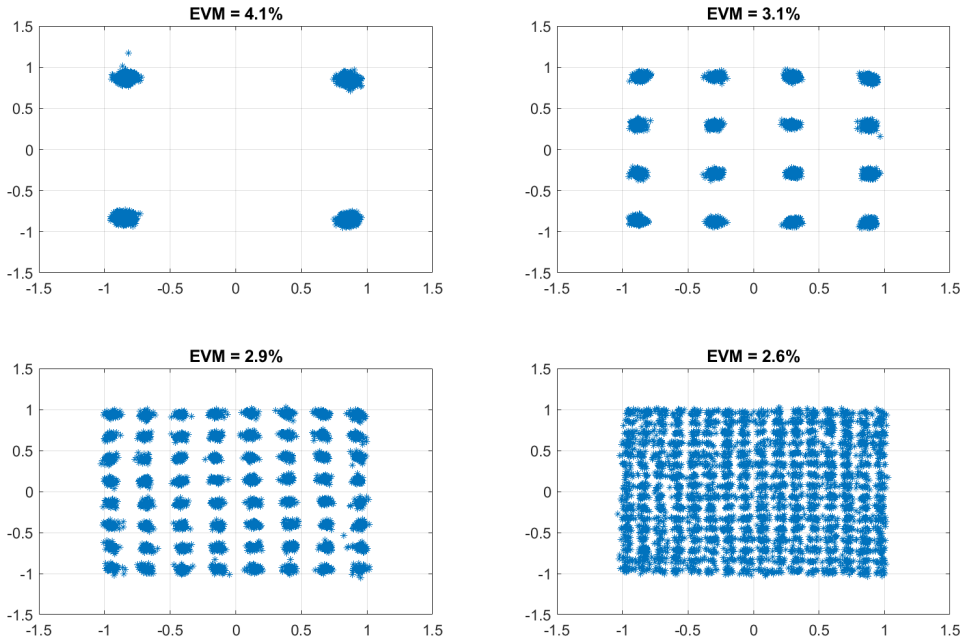

Received constellation pattern of the transmit signals in NR standard format.

Adaptative Multi-Carrier Modulation

Problem Statement	Multicarrier modulations provide robustness against multiple paths, simple equalization, and natural association with MIMO systems. However, these schemes still need improvement especially when it comes to Doppler resistance, out-of-band radiation, and PAPR. To tackle these drawbacks, a new flexible and robust multicarrier scheme is here proposed.
Methodology	As shown in the scheme below, the AMCM modulation is based on the disjoint processing of the in-phase and quadrature-phase channels of the data symbols where the IFFT is applied separately. In the frequency domain, the data processing consists of a sum between real (or imaginary) modulated symbols and the negative (or positive) value of their quadrature in delayed phase version. Then, phase rotations are applied to I and Q channels, respectively, to guarantee a quadrature between them to make exact restitution after demodulation at reception side.

Results

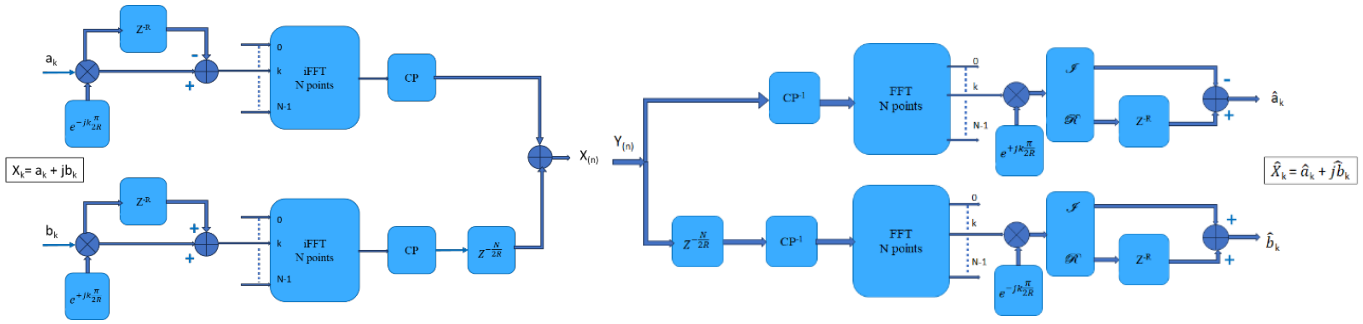

AMCM modulation and demodulation scheme

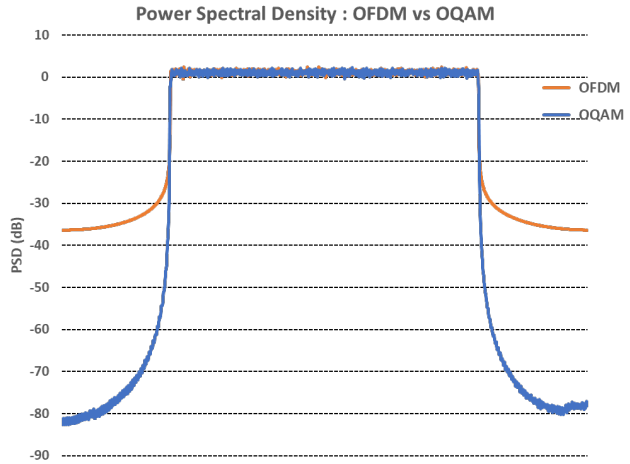

Significant out-of-band gain for AMCM when compared to CP-OFDM.

New LDPC code parity matrix design

Problem Statement	Error correcting codes are essential to the digital communication chain. LDPC codes have been selected by 3GPP for 5G due to their wide variety of size and code rate known as modulation and coding schemes (MCS). This work proposes a new parity matrix structure based on the 3GPP structure which improves the performance by reducing the number of decoding iterations and the overall system energy.
Methodology	To evaluate the gains of the new LDPC parity matrix, link simulations are performed over AWGN channel to compute the performance in terms of BLER with varying SNR.

Results

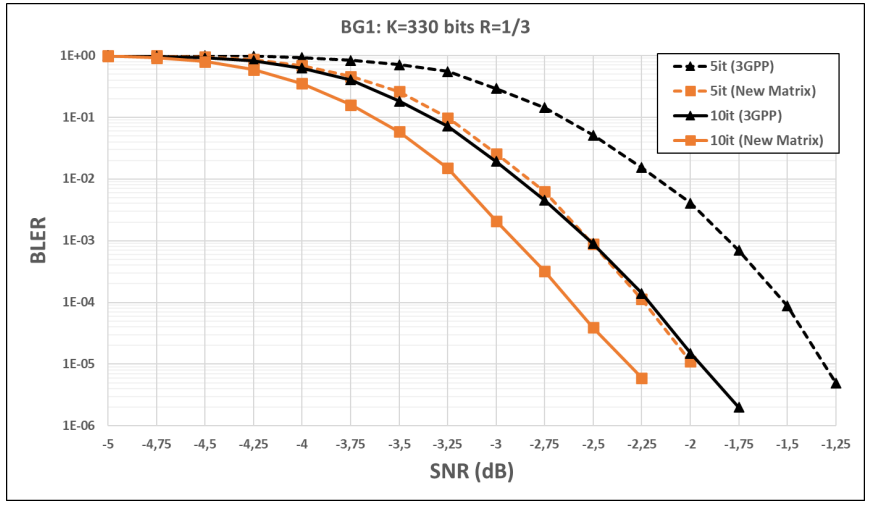

BLER Performance of the new BG1 (orange) and 3GPP (black) matrices for K=330 bits, R=1/3, and 5 and 10 iterations of decoding.

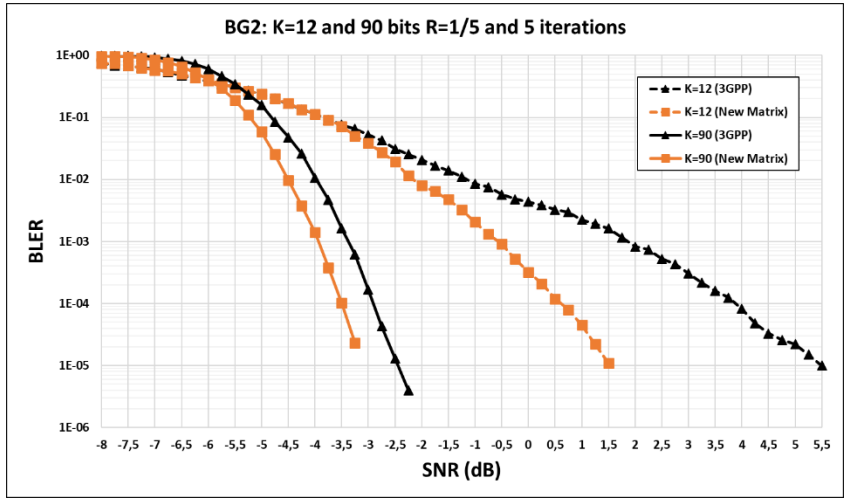

BLER Performance of the new BG2 (orange) and 3GPP (black) matrices for K=12 to 90 bits, R=1/5 for 5 iterations of decoding.

The new BG1 and BG2 matrices lead to better performance results when using 10 iterations at the decoder (gains between 0.2 dB and 1.5 dB depending on the MCS) compared to current 3GPP matrices and to the same performance when using 5 iterations with the matrices compared to 3GPP matrices with 10 iterations of decoding.

Optimised delayed bit interleaved coded modulation

Problem Statement	The aim is to optimise delay schemes for a given constellation using a low complexity algorithm compared to the conventional numerical integration method.
Methodology	A modified version of the Chernoff bound is used as a cost function to optimise delay schemes. The proposed method demonstrates strong performance only for Gray-labelled constellations, while the BICM performance on non-Gray labelled constellations is generally considered poor. Bit error rate and capacity curves are used to measure performance of the DBICM schemes. The best delay scheme has the highest capacity for a given SNR.

Results

- 64-QAM, 256-QAM, 1024-QAM and 16-APSK Gray labelled constellations are considered to initially obtain the capacity curves using numerical integration.
- The highlighted curves indicates the best delay schemes using the proposed low complexity method.
- The proposed low-complexity method can identify the best delay scheme at a given spectral efficiency with reasonable accuracy, especially at high SNR.

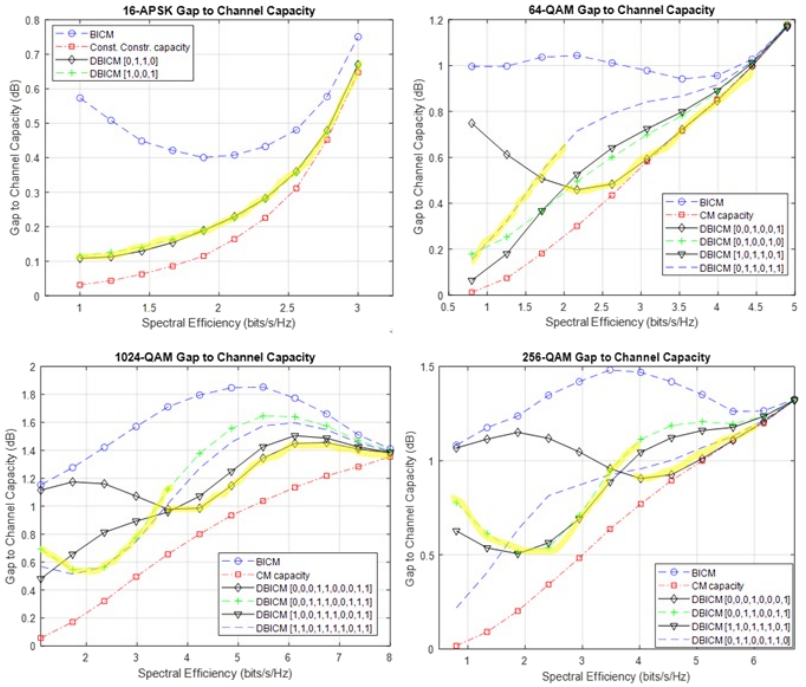

Intelligent radio air interface design

Summary

- The past few years have seen significant evolution in wireless technologies, paralleled by **machine learning breakthroughs** to meet the increasing demands for **spectral efficiency**, **reliability**, and **network flexibility**.
- This synergy is fostering the development of intelligent radio air interfaces aimed at **boosting network performance** and **adaptability** through **AI optimization**.
- The chapter explores innovative solutions that leverage AI to refine air interface design, marking a shift towards smarter, more efficient networks.
- Four areas for AI integration:
  - **Learning for Waveform, Modulation, and Coding**: Utilizing AI to enhance modulation and coding techniques, including the optimization of MIMO waveforms and error correction strategies.
  - **AI-Based CSI Acquisition**: Advancing CSI acquisition and prediction through AI, optimizing network spectral efficiency while reducing overhead.
  - **AI-Enhanced MIMO Transmissions**: Discussing AI's role in revolutionizing MIMO transmissions through advanced beamforming, antenna management, and user pairing strategies.
  - **AI solutions for HW impairments**: Highlighting AI's potential to address hardware challenges, specifically by compensating for power amplifier non-linearities.

Learning for Waveform, Modulation, and Coding

Problem Statement	Traditional modulation and coding techniques face limitations in meeting the high demands for spectral efficiency, transmission reliability, and service flexibility in future wireless systems, which can be surpassed by applying AI/ML based techniques in the design of the PHY layer
Methodology	AI/ML can be used at PHY layer for: • **MIMO Waveform Optimization** - utilizing end-to-end machine learning to train MIMO transmitters and receivers to use learned constellations for pilot-free communication • **LDPC matrix structures optimization -** for error correction • **Parametrization of beamformer and orthogonal matching pursuit (OMP)** algorithm to overcome unexpected hardware impairments that can impact **JCAS performance in estimating target position**

- The AI-optimized MIMO waveform led to a 15-20% improvement in spectral efficiency and transmission reliability at low SNR levels, demonstrating the feasibility of transmitting multiple MIMO streams successfully without pilots

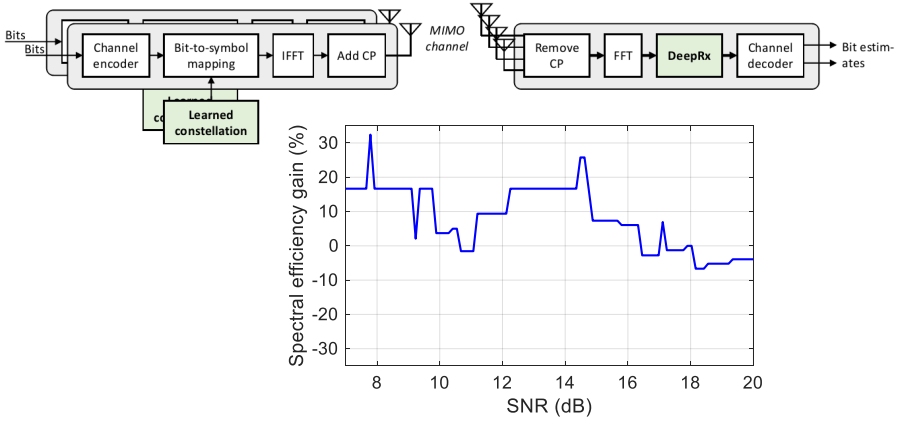

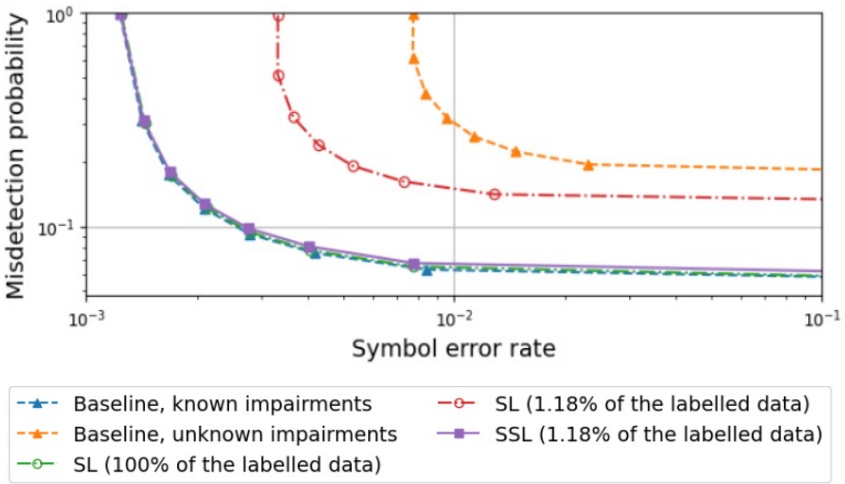

- Traditional JCAS transceiver is strongly impacted from HW impairments, which can be compensated with the proposed semi-supervised learning framework. The framework achieved similar performance to supervised learning with only 1.18% of labeled data and 98.82% of unlabeled data.
- Preliminary results from using RNNs to optimize LDPC codes indicate the potential for significant improvements in error-correcting performance within the 5G communication chain

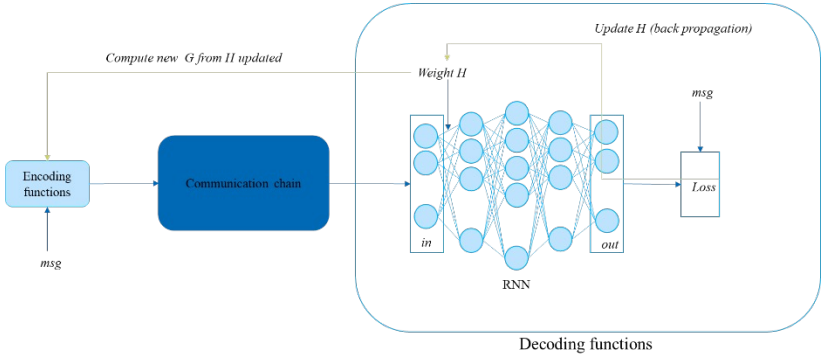

AI-Based Strategies for Enhanced CSI Acquisition

Problem Statement	As MIMO and beamforming grow more integral to system performance, the scalability challenge of CSI feedback becomes apparent, with codebook-based feedback risking accuracy for reduced overhead. There's a critical need for innovative solutions that maintain CSI feedback's accuracy without the associated overhead, especially in multi-vendor environments where interoperability and efficiency are key.
Methodology	Proposed solutions: • Demonstrate over-the-air feasibility of AI algorithms at both the device (UE) and network (gNB) levels to encode and decode CSI, respectively, leveraging shared datasets to improve model performance across different vendors. • Investigate more advanced CSI compression and precoding schemes such as the so called standardised eType2 scheme, or AI-based schemes • Developing a deep learning-based solution that allows the BS to accurately predict radio channel variations under the 3GPP CSI feedback mechanism.

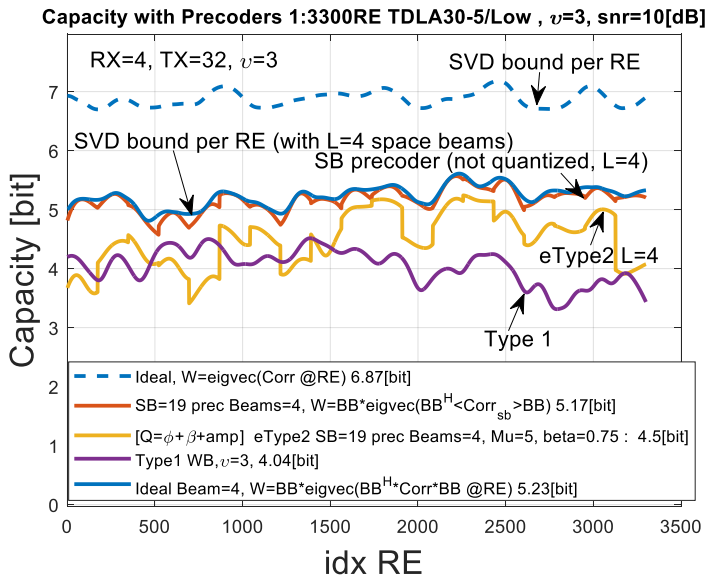

- Results shows that sequential training through dataset sharing is effective to deal with multi-vendor scenarios without disclosing the proprietary neural network (NN) architectures.
- A performance gap between 5G NR precoding scheme (Type1) and eType2 precoders is observed, confirming the advantage and importance of the latter
- Through the use of deep learning-based CSI prediction, a notable reduction in performance loss due to channel aging was observed. Specifically, the performance loss was reduced to 11% at a CSI aging of 9 slots.

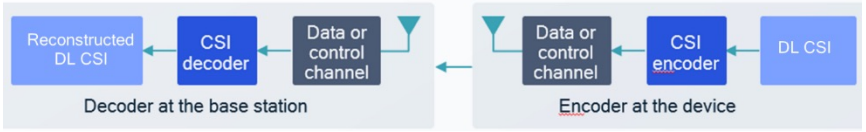

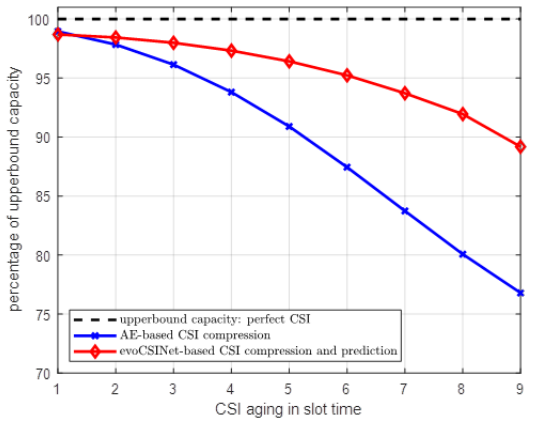

AI Enhancements in MIMO Transmissions

Problem Statement	In the realm of MU/D-MIMO transmissions, traditional techniques grapple with several issues such as: • **Imperfect CSI**: challenges arise in MU-MIMO transmissions due to performance degradation when CSI is not perfectly known at the transmitter, causing inefficiencies in beamforming, user pairing, resource allocations and pilot assignment for D-MIMO. • **Power Conservation**: in downlink MU-MIMO settings, optimizing the number of active antennas can significantly reduce power consumption while meeting user throughput requirements. These limitations underscore the necessity of leveraging AI-based solutions to address these inefficiencies.
Methodology	Proposed solutions: • **ML for beamforming** - utilizing machine learning to compute precoders based on estimated. • **Neural Antenna Muting (NAM)** - proposing a data-driven approach using a neural network to solve the transmit antenna muting optimization problem, minimizing active antennas while ensuring user QoS. • **Deep Q-Network (DQN) for User Pairing** - leveraging reinforcement learning, to optimize user pairing and scheduling based on partial CSI, modeling the problem as a Markov decision process. • **Graph Neural Network (GNN) for Pilot Assignment** - addressing pilot assignment as a coloring problem in a sparse graph, using GNN assisted reinforcement learning to reduce overhead and improve channel estimation in large-scale D-MIMO systems.

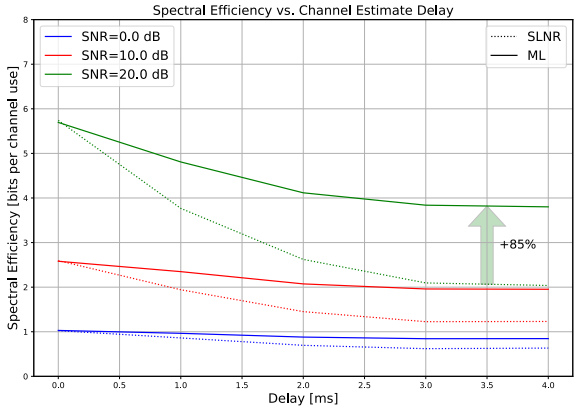

- ML beamforming is significantly more robust to channel aging than traditional solutions, showing improved spectral efficiency, especially at high SNR levels and for channel ageing exceeding ~2 ms.
- NAM approach can achieve similar spectral efficiency while reducing power consumption, demonstrating the feasibility of efficiently muting active antennas without compromising network performance.
- DQN method outperforms traditional round robin scheduling in terms of speed to empty user buffers by approximately 38% and closely matched the performance of genie-aided algorithms with full CSI knowledge.

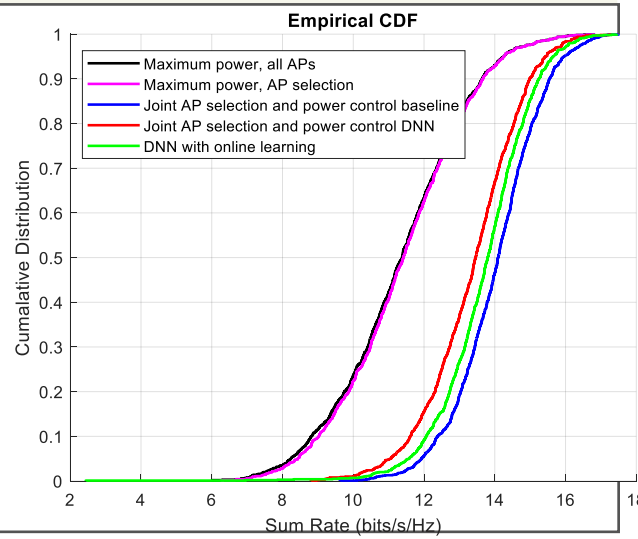

- The GNN-based method for pilot assignment in D-MIMO systems showed superior performance compared to traditional methods, ensuring more accurate channel estimation with reduced pilot overhead.

AI solutions for hardware impairments

Problem Statement	The non-linearity of power amplifiers (PAs) in wireless transceivers introduces significant in-band and out-of-band distortion, affecting system throughput, energy efficiency, and complexity. Traditional compensation methods like power back-off and digital predistortion (DPD) have limitations, such as reduced energy efficiency or increased transmitter complexity. AI-based approaches can be exploited to compensate for such non-linearities and mitigate hardware-induced distortions, leading to higher throughput and cost/energy efficient wireless communication systems.
Methodology	Proposed solution: • Adopting a receiver using Artificial Neural Networks (ANN) de-mapper to compensate for the PA non-linearity in the receiver side, when DFT-s-OFDM signal transmission is considered.

- In scenarios where the system is not power-limited, aiming for maximum operational efficiency, ANN-based de-mapper at the receiver side can lead to gains in energy efficiency ranging from 35% to 45% were observed at throughput levels of 1.6-2.0 Gbps with a class A PA model. In uplink scenarios, throughput can be improved up to 15%, both with and without standard changes in both non-power limited and power limited scenarios; UE energy efficiency can be improved 11-45% when transmitting with higher order modulations (up to 256-QAM).

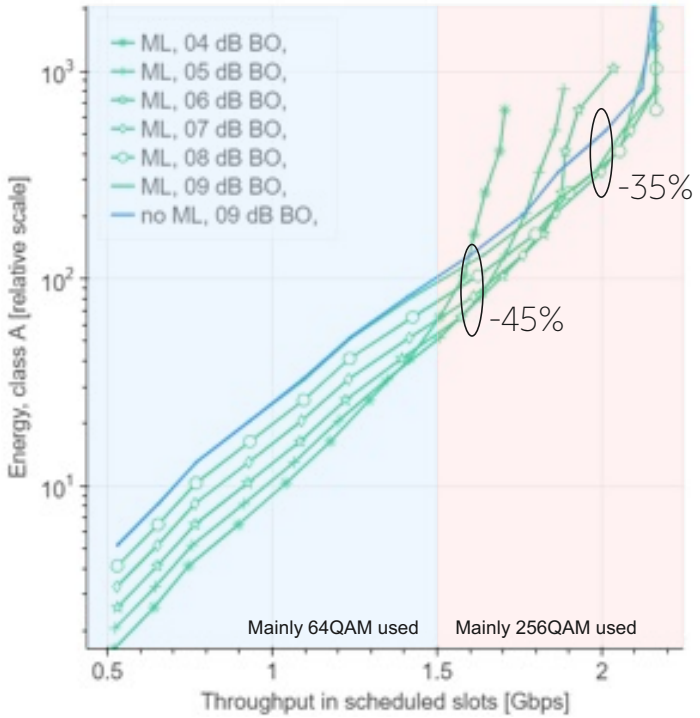

Joint Communication and Sensing

Summary

- Driven by innovative use cases like self-driving cars, unmanned aerial vehicles, indoor robotics, virtual reality, and digital twins, we are witnessing an unprecedented surge in demand for precise sensing and localization services in recent years.
- Accordingly, the International Telecommunications Union (ITU) identified joint communication and sensing (JCAS) as one of the main cornerstones for the 6th generation (6G) cellular communications
- Research on 6G JCAS involves exploration of various:
  - JCAS deployments scenarios
  - JCAS resource optimization schemes
- Deployment scenarios investigated in this chapter includes:
  - Utilization of non-terrestrial networks (NTN) and reconfigurable intelligent surfaces (RIS) for localization purposes
  - Integrated monostatic and bistatic sensing
  - Multistatic sensing
- Optimization scenarios considered encompass:
  - OFDM-based bistatic systems
  - Resource allocation of 6D (position and orientation) tracking in JCAS systems
  - Resource allocation and protocols for inter-UE JCAS systems
- Works include a spectrum of assumptions regarding 6G radio, ranging from hardware impairments to availability of diverse radio resources

Joint Communication and Sensing

JCAS Deployment Scenarios

NTN-RIS aided localization

Problem Statement	Localize the UE with the aid of NTN (single LEO satellite) and a single RIS.
Methodology	The LEO has access to a dish antenna (no beamforming) and the UE has access to an omnidirectional antenna. We compute the CRLB on delay, Doppler, and AOD estimation for various LEO azimuth and elevation angles with respect to the RIS

Results

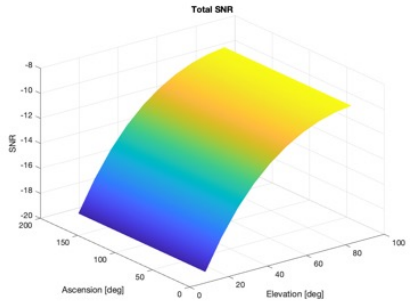

LEO-UE SNR

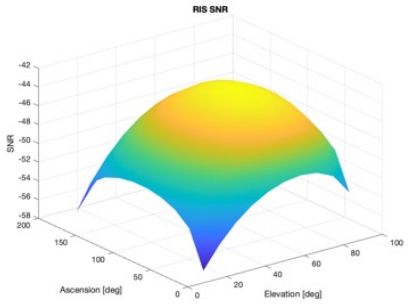

LEO-RIS-UE SNR

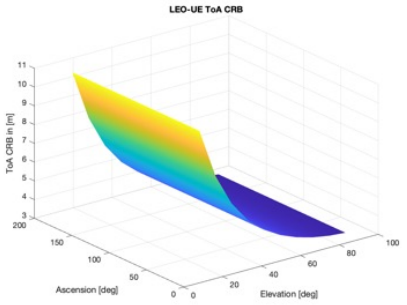

LEO-UE TOA CRLB

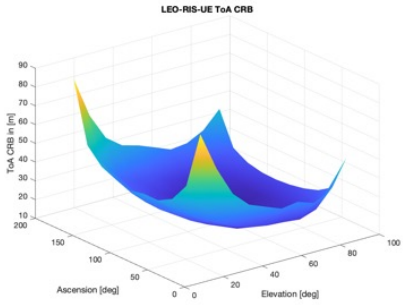

LEO-RIS-UE TOA CRLB

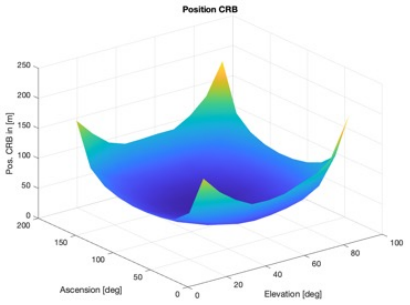

LEO-RIS-UE Position CRLB

Integrated monostatic and bistatic sensing

Problem Statement	Integrate two sensing modalities (monostatic and bistatic) to get a better sensing performance.
Methodology	The methodology includes simultaneous localization and mapping (SLAM) filter at the UE side for bistatic sensing, a mapping filter at the BS side for monostatic sensing, and a periodic fusion process at the fusion center.

Results

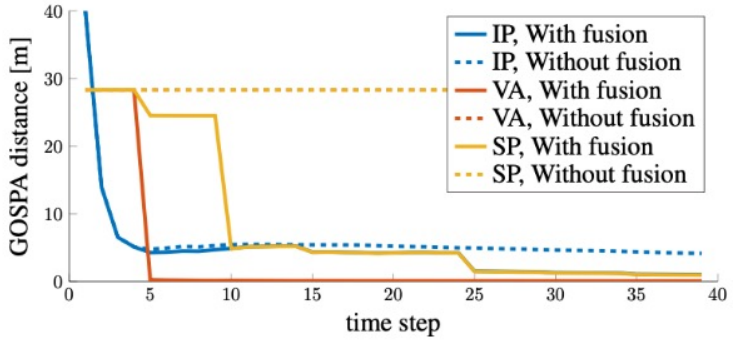

Mapping performance (monostatic)

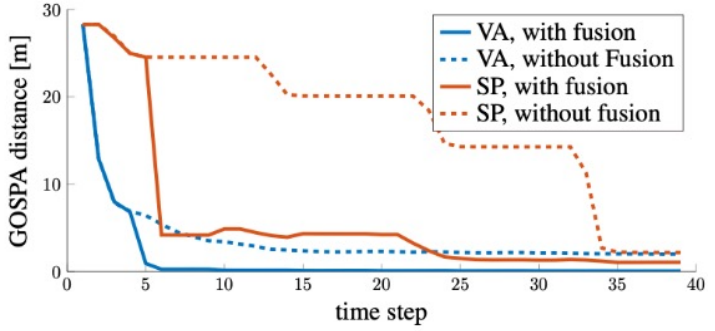

Mapping performance (bistatic)

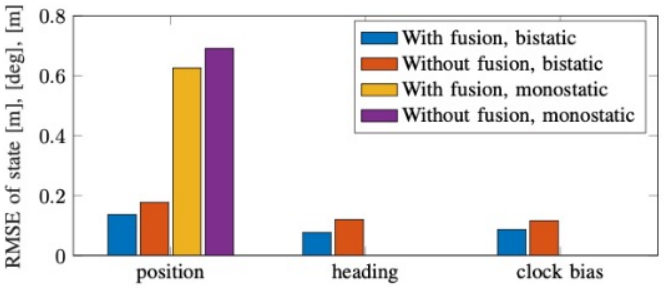

State estimation performance

Multistatic Sensing

Problem Statement	Explore the performance of multistatic sensing when it is composed by multiple bistatic sensing measurements.
Methodology	A single node transmits radar-like signal that is reflected by targets in the environment and sensed by multiple nodes. Each receiving node performs bistatic sensing and sends the measurements to a sensing processing unit for fusion and estimation of the position of targets.

Results

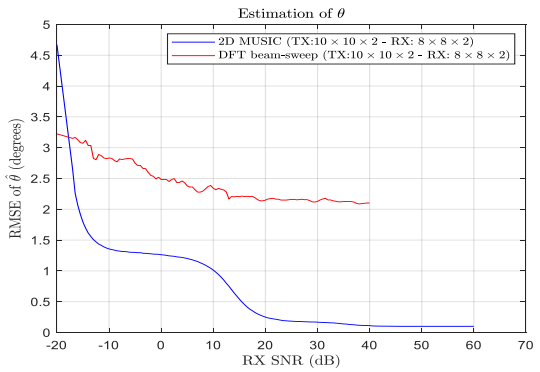

V-AOA estimation

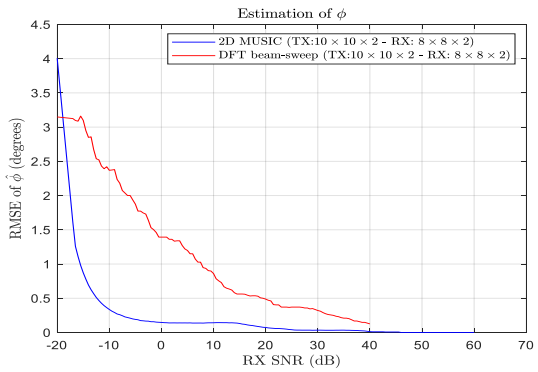

H-AOA estimation

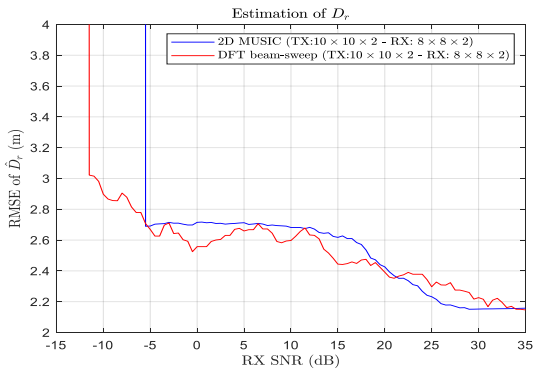

Target-receive range estimation

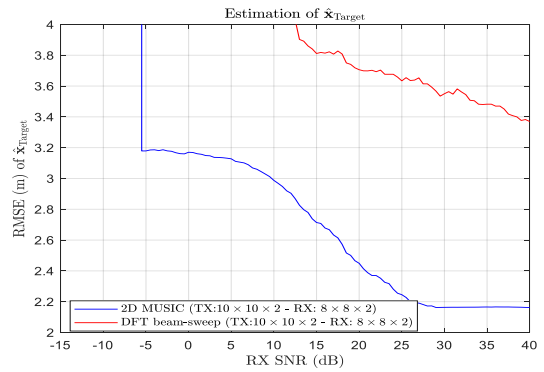

Target position estimation

Joint Communication and Sensing

JCAS Resource Optimization

Optimization of OFDM-based bistatic sensing

Problem Statement	Study the effect of OFDM cyclic prefix length on the maximum sensing distance.
Methodology	Calculate, in bistatic sensing, the maximum permitted target-to-receiver distance for a given value of CP length and given angles of arrivals of the incoming signal.

Results

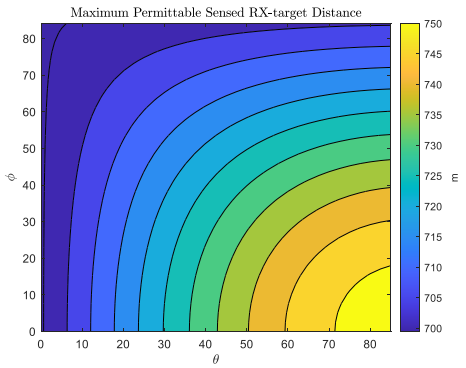

T_{CP}= 4.69 us

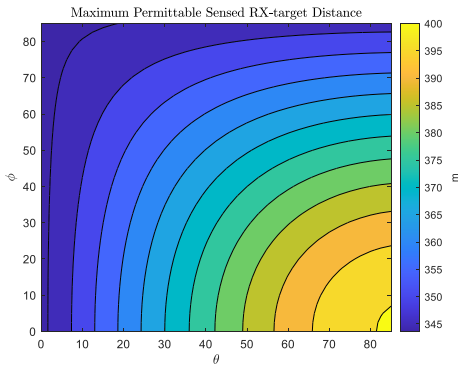

T_{CP}= 2.34 us

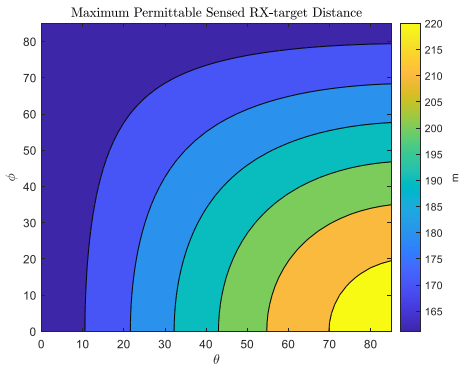

T_{CP}= 1.17 us

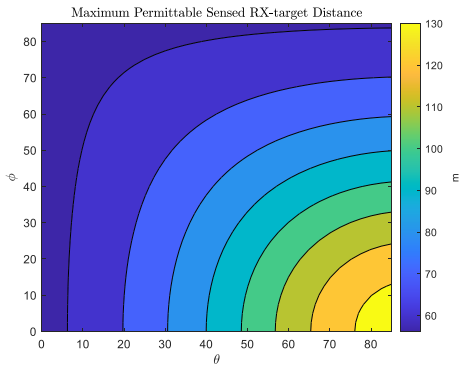

T_{CP}= 0.57 us

Resource allocation of 6D tracking scenarios

Problem Statement	Optimize the beamforming for communication and sensing purposes give 6D estimates of UE states are available.
Methodology	The 6D estimates along with their covariance matrix are already available via known localization algorithms. For UEs and RIS, only the beamformers are optimized. For the BS, both the beamforming and the resource allocation optimization problems are considered.

Results

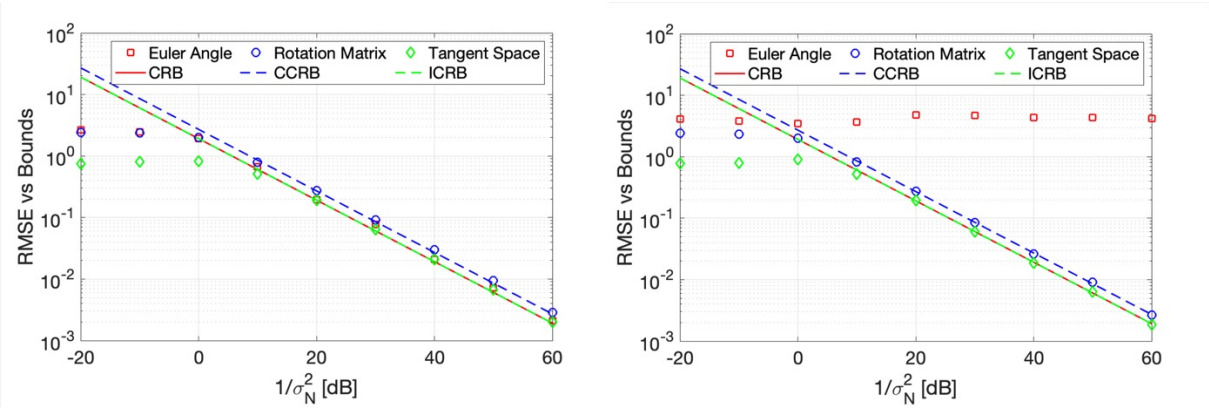

Performance vs bounds

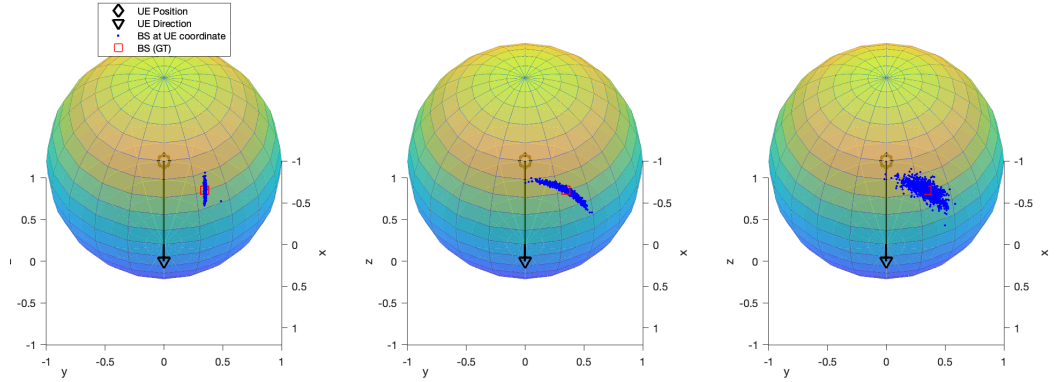

BS direction under various uncertenaties

Resource allocation and protocols for inter-UE sensing

Problem Statement	Explore resource allocation protocols to solve UE-UE sensing problems such as coordination and orchestration of air interface resources.
Methodology	Each UE is assumed to be connected via cellular technology to a central controller for sensing administration and orchestration. Sensing procedures define the waveforms and synchronization aspects as well as exchange of info such as orientation of the UEs involved.

Results

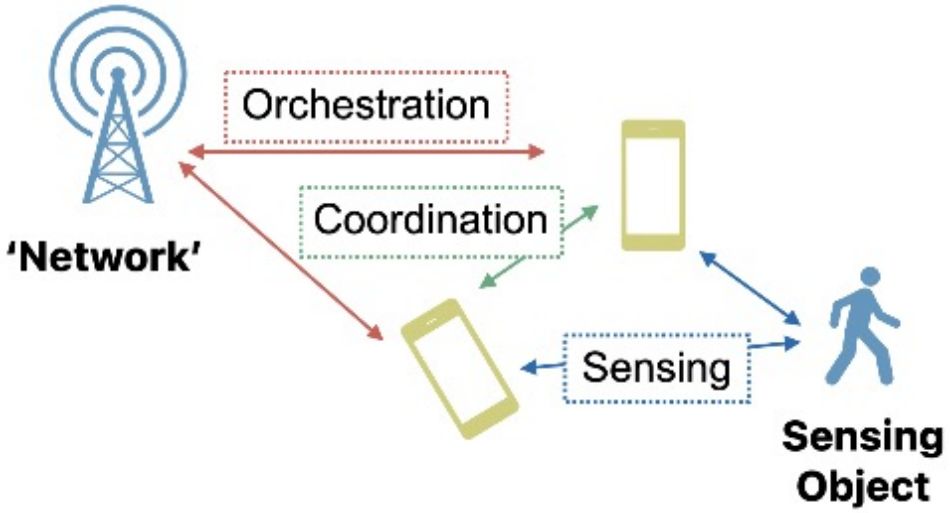

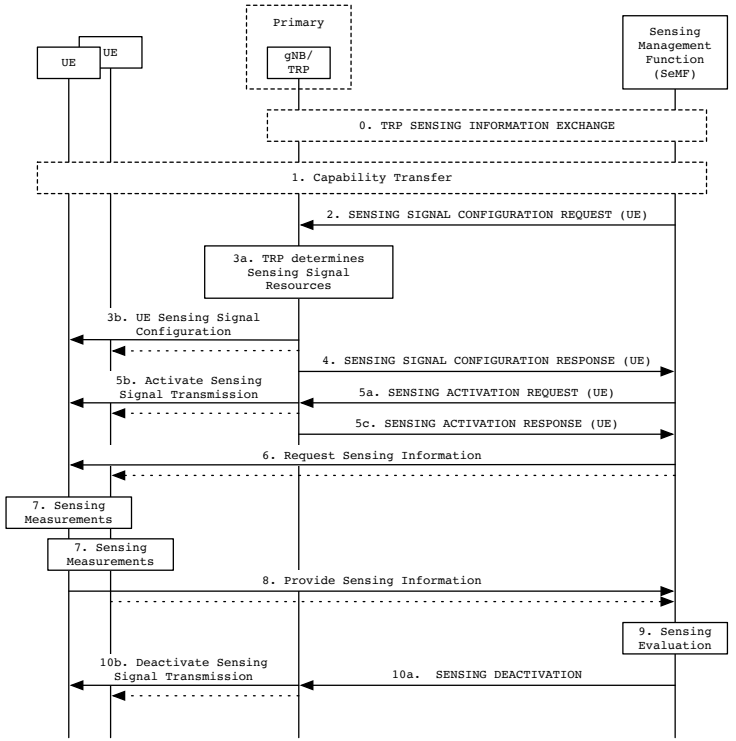

Flexible spectrum access solutions

Summary

WPO 4.5: Develop spectrum sharing and medium access mechanisms for enabling an efficient transition to 6G (coexistence) and low-latency service access

Enablers	Topics	Motivation
Spectrum sharing, coexistence	• assumptions and models to determine sharing possibilities with FSS ES • TN-NTN coexistence and spectrum sharing (S band, Ku band) • multi-RAT spectrum sharing	Spectrum is valuable and scarce. The ability to leverage spectrum that is already allocated to existing services is essential. Additional emerging non-terrestrial connectivity leads to new interference scenarios requiring further research.
Low-latency random access	• sub-THz access methods • risk-informed random access	Many services require low-latency access to spectrum for a good and reliable user experience. Sub-THz propagation characteristics as well as localised services require rethinking of spectrum access methods.
NTN enhancements	• NTN handover optimizations	A key topic for NTN is an efficient handover of users between cells given the highly dynamic environment especially in case of moving satellites.
Resource management	• interference prediction-based proactive resource management	Interference management is required to guarantee reliable low-latency services. Interference prediction can help to efficiently allocate resources.

Sustainability	*Inclusion*	*Trustworthiness*
NW- and device-side energy efficient solutions.	Fair access to spectrum for all.	Dependable access to spectral resources.

Flexible Spectrum Access: Assumptions to Determine Sharing Possibilities

Problem Statement	The assumptions and models of sharing and compatibility studies are crucial in understanding how mobile networks coexist with other radio services. The focus is on improving conditions to prevent interference between radio services, e.g., shorter separation distances between terrestrial stations operating in the same frequency band.
Methodology	Evaluation of co-channel separation distance to prevent interference from IMT base station (BS) using active antenna systems (AAS) to Fixed-Satellite Service earth stations (FSS ES). It compares factors, including refined assumptions on radiation patterns and user terminal (UE) deployments, using Monte Carlo simulations to determine separation distances.

Additional assumptions including more accurate FSS ES radiation patterns, UE deployments, and the BS activity factor are considered:

- Bessel functions provide a mathematical description of the electromagnetic fields within parabolic reflectors as used by FSS ESs
- A Rayleigh distribution for the UE ground distance from its BS is deemed more appropriate for scenarios like local networks
- It is reasonable to assume that a BS is active either 100% or 50% of the time, accounting for varying network loading factors

This analysis shows that taking into account the mentioned factors leads to a reduction in coordination distances from tens of km to just few km in some cases.

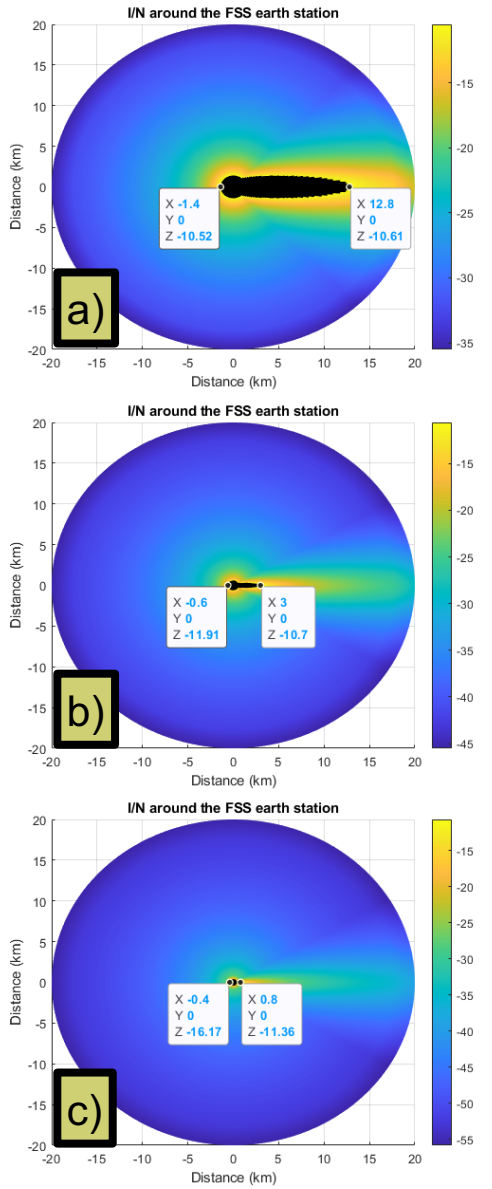

The darkened area indicates locations where the FSS ES long-term protection criterion is exceeded (I/N = -10.5dB)

a) Using conservative parameters for studies

b) Using more accurate FSS ES radiation patterns

c) Using more accurate FSS ES radiation patterns and UE deployment for certain scenarios

Flexible Spectrum Access: Spectrum Sharing with FSS Uplink

Problem Statement	Additional spectrum from the centimetric range (7-15 GHz) is identified as essential for realizing the high demanding use cases envisioned in future 6G networks. Coexistence and sharing possibilities in this frequency range focusing on spectrum sharing between 6G IMT and satellite networks, namely FSS UL, are investigated.
Methodology	*Frequency ranges:* 12.75-13.25 GHz and 14-14.5 GHz (UL for SpaceX Starlink and OneWeb) *Steps:* 1. An IMT network is created with a set of base stations (BS) in a hexagonal grid. UEs are distributed uniformly in the cell. At a given instant, each BS serves three random UEs simultaneously. 2. Multiple IMT networks are distributed randomly in the satellite footprint on the earth surface. 3. The average antenna gain from all BS to the satellite is calculated for different elevation angles. 4. An estimate of the cumulative interference to a satellite is calculated.

Sharing solutions need to address interference, specially with high BS power. IMT antennas can reduce emissions towards the sky via side lobe control mechanisms

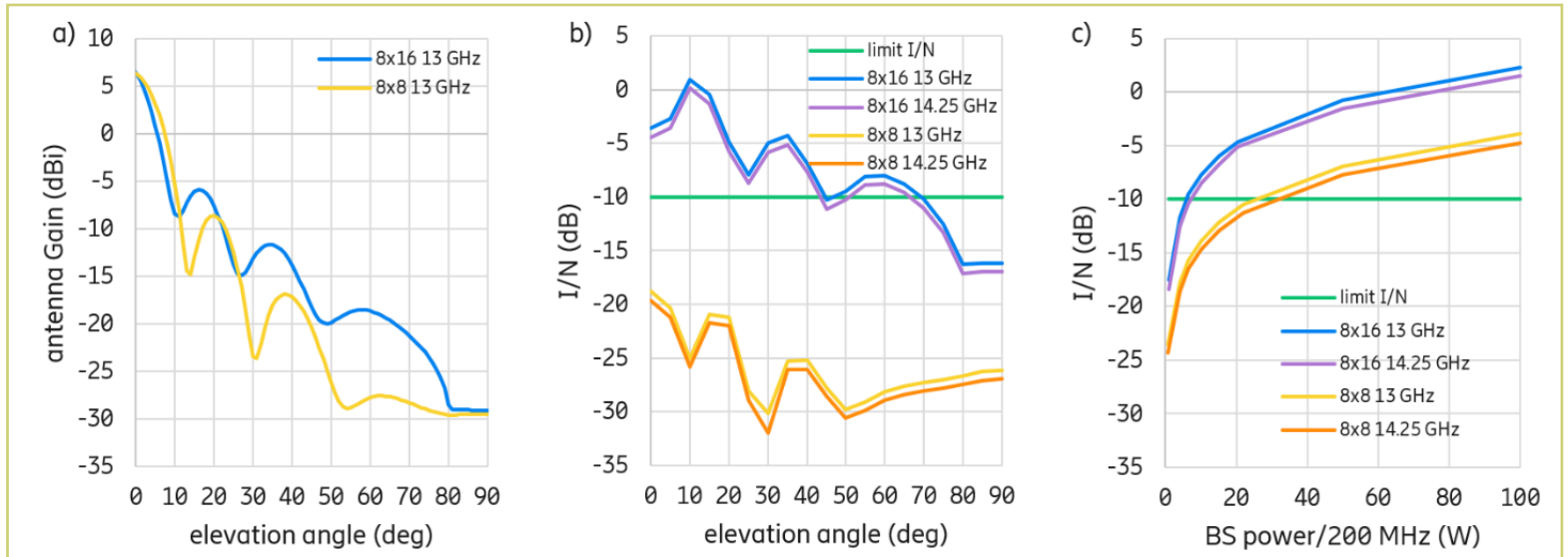

a) Antenna gain vs elevation angle generated for 13 GHz for the two sets of assumptions. The blue (8x16) and yellow (8x8) lines correspond to the ITU recommendations for 6450-10500 MHz and 24.25-33.4 GHz, respectively. b) I/N for both sets of assumptions and frequencies. The green horizontal line is the typical level for an acceptable I/N in coexistence studies. c) I/N for different BS power at 35 degrees of elevation angle.

Flexible Spectrum Access: TN-NTN Spectrum Sharing Using Stochastic Geometry

Problem Statement	Coexistence and sharing possibilities between TN and NTN may be needed in order to allow an efficient use of limited spectral resources. In this study we investigated the interference level generated by an NTN network on the uplink of a TN.
Methodology	The NTN satellite serves users outside the coverage area of the TN in the frequency range of 2 GHz. Stochastic geometry was used to derive analytical results, which were verified with simulation results.

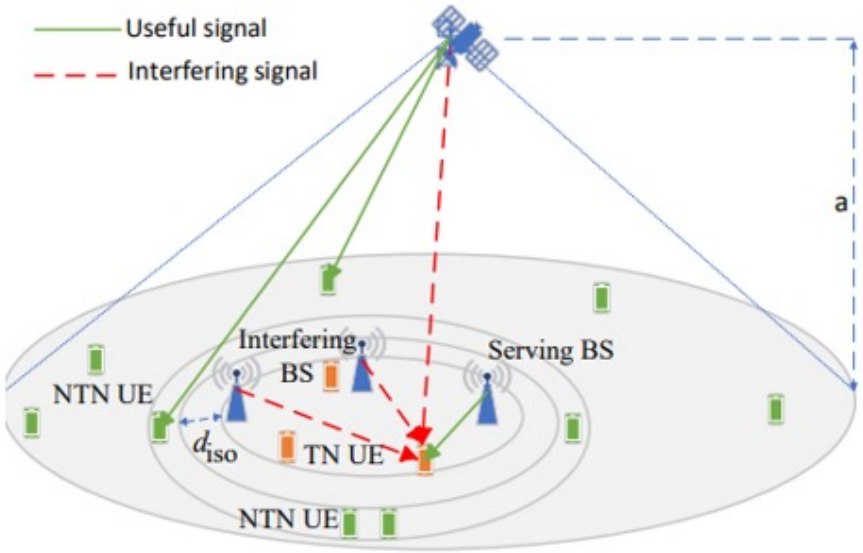

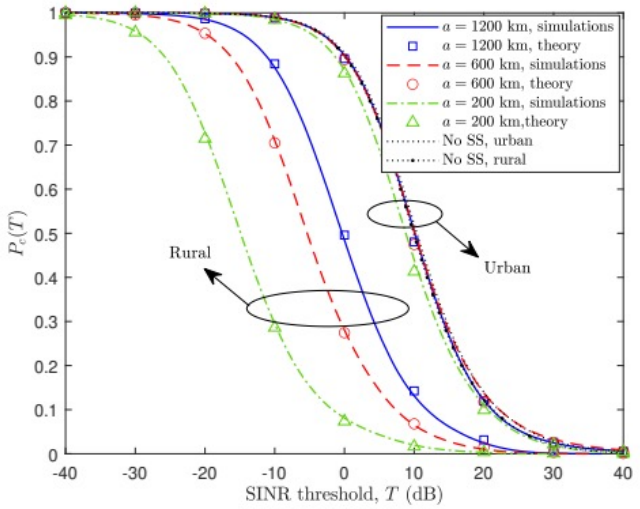

(a) 100% load.

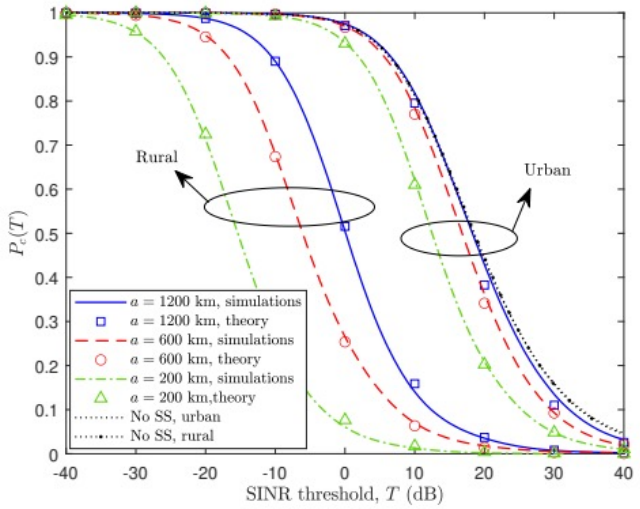

(b) 25% load.

Interference is higher for rural areas (larger distance between UEs and BSs), and lower satellite heights.

Flexible Spectrum Access: Multi-RAT Spectrum Sharing

Problem Statement	Dynamic sharing between different RAT generations (5G-NR and 6G) is required to allow a smooth transition with high spectral efficiency.
Requirements	A flexible low-overhead scheme for sharing between generations

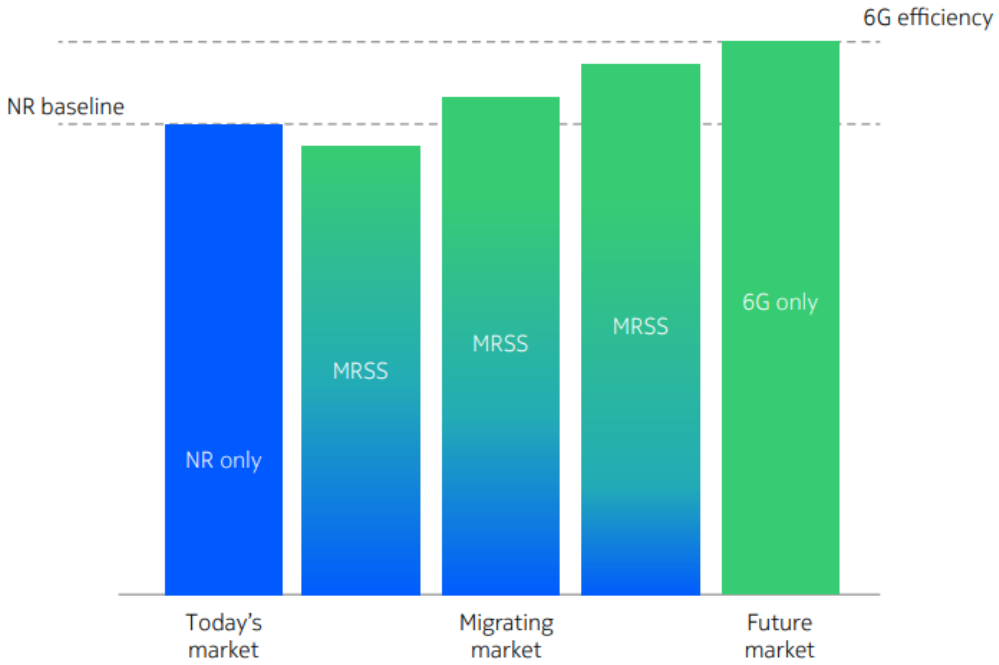

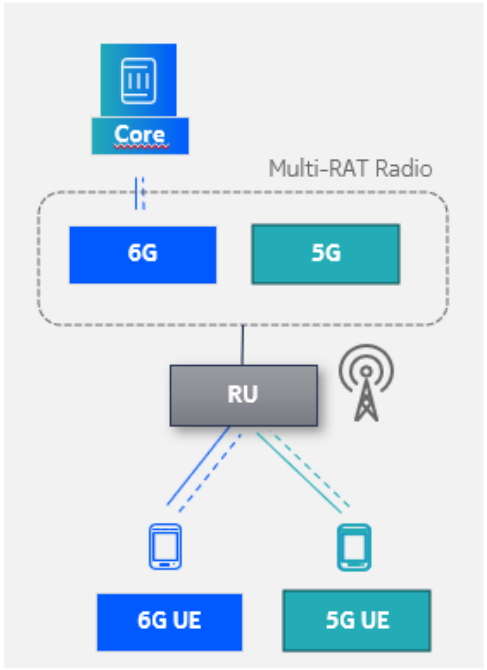

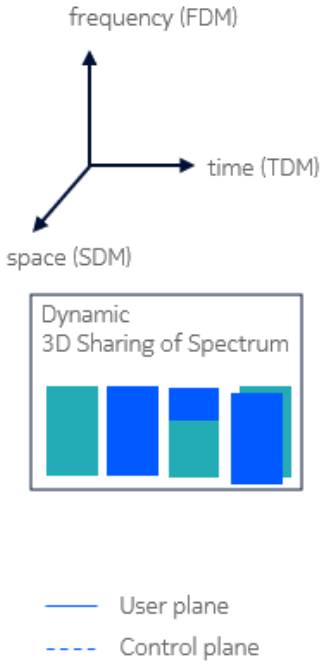

Flexible Spectrum Access: Low-Latency Spectrum Access

Problem Statement	Many services require low-latency spectrum access. Sub-THz characteristics as well as localised services require rethinking of spectrum access. Different access steps are described and tailored to sub-THz.
Methodology	A two-step spectrum access including an omni-directional anchor RAT (e.g., FR 1) and a directed low-latency high-data-rate sub-THz booster RAT is assumed.

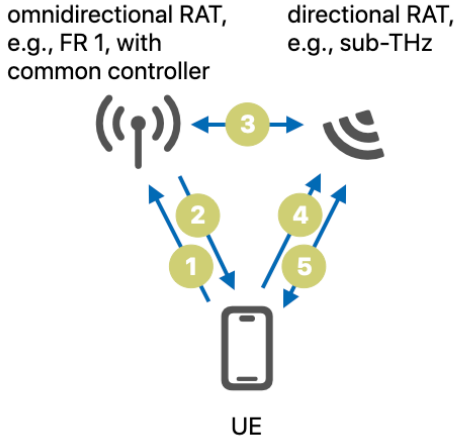

step 1: configuration via omnidirectional RAT
1. registration, capability sharing
2. directional RAT info
3. access scheme configuration

step 2: beam pairing and data transfer via directional RAT
4. directional access
5. data transfer

Pre-configuration of the directed access avoids conflicts between multiple UE and allows tailoring of sub-THz access parameters.

For 10 GHz bandwidth a data transfer latency of 100–150 µs can be achieved. The limiting factor for latency is the detection and response period.

A frequency-domain decoupling of beam pairing (within 100–500 MHz) from the data transfer period can further reduce latencies down to 20 µs. Control overhead is increased to 10–20 %. Due to the large available bandwidth this is deemed acceptable.

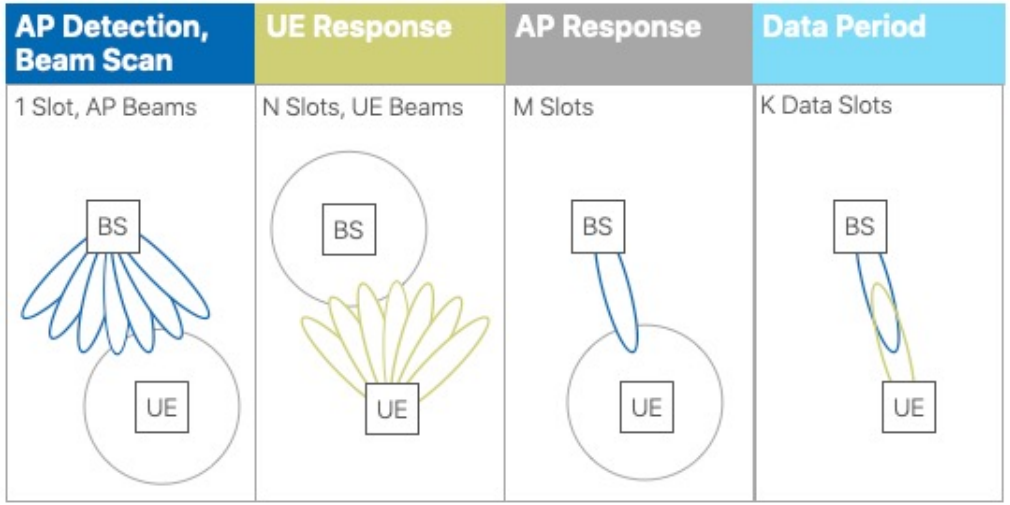

Flexible Spectrum Access: Risk-Informed Random-Access

Problem Statement	Non-coordinated risk-informed random access to localized communication can augment scheduled access, if the risk for interference is expected to be low. Interference assessment is central as it helps in understanding potential risks and their occurrences during sharing.
Methodology	**Methodology:** Aloha and CSMA based device-to-device communication for a shared frequency band is performed in a simulation environment 'Wireless InSite'. The key objective of this simulation is to understand the dynamic spectrum access with the consideration of risk-based interference management. **Initial Results:** The figure below presents comparison of mean aggregate interference and throughput against the channel load which shows that for Aloha interference and throughput do not depend on each other while there is an exponential increase in interference against the throughput for CSMA. Figure on the right presents the information about the time of maximum interference against the channel load. It can be seen from the figure that there are different reasons for both Aloha and CSMA.

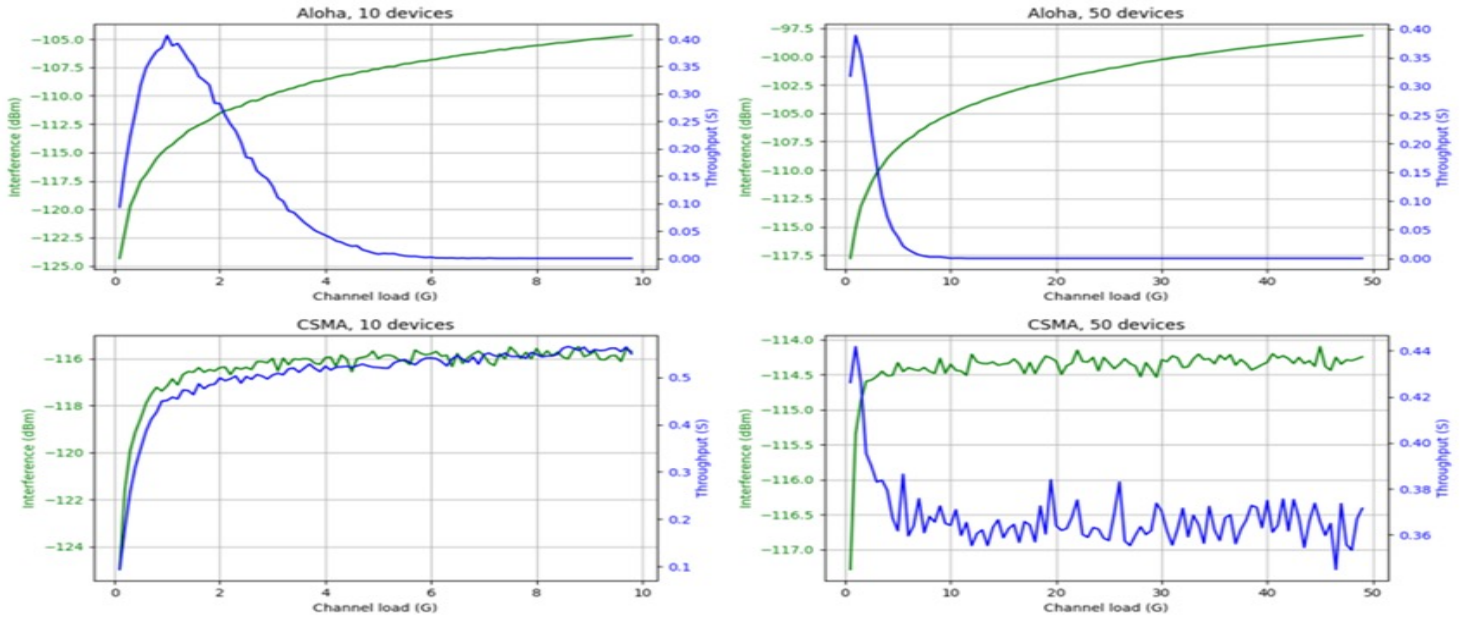

Channel load and mean aggregate interference plotted against channel load.

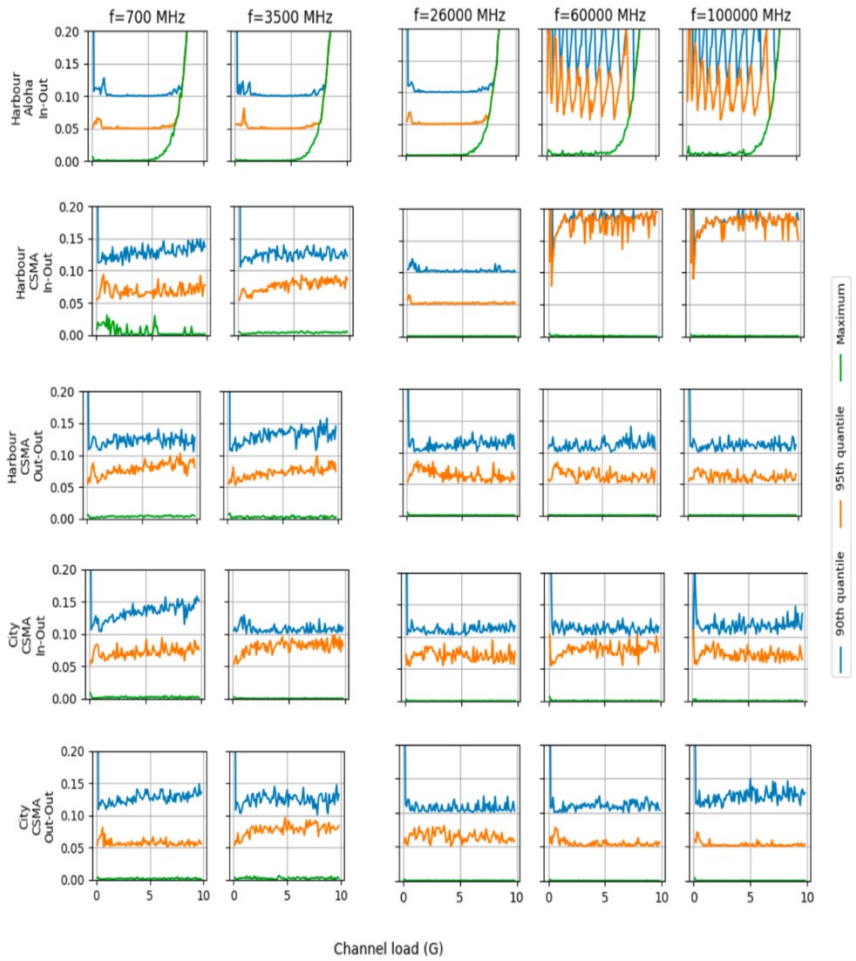

Proportion of observations exceeding indicated limits for aggregate interference

Flexible Spectrum Access: TN/NTN Enhancements

Problem Statement	A critical aspect for TN and NTN integration, and key topic for specified NTN enhancements in 3GPP Rel. 18, is the handover (HO) of users between cells. In satellite NGSO scenarios frequent HO (as perceived in legacy TN) of multiple, even stationary, UEs together will be unavoidable. This leads to significant signalling overhead, service interruption and energy consumption at device.
Methodology	The NTN-NTN HOs can be predicted to some extent and new designs are encouraged compared to legacy NT networks, e.g., group-based HO or broadcasting of required neighbor cell specific information instead dedicated signalling. In this work we investigate efficient solution designs for HO procedures <u>Deployment considerations</u>: Following main assumptions and HO concepts considered in 3GPP Rel. 17/18 work for NTN (e.g., sub-6 GHz bands, transparent payload, 3GPP power class 3 UE with navigation satellite reception capability, earth-fixed or earth-moving cell NTN configurations)

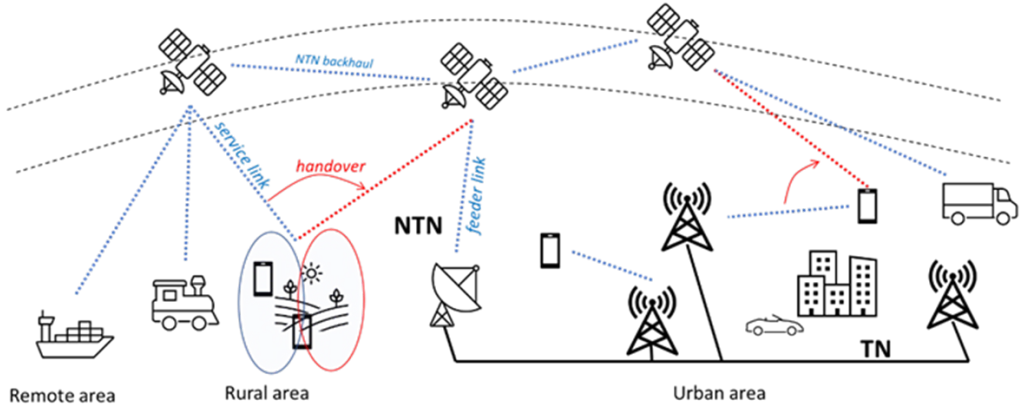

- Solution-1: *QoS-aware signalling of common information*
  - Omit HO common information in HO message for UEs with sporadic data or delay tolerant traffic
  - Legacy behaviour for other UEs, e.g., with ongoing voice calls
    - Possible to omit common information, if can get parameters from source cell other signalling during overlap time
- Solution-2: *Random time-based conditional HO*
  - UEs configured to perform time-based CHO at a random time during the overlapping time period broadcasted by network
  - Addresses dense signalling when many UEs concurrently need to perform RACH for HO execution
- Solution-3: *Satellite switching with "PCI change only"*
  - Avoids HO procedure altogether
  - Addressed shortcomings of current specified "PCI unchanged" solution
  - For low complexity UEs that cannot support DAPS feature

Flexible Spectrum Access: Interference Prediction-Based Resource Management

Problem Statement	Efficient management of inter-cell interference is a major challenges in wireless networks. It is even more important for guaranteeing the stringent reliability and latency requirement of URLLC. Solutions that can predict the interference conditions and allocate resources proactively are found to be more effective.
Methodology	This work investigates efficient yet accurate interference prediction based on decomposing the interference signal using the Empirical Mode Decomposition algorithm The interference signal is decomposed into N+1 components, each of which are predicted independently This results in more accurate prediction compared to predicting the interference signal as a whole

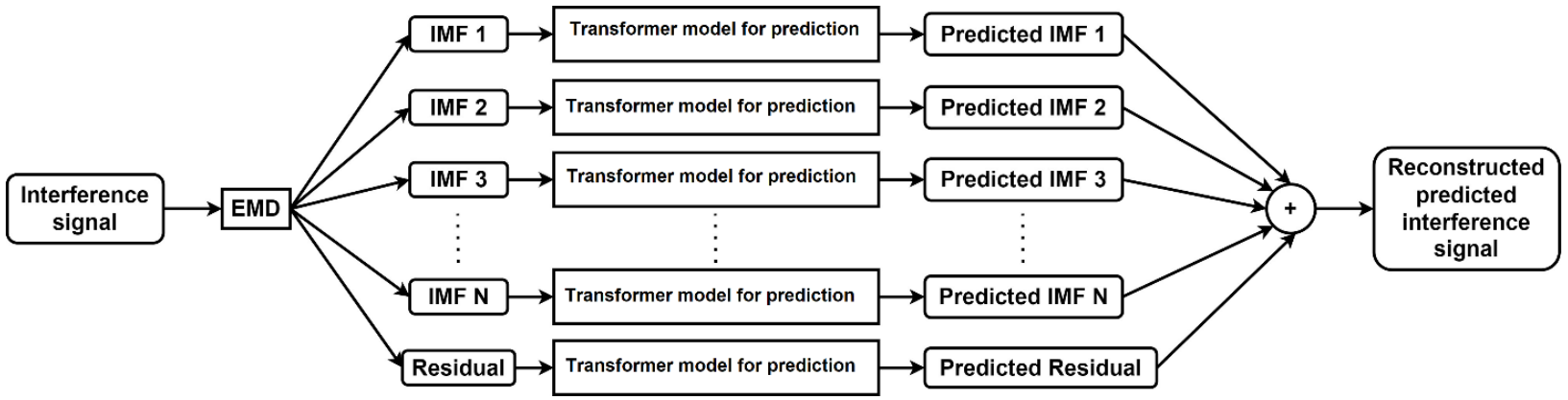

Algorithm	RMSE of conventional method	RMSE of proposed method
Transformers	0.77	0.54
LSTM	1.53	1.71
ARIMA	1.00	0.57

Trustworthiness

Summary

- Trustworthiness is one the three core values targeted by Hexa-X-II. Different aspects of a trustworthy 6G radio design are explored in Chapter 10. These include, physical layer based solutions exploiting the physical properties of the wireless channel and device hardware to ensure security against eavesdropping attack in a device to device communications scenario; investigating methods to assess the impact of jamming against and localize a jammer; and analysing the security and privacy analysis of a general cellular JCAS system, including the UE related aspects.

Secret key generation for D2D communication

Problem Statement	Physical layer security (PLS) based secret key generation (SKG) is a promising approach that can be used in hybrid crypto-PLS systems to achieve confidentiality at the physical layer. SKG uses the reciprocity and randomness of the wireless channel as a source of entropy using which shared secret keys can be generated. This work implements SKG in the presence of passive eavesdropping attack for device to device (D2D) communication systems.
Methodology	Three universal software radio pheripherals (USRPs) are used as legitimate users and an eavesdropper at multiple locations. The property of spatial decorrelation at the eavesdroppers is investigated with the eavesdroppers being very close to the legitimate users. The information leaked during the process is measured and compressed to obtain secret keys and the secret key rates are measured for dynamic channel conditions for both line of sight (LoS) and non line of sight (NLoS) channels.

Results

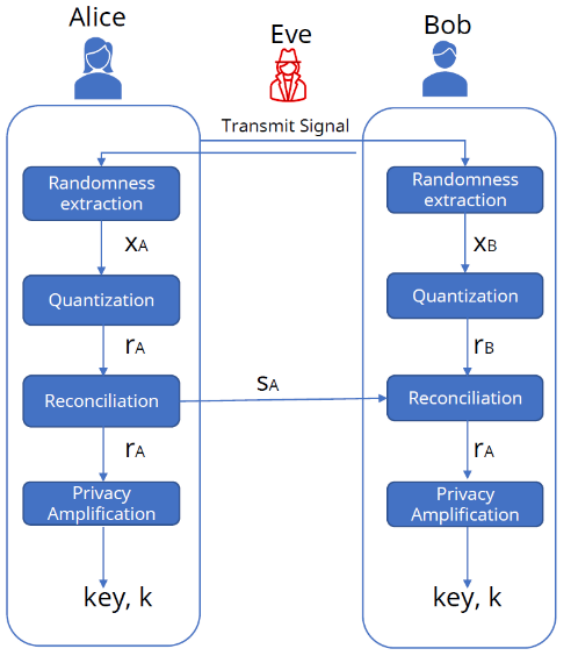

SKG protocol with Alice Bob and Eve

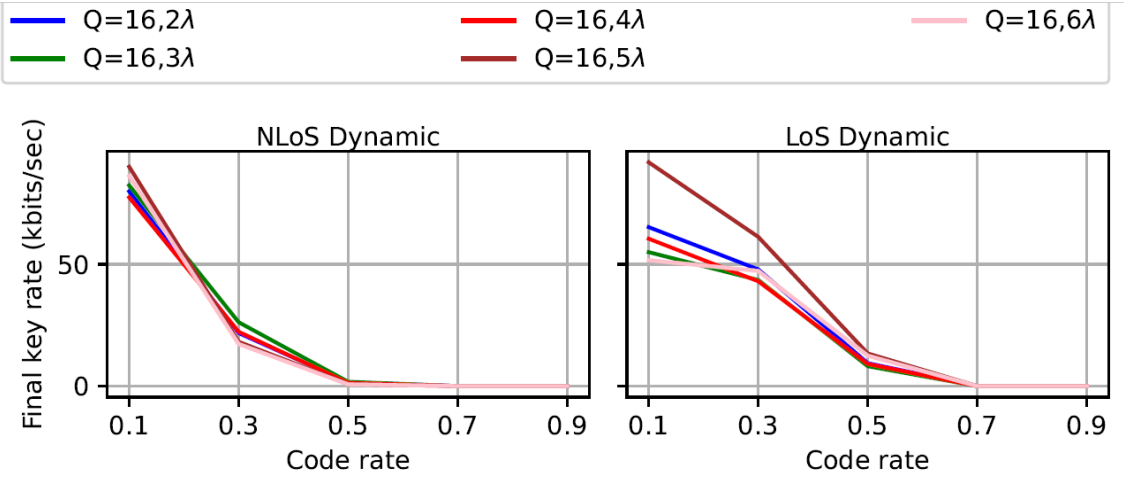

SKG rates achieved for K=16, Q=16 at different positions of Eve

Impact of jamming as a foundation towards

Problem Statement	With the envisioned support of critical use cases and the broader availability of software defined radio (SDR) devices, jamming is becoming a relevant threat for modern wireless communications. To develop effective reaction mechanism to the jamming attacks, jamming models and their impact on the communications performance have to be evaluated.
Methodology	For the initial analysis a general single-input single-output (SISO) orthogonal frequency division multiplexing (OFDM) system in an additive white Gaussian noise (AWGN) channel with fixed signal-to-noise ratio (SNR) is considered. We have selected five different types of jamming signals. Through adjustment of the jamming-to-signal ratio (JSR), the impact of the jamming signals on the SISO-OFDM transmission is captured at a bit error rate (BER) simulation of the aforementioned prototype system.

Results

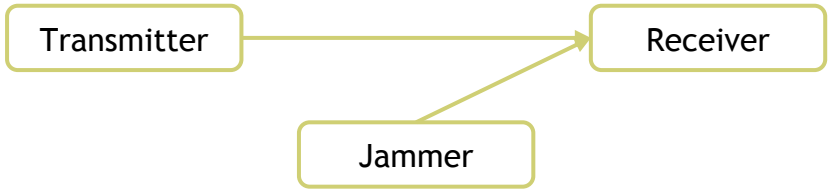

Considered jamming patterns

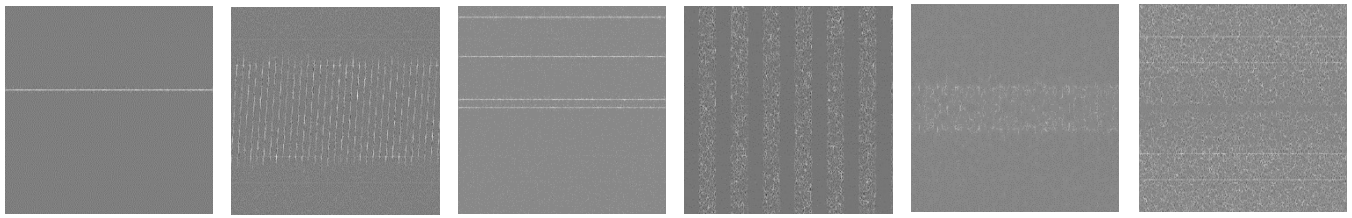

Single Tone | Chirp | Multi Tone | Pulse Noise | Narrowband | Unjammed

BER of a jammed OFDM system (SNR = 10 dB)

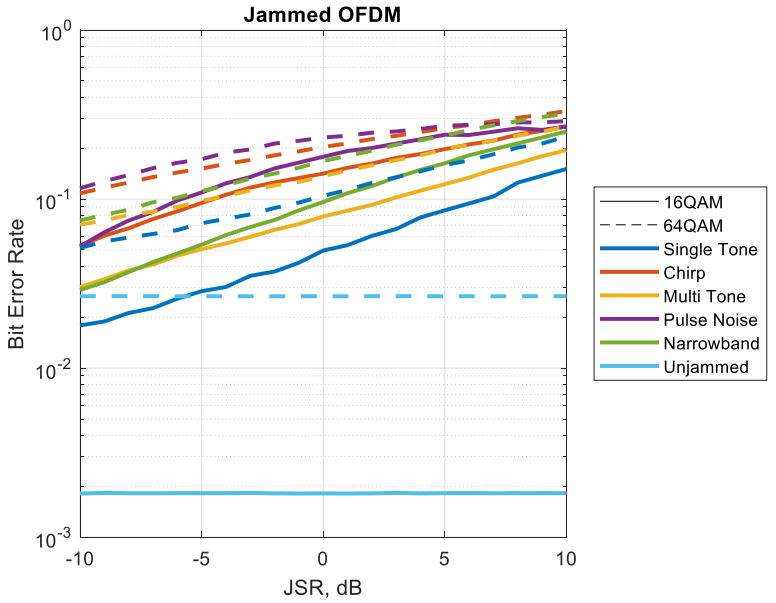

Indoor jammer localisation

Problem Statement	Determining the location of a blind transmitter or jammer without using any prior information about its location or the environment. The jammer will transmit various waveforms, not aimed at compliance but aimed at disrupting communication. The question is whether we can accurately locate the jammer by only the received signal strength.
Methodology	We have six sensing units (SUs) and one transmitter Tx1 with known positions. We assume we have a jammer with an unknown location Tx2. RSSI is measured at the SUs assuming that we are receiving power from Tx1. A log-normal path-loss model is used to obtain the respective distances between SUs and Tx1. Considering the distances and the present Gaussian noise we can identify and estimate the presence and location of Tx1. RSSI distance estimation apart from others is affected by the presence of a jammer too, thus we can use this. We conduct simulations on Dilution of Precision (DoP) to optimize the geometric placement of the SUs, aiming to minimize the Tx1 position estimation error.

Results

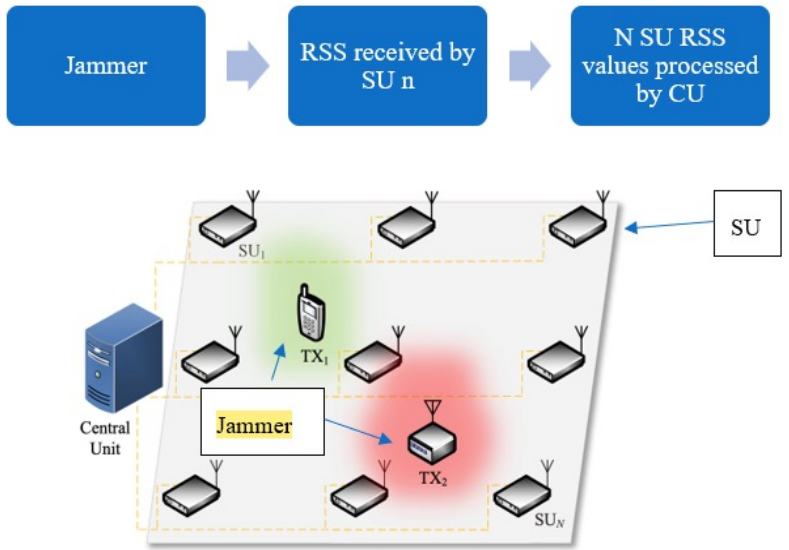

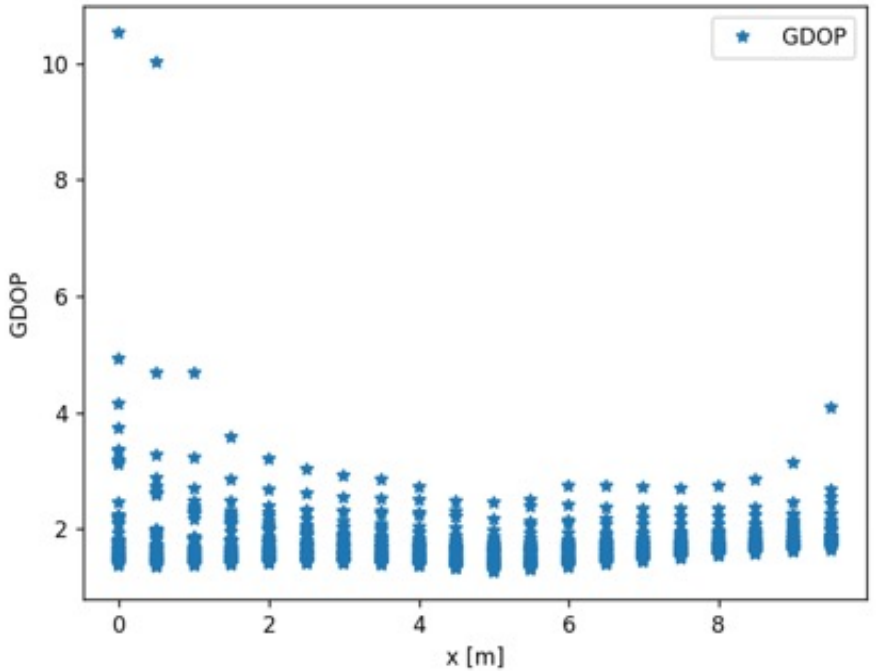

Security and privacy analysis of a general cellular JCAS system

Problem Statement	Due to the sensitive nature of the information produced from a sensing procedure of JCAS system and the way that it can be used, the aspects of privacy and security are very important. Thus, new privacy and security requirement, beyond the existing ones connected to communication, need to be introduced to the future communication networks that support JCAS.
Methodology	This study considers a general cellular JCAS system and uses the Spoofing, Tampering, Repudiation, Information disclosure (breach or leak), Denial of service, and Elevation of privilege (STRIDE) framework and the known Linking, Identifying, Non-repudiation, Detecting, Data Disclosure, Unawareness, and Non-compliance) LINDDUN framework in order to identify it possible security and privacy threads.

Results

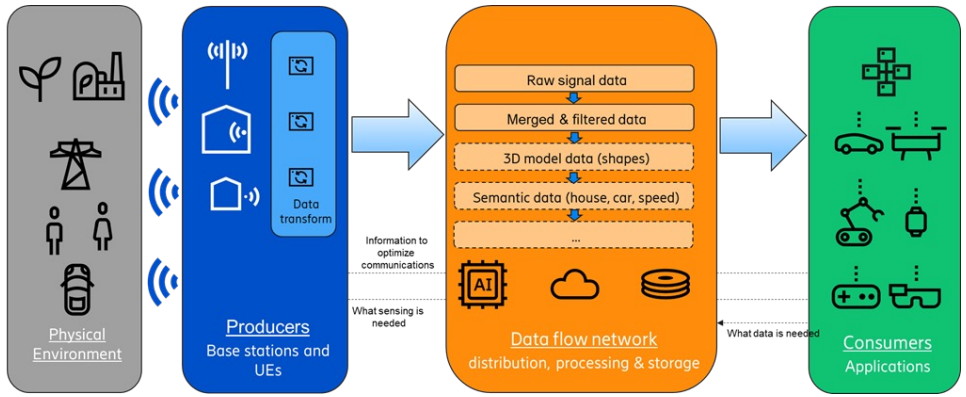

Abstract architecture of a cellular JCAS system.

- Security Risks (STRIDE):
  - **Spoofing** (synchronization attacks, raw data spoofing, etc); **Tampering** (beamforming tampering, timing tampering, etc; **Repudiation** (false claim and miss-correlation); **Information Disclosure (**raw and semantic data, object reveal, etc); **Denial of Service** (physical denial of service and noise addition); **Elevation of privilege** (sensing of unintended or prohibited areas and 2) object reveal).
- Privacy risks (LINDDUN):
  - **Linking** (unauthorized connection of sensing data with an entity); **Identifiability** (unauthorized use of sensing data for the extraction for identity extraction); **Non-Repudiation** (false attribution of actions or states to entities using sensing data); **Detection** (unauthorized extraction of private information, action or state, using the observation or transfer of sensing data); **Data Disclosure** (unauthorized collection, processing, storage, and sharing of private sensed data); **Unawareness** (unauthorized collection and processing of sensing data of private entities without their consent or with insufficient disclosure of the resulting privacy implications, failure of allowing sensed entities to access and manage their data, and the failure to informs the consumer applications about the privacy implications of using the sensing infrastructure); **Non-Compliance** (use and processing of data and the use of sensing infrastructure that violate the industry practices and standards, and the local legislations and regulations).

Proof of the Concept

Summary

Chapter 11 presents advancements and research findings in the development of 6G technology through proof of the concept case scenarios. Key areas of focus include the development of a link-level simulation tool for the 6G physical layer, showcasing significant enhancements in PHY schemes like D-MIMO and beamforming. These advancements aim to optimize system performance, particularly in mmWave and sub-THz frequency bands. Moreover, the report introduces an AI-native air interface, demonstrating the practical applications of machine learning in enhancing channel state feedback compression and facilitating pilotless OFDM transmissions. Additionally, the report delves into innovative approaches for flexible modulation and transceiver design, emphasizing the integration of AI and machine learning in air interface design. Joint communication and sensing (JCAS) capabilities are explored, highlighting the potential of using the same hardware for both communication and sensing purposes. Furthermore, the report addresses the crucial aspect of power consumption in JCAS systems, providing insights into power efficiency strategies. An important component of the report is the EMF assessment, evaluating the EMF exposure from advanced MIMO systems, and the evaluated environmental EMF exposure levels from D-MIMO deployments are found far below the international and EU recommended EMF limits. Lastly, comprehensive channel measurement data and models are presented, offering valuable resources for further research and development in 6G technology.

Link modelling of 6G physical layer

Problem Statement	A link-level simulation tool of the downlink 5G PHY has been developed, including models of multi-cluster propagation channels in the sub-THz bands. The simulator provides performance evaluation of D-MIMO and beamforming. The aim is to understand the impact of these enhanced PHY schemes to improve the system performance and to optimize the parameters, especially in mmWave (FR2 frequency bands) and sub-THz.
Methodology	The simulation chain presented in the figure below has been implemented, based on the 3GPP specifications. The blocks are developed in Python, using the Sionna open-source libraries as a starting point, offering substantial flexibility in the development, choice of the use cases, etc. It allows the integration of new algorithms/configurations so that the chains can easily evolve.

Results

- The data flow is randomly generated by a bit generator, and feeds the chain of baseband signal processing blocks: segmentation, cyclic redundancy check (CRC), interleaving, etc. The forward error coding scheme is the LDPC specified in [38.212]. OFDM modulation is implemented, and the signal samples are convolved with a randomly generated channel impulse response. The reception part of the chain includes the demodulators and decoders, leading to an estimation of the transmitted bits. A dedicated block compares the initially generated bits with the estimated bits and computes the bit error rate (BER) and block error rates (BLER).
- The first version of the simulator includes an ideal digital MIMO precoding (e.g., based on the singular value decomposition of the channel matrix). In a future deliverable, the obtained BER vs. SNR results will be used as reference, and further compared with other MIMO schemes, such as D-MIMO and hybrid beamforming, as discussed in sections 5.1.1 and 5.2.5.

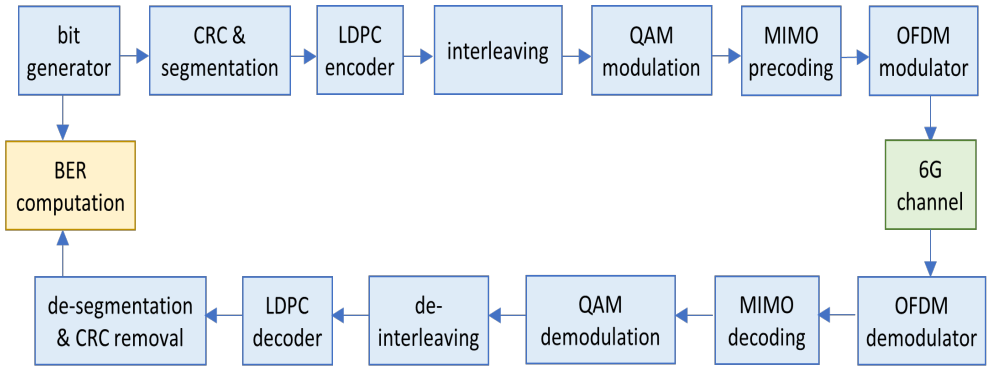

AI Native Air Interface, Part 1: ML-based channel state feedback compression in a multi-vendor scenario

Problem Statement	This enabler is a proof-of-concept (PoC) that aims to demonstrate the feasibility of cross-vendor cooperation, between UE-side ML Model (also referred to as Encoder) and NW-side ML Model (also referred to as Decoder), to enable joint AI solutions for enhanced channel state feedback compression.
Methodology	ML-based channel state feedback compression in a multi-vendor scenario, a simulation study is presented that demonstrates that sequential training of multi-vendor ML models achieves similar performance compared to a joint training solution and that a common NW decoder model can be trained through sequential training to deal with multi-UE vendor scenarios. Given the simulation results, the next step is the lab testing and Over-The-Air (OTA) evaluation of the proposed scheme

Results

- It is composed of two parts: a lab test and an OTA test. For the lab test, a gNB and a UE device will be connected through an 8x4 channel emulator. Certain fading channel types (to be defined upon OTA evaluation) will be configured for data collection and testing. To emulate a multi-vendor scenario, the lab testing and OTA evaluation will use a Nokia gNB and a Qualcomm UE.

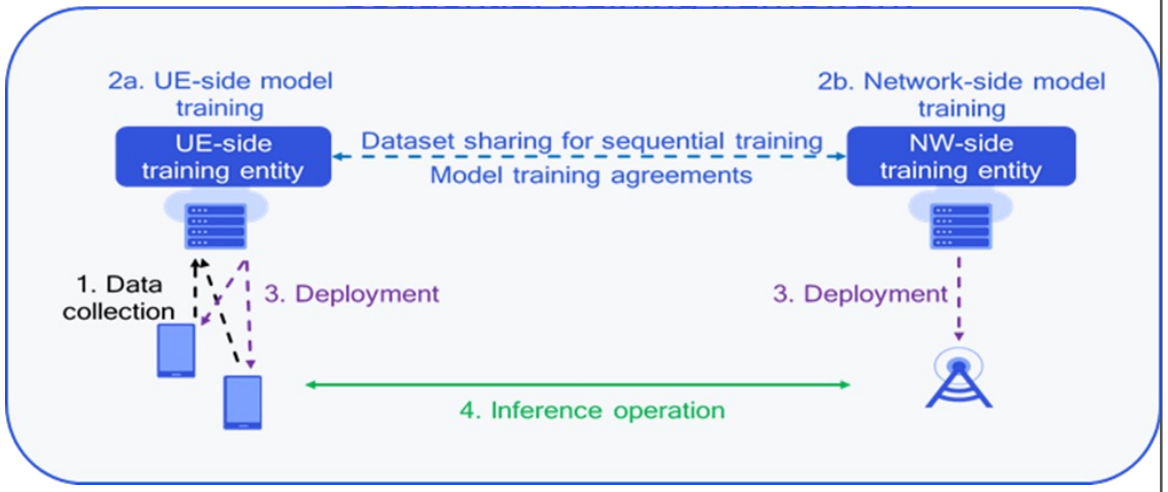

AI Native Air Interface, Part 2: Pilotless operation with a partially learned air interface

Problem Statement	The primary target of this PoC is to demonstrate the practical feasibility and performance gains of an ML-based pilotless air interface. The concept is shown in the left figure below, which illustrates the considered OFDM link. In particular, the approach involves learning the transmitter constellation (DeepTx) and receiver algorithm (DeepRx) to achieve a system which can communicate without any channel estimation pilots. This will result in throughput gains via the reduced overhead.
Methodology	The basic approach of the considered PoC is depicted in the right figure below, which shows the training and validation methods. In particular, the required ML models are trained in a simulator, after which the models are deployed to the target hardware and the performance is validated with real RF measurements. This ensures that the results show two aspects: (i) a simulator-trained model can generalize to unforeseen real-life channels, and (ii) a ML-based air interface can outperform a pilot-based system. It should also be noted that this PoC is a SISO variant of the approach described in Section 7.1.1.

Results

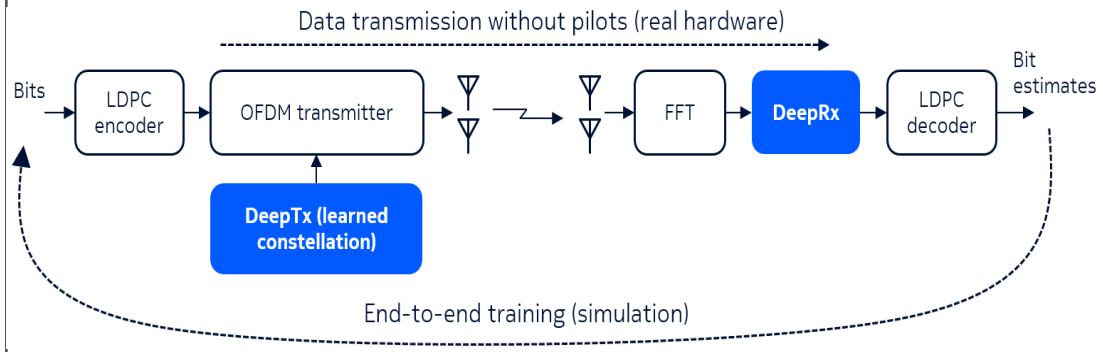

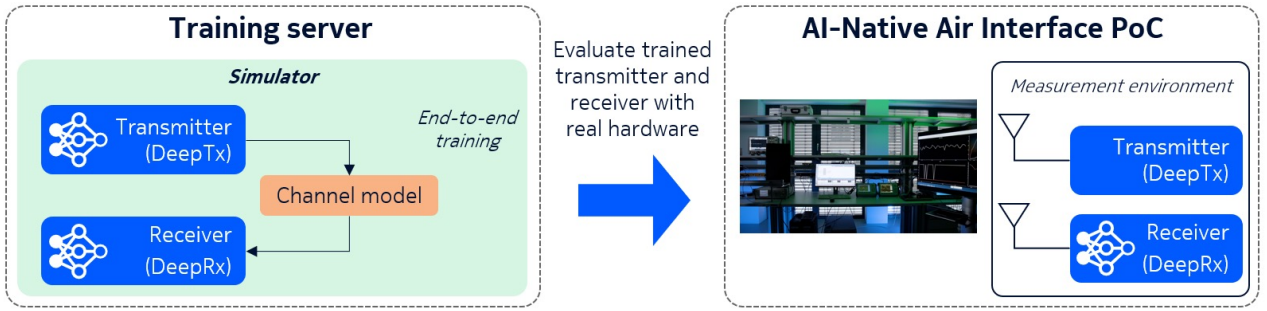

Bistatic joint communication and sensing

Problem Statement	The implemented bistatic sensing system leverages evaluation kits (EVK) from Sivers Semiconductors in 57-71 GHz for the transmitter and receiver radios, coupled with the RFSOC from Xilinx for efficient and high-speed signal processing according to the left figure below. This setup is specifically designed to utilize 5G waveforms, enabling us to explore the capabilities of joint bistatic sensing and communication within a communication framework. The objective is to demonstrate a joint communication and sensing proof of concept that showcases the potential of using the same hardware for both communication and sensing.
Methodology	Using the 5G NR standard waveform, different waveforms can be transmitted using QPSK and 16-QAM to 256-QAM signals for the communication demonstration. The SSBs for synchronization is used according to 5G NR standard.

Results

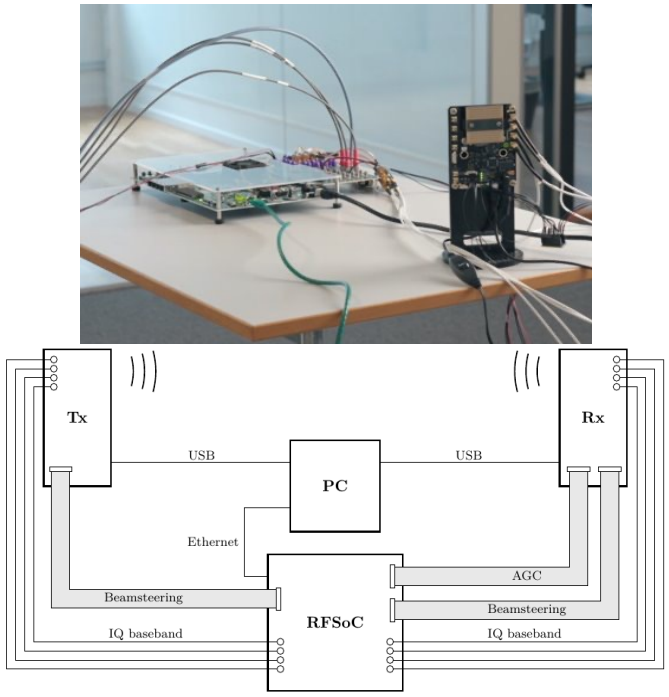

Qamcom RF setup (including the Xilinx board and Sivers EVK) for joint communication and sensing

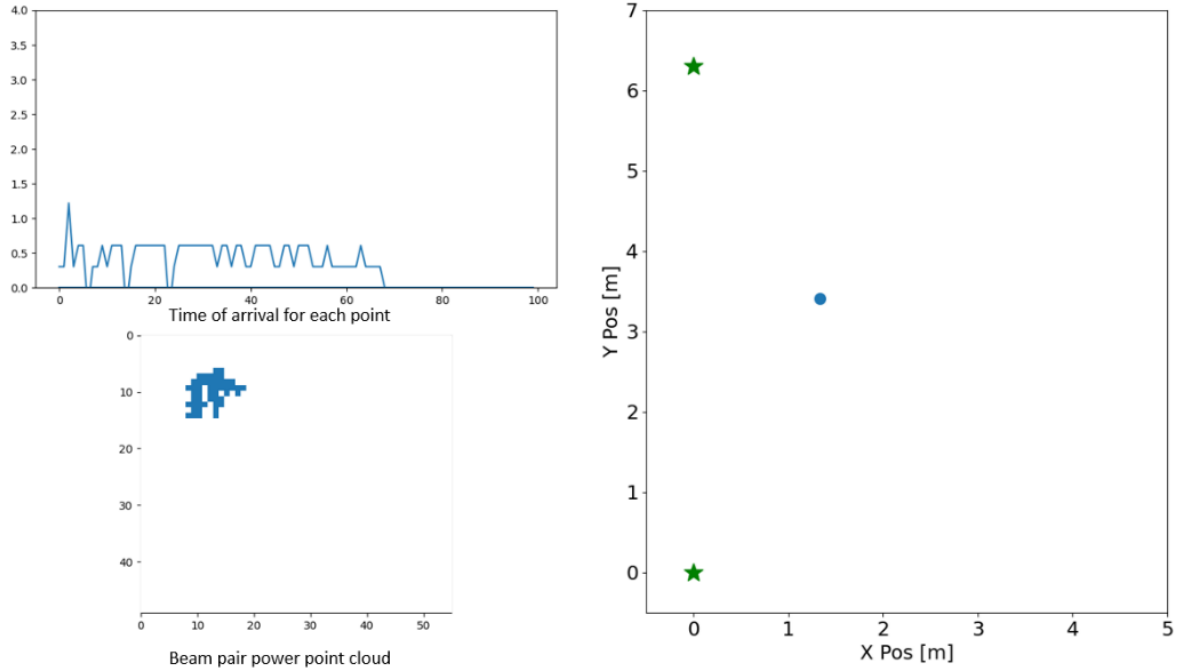

Beam-power map on lower left figure (point cloud power of detected targets), TOA on upper left figure, and estimated position using Qamcom JCAS setup on the right figure

Power consumption of JCAS

Problem Statement	Considering the expected power consumption and consumption factor changes on mmWave systems, it is decided to use the Qamcom Joint Communication and Sensing setup presented in Figure 11-7 to perform the power consumption measurements.
Methodology	The setup contains the RF Module EVKs that are “plug and play” platforms, including patch antennas to evaluate the Sivers Semiconductors beam steering RFICs - TRX BF/01 for unlicensed 5G (IEEE 802.11ad) and TRX BF/02 for licensed 5G. Frequency ranges include 24-29.5 GHz (TRX BF/02) and 57-71 GHz (TRX BF/01). The maximum power lies between 15-40 W. The power consumption measurements and analyses will include different states: (i) power required to turn the device on while the radio interface is down; (ii) power consumption required to generate traffic when the radio interface is up; (iii) power consumption of on and off beacon period; (iv) power consumption during the transmission and reception modes ; (v) power consumption when changing propagation conditions (LoS, NLoS).

Results

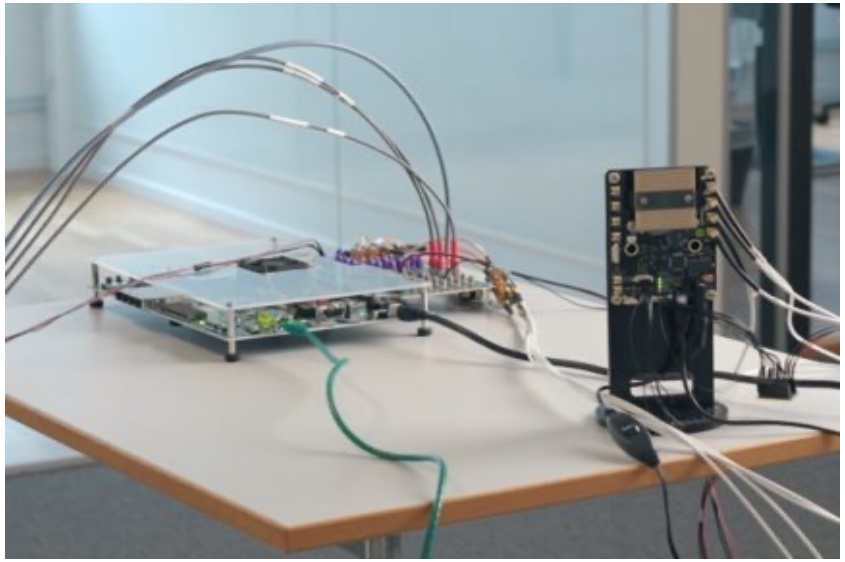

Frequency ranges: 57-71 GHz

Frequency ranges: 24-29.5 GHz

EMF Assessment

Problem Statement	When a new generation of mobile technology is introduced, questions about electromagnetic field (EMF) exposure may be raised. The EMF exposure limits are given in terms of basic restrictions (physical quantities inside the body) and reference levels (external field quantities derived from the basic restrictions) according to the EU recommended limits and the international EMF exposure guidelines, such as those provided by the International Commission on Non-Ionizing Radiation Protection (ICNIRP). To simulate EMF exposure from a D-MIMO system, a full-wave analysis of the antennas and of the surrounding electrically large environment is infeasible due to the extremely large computational demand.
Methodology	A solution is to use hybrid simulation approaches, with which the antennas and the human body model (phantom) are simulated by full-wave methods, while the field propagation is simulated by asymptotic approaches, such as the ray-tracing method. In this study, a hybrid simulation scheme is developed to assess the downlink EMF exposure from 6G D-MIMO deployments. The same scheme is also applied to 5G massive MIMO (mMIMO) deployment for the sake of comparison. Two precoding schemes, including single-user equal-gain transmission (EGT) and multi-user centralized zero-forcing (CZF), are considered. The study is conducted in a realistic industrial indoor environment at 3.5 GHz using representative array antenna designs and a full-body phantom.

Results

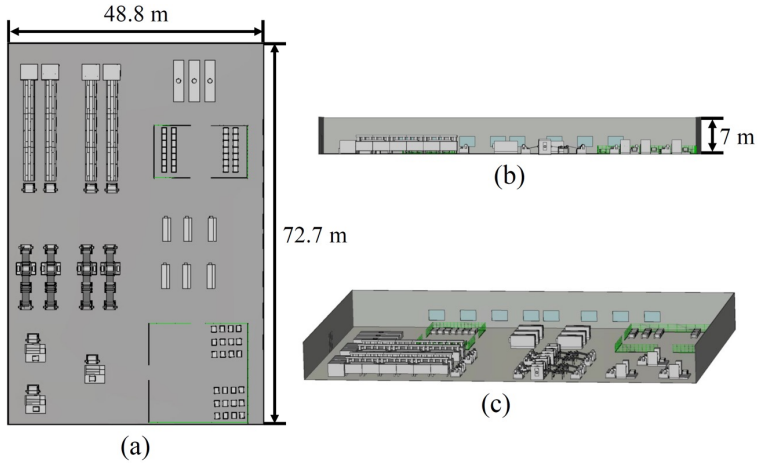

Battery factory model used for the study: (a) top view, (b) side view, and (c) perspective view.

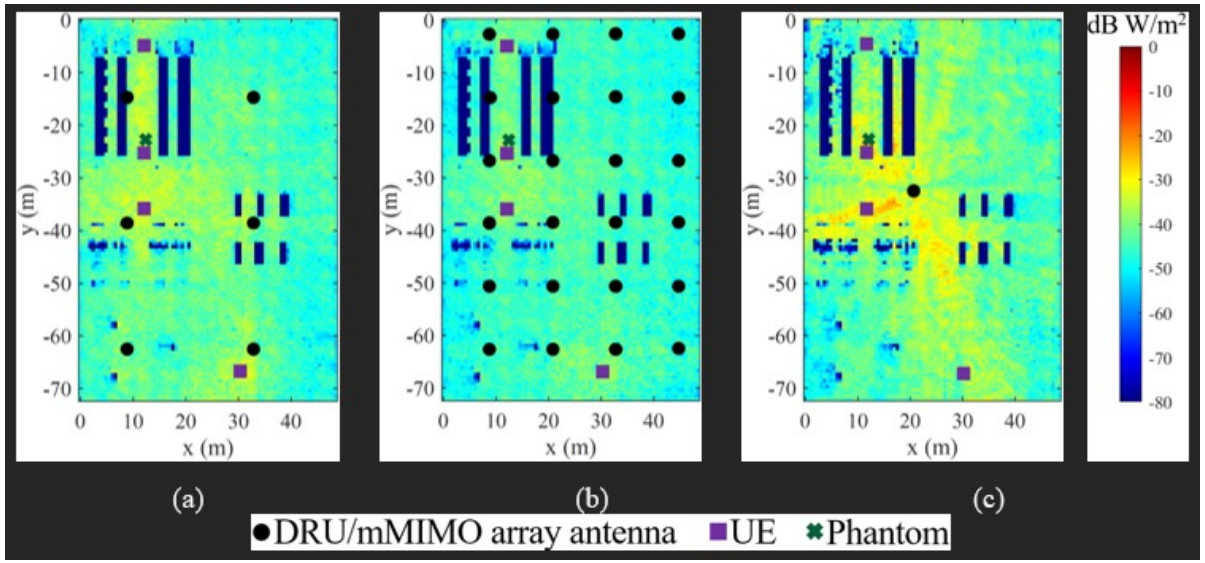

Incident power density (Sinc) distribution for CZF-precoding with K = 4 UEs for one of the studied scenarios for a total configured power of 1 W for: (a) D-MIMO with 6 DRUs, (b) D-MIMO with 24 DRUs, and (c) mMIMO.

Channel measurement data and model

Problem Statement	The most common methods of channel modelling, such as the stored channel, deterministic, and stochastic channel models, are based on multipath data obtained from measurements. A stored channel model directly replays the measured channel impulse responses. Measured channels are also indirectly used in deterministic channel modelling, where the channel response is calculated by allowing rays to propagate and interact with different objects in the environment. The amplitude and phase contribution of each interaction depend on the electromagnetic characteristics of each object, which may either be based on a standard or estimated from the measurements. The latter also pertains to the so-called calibration of ray-based propagation tools used for deterministic channel modelling. Finally, stochastic channel models heavily rely on measured multipath data to determine the input channel parameter values. These models can produce large amounts of multipath data with probability density functions consistent with the measured channels for a given scenario.
Methodology	Radio channel measurements were performed in an indoor entrance hall and outdoor sites, including suburban, residential, and city centre environments both in line-of-sight (LoS) and non-LoS (NLoS) link conditions. The measurements were taken over a maximum distance of 65 meters for the indoor site and up to 170 meters for outdoor sites. The frequency range scanned was 140 GHz to 144 GHz, using a vector network analyser with frequency converters. The Tx and Rx have omnidirectional and rotator-mounted directional horn antennas, respectively. Other measurements in 150 GHz and 15 GHz are also maintained for different environments

Results

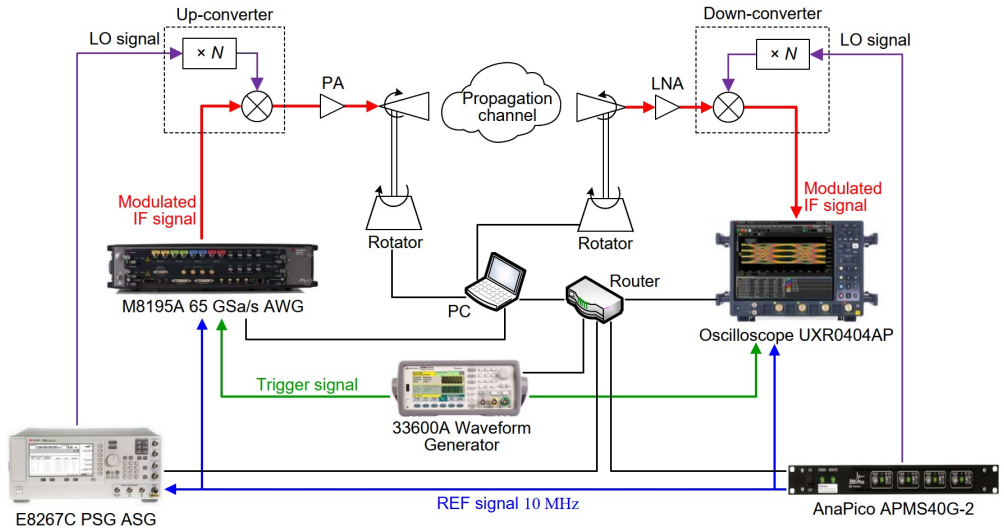

COTS instrument-based channel sounder used for measurements at 150 GHz.

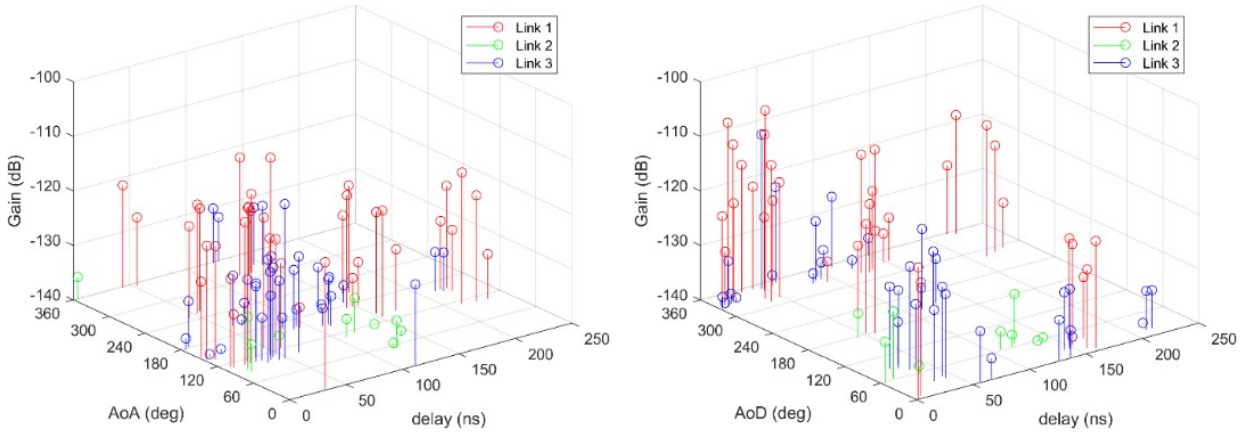

Channel model with the measured 142 GHz channel model parameter values. (left) Azimuth angle of arrival (right) Azimuth angle of departure.

HEXA-X-II.EU //

Co-funded by the European Union

6GSNS

Hexa-X-II project has received funding from the Smart Networks and Services Joint Undertaking (SNS JU) under the European Union's Horizon Europe research and innovation programme under Grant Agreement No 101095759.